ANALYSIS AND DESIGN OF ROTOR BLADES DUE TO THE TRANSIENT THERMAL AND VIBRATORY LOADS

RAJEEVE BAHREE

ANALYSIS AND DESIGN OF ROTOR BLADES DUE TO THE TRANSIENT THERMAL AND VIBRATORY LOADS

by

© Rajeeve Bahree

A thesis submitted to the School of Graduate Studies
in partial fulfillment of the
requirements for the degree of
Master of Engineering

Faculty of Engineering and Applied Science
Memorial University of Newfoundland

September 1987

St. John's Newfoundland Canada

ISBN 0-315-43326-4

ABSTRACT

The research work carried out in this thesis deals with the transient thermal and vibratory analysis of a gas turbine rotor blade. The design criteria of a rotor blade is suggested after studying the combined effects of the vibratory and thermal stresses on the turbine blade.

The non-linear equations for the transient temperature distribution within the airfoil cross-section of the blade are derived using the finite element analysis. The non-linearity in these equations is due to the radiative heat transfer and also due to the variation of the material properties of the blade with temperature. The non-linear differential equations are transformed to the non-linear algebraic equations in the time domain using a finite difference scheme. The temperature gradients and the thermal stresses are calculated from the transient temperatures obtained from the heat transfer analysis.

The mathematical model for the vibratory analysis is formulated using solid, quadratic, isoparametric finite elements. The stiffness and mass matrices are integrated using Gaussian quadrature. A dynamic matrix reduction technique is used to condense the global stiffness and mass matrices of the blade. The free vibration analysis of the blade is carried out using the condensed system matrices. The effects of the transient temperature distribution and the angle of pre-twist on the undamped natural frequencies of the rotor blade are studied.

The vibratory stresses are calculated due to nozzle excitation and centrifugal forces. The nozzle excitation forces are modelled as a series of impulses using the kinematic equations. The principal stresses are obtained from the vibratory stress vector and the design of the rotor blades is based on the distortion energy stress.

ACKNOWLEDGEMENTS

I am thankful to Dr. Anand M. Sharan for his guidance and encouragement during the course of this investigation. His contribution of time and technical expertise have helped me immensely.

I would like to express my gratitude to Dr. F. A. Aldrich, Dean of Gradute Studies and Dr. G. R. Peters, Dean of Engineering for providing me with a University Fellowship during my studies. I am also indebted to Dr. T. R. Chari, Associate Dean of Engineering, for all his assistance during my graduate studies.

Finally, a special word of thanks goes to Ms. Wanda Butler for her quick and efficient typing of this thesis.

To My Parents and

My Sister

TABLE OF CONTENTS

	Page
ABSTRACT	ii
ACKNOWLEDGEMENTS	iv
TABLE OF CONTENTS	vi
LIST OF FIGURES	ix
LIST OF TABLES	xii
NOMENCLATURE	xiii
CHAPTER 1	
INTRODUCTION AND LITERATURE SURVEY	
1.1 Introduction	1
1.2 The Literature Survey	5
1.2.1 The Thermal Stress Analysis	5
1.2.2 The Vibratory Stress Analysis	6
1.3 The Objectives of this Investigation	7
CHAPTER 2	
THE TRANSIENT THERMAL STRESS ANALYSIS	
2.1 Introduction	10
2.2 The Mathematical Formulation	11
2.2.1 The Transient Temperature Determination	11
2.2.2 The Transient Thermal Stress Determination	21
2.3 Numerical Example	22
2.4 The Transient Thermal and Thermoelastic Studies of the Turbine Blade	24
2.4.1 The Effect of the Radiative Heat Flux on the Temperature Distribution	24
2.4.2 The Temperature Gradient Distribution across the Airfoil Cross-section of the Turbine Blade	29
2.4.3 The Thermal Stress Distribution	38
2.5 Conclusion	44
CHAPTER 3	
THE FREE VIBRATION ANALYSIS OF THE TURBINE BLADE	
3.1 Introduction	47
3.2 Mathematical Formulation	49

		Page
3.2.1	The Isoparametric Finite Element Formulation	49
3.2.2	The Free Vibration Analysis	57
3.3	Numerical Example	59
3.3.1	Verification of the Formulation and the Computer Software	59
3.3.2	The Description and Details of the Turbine Blade	62
3.4	A Study of the Undamped Natural Frequencies of the Blade	65
3.4.1	The Variation of the Undamped Natural Frequencies with Temperature	65
3.4.2	The Coordinate Reduction Using the Dynamic Matrix Reduction Scheme	67
3.4.3	The Effect of Pre-Twist on the Undamped Natural Frequencies	67
3.5	Conclusion	69

CHAPTER 4

THE TRANSIENT STRESS ANALYSIS DUE TO THE VIBRATORY AND THERMAL LOADING

4.1	Introduction	72
4.2	The Mathematical Formulation	72
4.2.1	The Modelling of Transient Nozzle Excitation Forces	72
4.2.2	The Transient Response Due to Nozzle Excitation Forces	75
4.2.3	The Transient Response Due to Centrifugal Forces	76
4.2.4	The Calculation of Vibratory Stresses	77
4.3	Numerical Example	78
4.4	A Study of the Coupled Effects of Thermal and Vibratory Loads on the Transient Stresses in the Blade	79
4.4.1	The Thermal Stress Analysis of the Turbine Blade	79
4.4.2	The Vibratory Stress Analysis of the Turbine Blade	80
4.4.3	The Stress Analysis of the Turbine Blade Due to the Combined Effects	86
4.5	Conclusion	89

CHAPTER 5

CONCLUSIONS AND RECOMMENDATIONS

5.1	A Brief Discussion About the Investigation and the Conclusions	91

		Page
5.2	Limitations of the Present Investigation and Recommendations for Future Work	93
REFERENCES		95
APPENDIX A:	THE EXPRESSIONS FOR THE ELEMENTAL MATRICES AND VECTORS FOR THE LINEAR TRIANGULAR ELEMENT	98
APPENDIX B:	DECOUPLING OF THE EQUATIONS OF MOTION FOR MODAL ANALYSIS	102
APPENDIX C:	THE TURBINE BLADE AIRFOIL CROSS-SECTIONS	104
APPENDIX D:	DESCRIPTION AND LISTING OF THE COMPUTER PROGRAMS	111

LIST OF FIGURES

No.	Description	Page
1.1	The Aircraft Engine	2
1.2a	The Gas Turbine Rotor Disk-Blade Assembly	3
1.2b	The Turbine Blade	4
2.1	The Finite Element Discretization of the Turbine Blade Cross-section	23
2.2	Heat Transfer Distribution Around The Blade Surface at Full Load Operation	25
2.3	Heat Transfer Coefficient During Quick Start as a Function of Time	26
2.4	The Transient Temperature Distribution With and Without Radiation (T_g = 870°C)	28
2.5	The Variation of the Temperature Gradient-X Along the Pressure Surface (T_g = 870°C)	30
2.6	The Variation of the Temperature Gradient-Y Along the Pressure Surface (T_g = 870°C)	33
2.7	The Variation of the Temperature Gradient-X Along the Mid-Section (2-2') at T_g = 870°C	34
2.8	The Variation of the Temperature Gradient-Y Along the Mid-Section (2-2') at T_g = 870°C	35
2.9	The Variation of the Temperature Gradient-X Along the Suction Surface (T_g = 870°C)	36
2.10	The Variation of the Temperature Gradient-Y Along the Suction Surface (T_g = 870°C)	37
2.11	The Variation of the Normalized Stresses and ΔT as a Function of Time Corresponding to the Turbine Heating Rate of 56°C/sec. and Final T_g = 870°C	39

No.	Description	Page
2.12	Calculated Temperature and Stress Distribution During Start for Leading Edge, Mid-Part and Trailing Edge	41
2.13	The Temperature Contours Across the Airfoil Section at t = 88 seconds	45
2.14	The Stress Contours Across the Airfoil Section at t = 88 seconds	46
3.1	The Blade Airfoil Cross-sections at the Root and the Tip	48
3.2	The Solid Isoparametric 'Serendipity' 20-noded element (a) Local Coordinate System (b) Global cartesian coordinate System	50
3.3	The Turbine Blade Finite Element Model	63
3.4	Plot Showing the Effect of Guyan's Reduction on the First Five Blade Natural Frequencies	68
3.5	The Variation of Natural Frequency with Pretwist	70
4.1a	Schematic of the blade, nozzle and rotor configuration	73
4.1b	The representation of the nozzle excitation forces as a series of impulses	73
4.2	The Transient Temperature and Thermal Stress Distribution in the Blade for the feasible heating rate of 31-33°C/sec. and Final T_g = 870°C	81
4.3	The Variation of Nozzle Excitation Stresses at the Leading Edge at Various Speeds	83
4.4	The Variation of Nozzle Excitation Stresses at the Trailing Edge at Various Speeds	84

No.	Description	Page
4.5	The Variation of Nozzle Excitation Stresses at the Element No. 78 at Various Speeds	85
4.6	The Variation of Centrifugal Stresses at the Rotor Speed of 4000 RPM	87
A.1	The Details of the Triangular Element	99
C.1	The Turbine Blade Airfoil Cross-section at the Root (z = 0.0m)	105
C.2	The Turbine Blade Airfoil Cross-section at z = 0.025 m	106
C.3	The Turbine Blade Airfoil Cross-section at z = 0.05 m	107
C.4	The Turbine Blade Airfoil Cross-section at z = 0.075 m	108
C.5	The Turbine Blade Airfoil Cross-section at z = 0.1 m	109
C.6	The Turbine Blade Airfoil Cross-section at the Tip (z = 0.11 m)	110
D.1	The Flow Chart for the Transient State Thermal Analysis	113

LIST OF TABLES

No.	Description	Page
2.1	The Variation of the Material Properties of the Blade with Temperature	27
2.2	The Calculation of Overall Temperature Gradient of Elements Having High Stress State (t = 88 seconds)	43
3.1	A Comparison of the Natural Frequencies of a Cantilever Beam	61
3.2	The Geometric Properties of the Blade	64
3.3	The Variation of Natural Frequencies (Hz.) with Time	66

NOMENCLATURE

$[D]$	material property matrix
$[B]$	strain-displacement matrix
$[N]$	shape function matrix
$[CP]$	capacitance matrix
$[K]$	conduction matrix
$[C]$	damping matrix
$[KS]$	stiffness matrix
$[M]$	consistent mass matrix
$[\phi]$	matrix of modal vectors
$[J]$	Jacobian matrix
$[\psi]$	transformation matrix
$[\overline{KS}]$	reduced stiffness matrix
$[\overline{M}]$	reduced mass matrix
$[\overline{C}]$	reduced damping matrix
$\{T\}$	nodal temperature vector
$\{\gamma\}$	strain vector
$\{F_r\}$	force vector due to radiation
$\{F_c\}$	force vector due to convection
$\{F\}$	dynamic force vector
$\{\overline{F}\}$	reduced dynamic force vector
$\{U\}$	nodal displacement vector
$\{Q\}$	force vector transformed in modal coordinates by normalized modal matrix
$\{QF\}$	force vector transformed in modal coordinates by m-orthonormalized modal matrix
T_∞	gas temperature

S	surface subjected to convection, radiation and specified heat flux
χ	a functional
θ_p	angle of pre-twist
θ	angle between two nozzles
θ_R	angle of pre-twist at root
θ_T	angle of pre-twist at tip
θ_N	angle subtended by a nozzle at the centre of rotation
ω	angular speed of the rotor
ω_{nk}	natural frequency of k^{th} mode
ω_{dk}	damped natural frequency of k^{th} mode
ξ_k	damping ratio of k^{th} mode
n	number of elements
c	specific heat
h	convective heat transfer coefficient
h_0	convective heat transfer coefficient at $30^\circ C$
K_x	thermal conductivity in the x-direction
K_y	thermal conductivity in the y-direction
K_z	thermal conductivity in the z-direction
ℓ_x, ℓ_y, ℓ_z	direction cosines normal to the surface
Q	heat generated within the body
q	specified heat flux
W_i, W_j, W_k	weights used in Gaussian-quadrature
t	time
Δt	time increment
Δt_{imp}	duration of the impulse
Δt_0	time gap between occurence of two impulses

ρ	mass density of the material
σ	Stefan-Boltzman constant
$\sigma_x, \sigma_y, \sigma_z$	normal stresses
$\tau_{xy}, \tau_{yz}, \tau_{xz}$	shear stresses
α	coefficient of thermal expansion
ν	Poisson's ratio of the material
ϵ	emissivity of the body
ξ, η, ζ	local coordinate directions
V	volume of the blade
NG	number of Gauss points
x_c, y_c	coordinates of the centroid of the triangular element
E	modulus of elasticity
A	area of cross-section
R	radius of the rotor
σ_d	distortion energy stress
σ_d^*	normalized distortion energy stress
G	global
e	elemental
C	chord length

CHAPTER 1

INTRODUCTION AND LITERATURE SURVEY

1.1 Introduction

The turbines are one of the most widely used machinery in power generation or in jet propulsion. For example, the application of turbines is well known in the areas of hydroelectric power generation, steam power generation and in the propulsion of jet planes. Fig. 1.1 shows the turbine as one of the components in the aircraft engine. In this figure the air is let in through the diffuser, is compressed in two stages, and then the pressure and temperature of the air is increased in a combustor. The air-fuel mixture is then injected through the nozzles of the gas turbine chamber onto the turbine blades. This produces mechanical power which is then used to drive the propeller attached to the turbine shaft. Fig. 1.2a shows the rotor disk-blade assembly and Fig. 1.2b shows the twisted shape of the blade.

This rotor blade, while in operation, is subjected to a combination of stresses such as thermal, centrifugal and due to the nozzle excitation forces. Hence, a reliable design of the blade depends upon a careful and detailed analysis of these type of stresses and this is the intent of the investigation in this thesis.

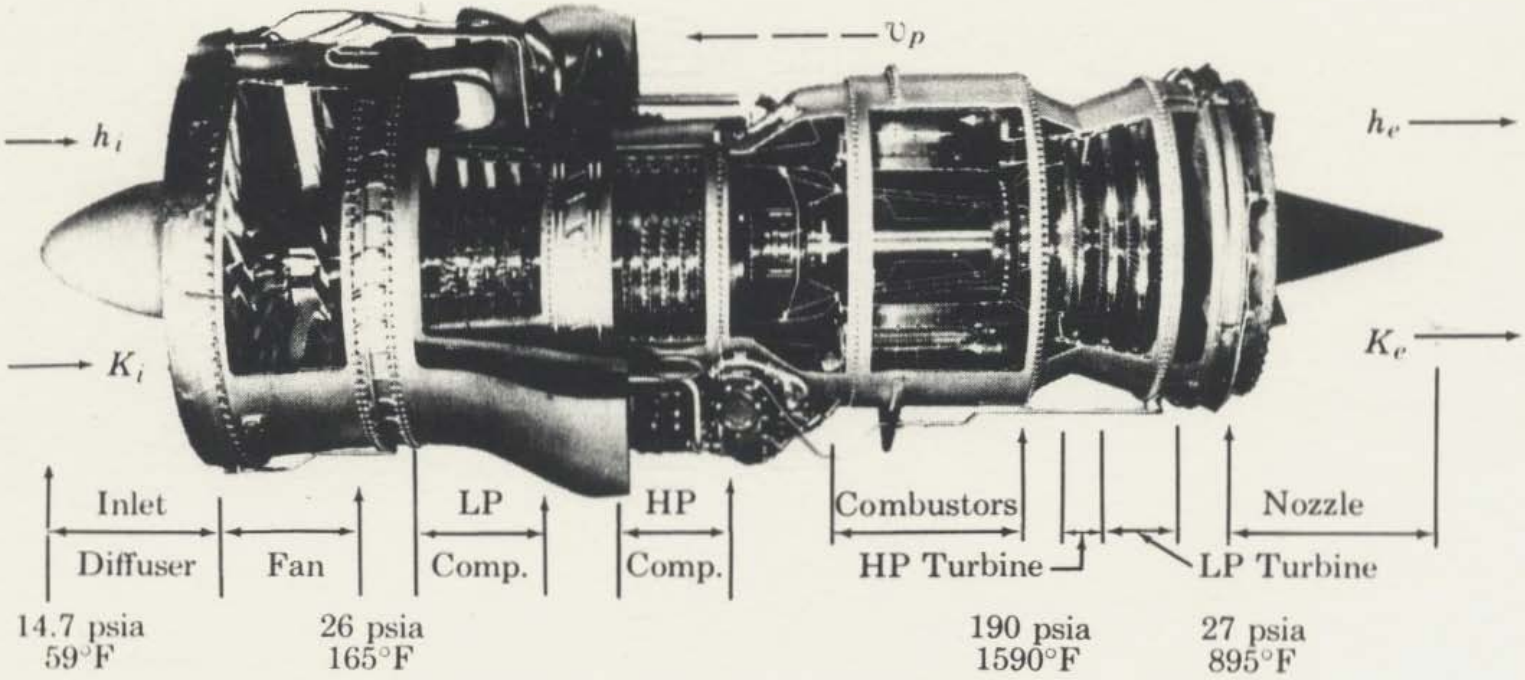

FIG.1.1 THE AIRCRAFT ENGINE [1]

FIG.1.2a THE GAS TURBINE DISK-BLADE ASSEMBLY [2]

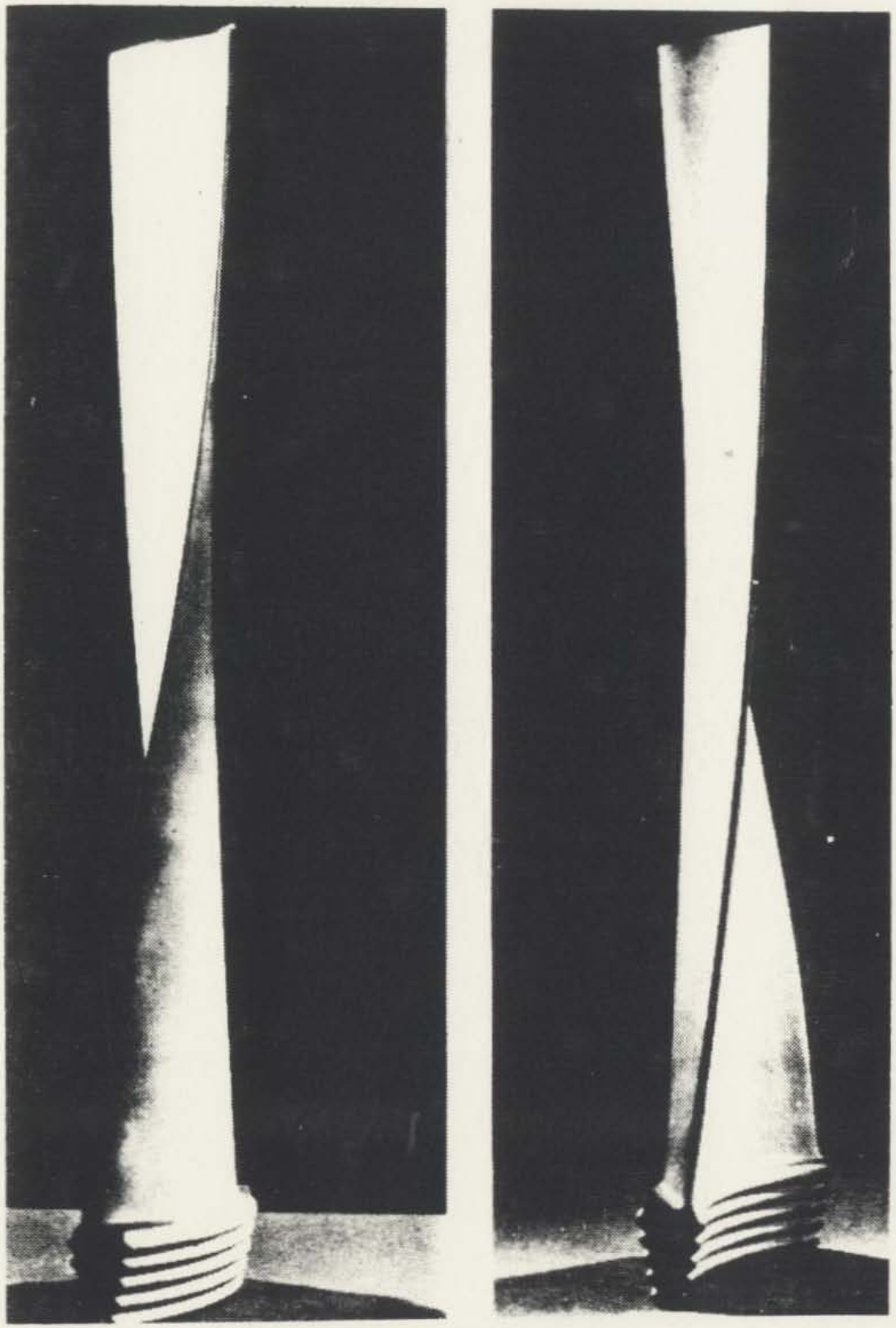

FIG.1.2b THE TURBINE BLADE [3]

1.2 The Literature Survey

1.2.1 The Thermal Stress Analysis

Ever since the inception of a gas turbine engine there has been a considerable amount of interest in carrying out its heat transfer and thermal stress analyses. However, as the demand on the engine for more power output became the primary factor in its design, it caused the engine to be operated under optimum conditions of pressure and temperature. Hence, the heat transfer and thermal stress analysis should be carried out as accurately as possible. Some of the more recent advances in heat transfer can be found in [4,5].

The heat transfer process of the gas turbine blades has been studied by Maya, et al [6] and Mukherjee [7]. In their work they considered the heat exchange process at the surface by convection only. They also calculated the transient thermal stresses; however, their analyses lack accuracy in prediction of the thermal stresses and temperature distributions because the radiative heat exchange mechanism is quite significant at the operating temperatures. In addition, they investigate the stresses only at a few points such as the leading edge, the trailing edge and at the corner of a cross-section of the blade and carried out their analyses by assuming that the maximum stresses would take place at one of these points only during the transient period. The effect of temperature dependent mechanical properties on thermal stresses in cooled turbine blades was studied in [8]. The influence of turbine blade airfoil and root thickness variation along the blade height on its thermal stress state was studied in [9].

Also, an experimental investigation of the thermal stresses in gas turbine blades was carried out in [10]. The effect of radiative heat transfer was not included by any of these researchers.

1.2.2 The Vibratory Stress Analysis

The blade dynamics has been an area of extensive research for a long time. One of the important tasks in the dynamic analysis of the rotor blade is to carry out its free vibration analysis. The dynamic equations of motion of the blade can be arrived at by using various mathematical techniques. Some of these are based on the Newtonian approach. The geometry of the blade, as a first approximation, can be modelled as a tapered beam having a rectangular cross-section.

The bending frequencies for the first three modes of vibration of tapered cantilever blades having rectangular cross-section were obtained by Rao and Carnegie [11]. They used the Ritz-Galerkin method to arrive at the equations of motion. The natural frequency determination due to various boundary conditions was studied by Mabie and Rogers [12]. They used the Bessel's functions in their work. The effect of axial force on the frequencies of blades with ends restrained elastically against rotation was carried out by Sato [13]. He used the Ritz method for his formulation. The free vibration studies were also carried out by Banerji and Williams [14], Hutchinson and Zillmer [15] and various other researchers [16,17].

Sisto and Chang [18] used the finite element method to calculate the blade natural frequencies, however, their model was

appropriate for thin ahd high aspect ratio blades only. Nagarajan and Alwar [19] analysed the free vibration behaviour of the blade packet assembly using twenty-noded finite elements. The details of the ongoing research in this field and the latest state-of-art can be found in [20-23].

Based on this literature survey it was found that the non-linear transient temperature and thermal stress determination in case of a turbine blade has not been done so far. Also, it was fairly certain that the blade dynamics had not been studied using twenty-noded isoparametric finite elements. The modelling of nozzle excitation forces using kinematics had also not been done so far.

1.3 The Objectives of this Investigation

The problem under consideration in this thesis is multi-disciplinary; hence the objectives of this investigaion are manifold. In order to calculate the state of stress in the blade in the transient state, extensive studies into the heat transfer and dynamics of rotor blades have to be carried out. Thus, the objectives of this investigation can be summarized as:

1. The derivation of the transient temperature distribution equations in a turbine blade using finite element analysis.
2. The determination of temperatures at various points on the airfoil cross-section of the blade by solving a non-linear system of equations. Here, the non-linearity arises due to the

radiative boundary conditions at the surface of the turbine blade.

3. To study the free vibration characteristics of the turbine blade using twenty-noded, curved, isoparametric finite elements.
4. To study the dynamic stresses in the blade due to nozzle excitation forces and centrifugal forces.
5. To study the state of stress in the blade due to the combined effects of thermal and dynamic loading.

In Chapter 2, the non-linear equations for the transient temperature determination in a turbine blade are derived using the finite element method. The non-linear system of differential equations are transformed into a non-linear system of algebraic equations in the time domain by using the Crank-Nicolson finite difference scheme. The thermal gradients and thermal stresses are calculated once the transient temperatures are known.

In Chapter 3, a mathematical model for the free vibration study of a rotor blade is developed. The twenty-noded isoparametric finite element formulation is used to study the free vibration characteristics of the blade. A coordinate reduction scheme is used to reduce the dynamic equations of motion. The effect of the heating of the blade on its natural frequencies is studied in this chapter. Also, the effect of the variation of the pre-twist angle on the natural frequencies is studied.

In Chapter 4, a feasible heating path for the gas turbine engine, while in acceleration, is used to carry out the thermal analysis. The thermal stresses are then calculated for this heating

path. The nozzle excitation forces have been modelled as a series of impulses using the kinematic equations. The response due to nozzle excitation forces and centrifugal forces is used to calculate the dynamic stresses in the blade. The occurance of the stress due to the combined effects of thermal and dynamic loading has been studied at various locations along the height of the blade. The distortion energy criteria is used to calculate the stresses.

The conclusions and recommendations for future work are presented in Chapter 5.

CHAPTER 2

THE TRANSIENT THERMAL STRESS ANALYSIS

2.1 Introduction

The efficiency of a turbine is greatly enhanced by using higher inlet pressures and temperatures. Although higher inlet temperatures are desirable from the thermodynamic point of view, they severely increase the thermal loading on the turbine blades and consequently cause high thermal stresses in the blades. These thermal stresses are known to peak during acceleration or deceleration of the gas turbine engine. This is because, in the transient state, there is a large difference of temperature between various points of the blade. Therefore, one should calculate the temperature distribution within the blade as accurately as possible. In this work, the heat transfer problem has been formulated as a two-dimensional heat-flow problem because it has already been shown by [6] that the thermal gradient along the height of the turbine blade is negligible during the transient state as compared to the thermal gradient along the airfoil cross-section of the blade. The mathematical model for the non-linear transient heat transfer analysis is formulated using the finite element method. The boundary elements on the blade exchange heat with the surrounding hot gases by the convection and radiation processes. The inclusion of radiation into this analysis results in a non-linear system of differential

equations. These non-linear system of differential equations are transformed into a non-linear system of algebraic equations in the time domain using the Crank-Nicolson finite difference scheme. These non-linear system of algebraic equations are then solved for the nodal temperatures by using an iteration technique. Once the transient nodal temperatures are known, the thermal gradients across the airfoil cross-section and the thermal stresses can be calculated.

2.2 The Mathematical Formulation

2.2.1 The Transient Temperature Determination

The governing three-dimensional partial differential equation for heat flow in any solid can be written as [24]

$$k_x \frac{\partial^2 T}{\partial x^2} + k_y \frac{\partial^2 T}{\partial y^2} + k_z \frac{\partial^2 T}{\partial z^2} + Q = \rho c \frac{\partial T}{\partial t} \tag{2.1}$$

with the boundary condition

$$k_x \frac{\partial T}{\partial x} \ell_x + k_y \frac{\partial T}{\partial y} \ell_y + k_z \frac{\partial T}{\partial z} \ell_z + q + h(T - T_\infty) + \sigma \epsilon (T^4 - T_\infty^4) = 0 \tag{2.2}$$

The calculus of variations can be used to solve the governing partial differential equation, Eqn. (2.1), and its boundary condition, Eqn. (2.2). This can be achieved by minimizing the corresponding variational functional and solving the resulting system of algebraic equations.

Now, Eqn. (2.1) can be rewritten as

$$- k_x \frac{\partial^2 T}{\partial x^2} - k_y \frac{\partial^2 T}{\partial y^2} - k_z \frac{\partial^2 T}{\partial z^2} - \left(Q - \rho c \frac{\partial T}{\partial t}\right) = 0 \tag{2.3}$$

The variational functional can be set up by multiplying Eqn. (2.2) and (2.3) by the first variation of T i.e. δT and integrating over the whole domain as

$$\delta\chi = \int_V \left[-k_x \frac{\partial^2 T}{\partial x^2} - k_y \frac{\partial^2 T}{\partial y^2} - k_z \frac{\partial^2 T}{\partial z^2} - \left(Q - \rho c \frac{\partial T}{\partial t} \right) \right] \delta T \, dV + \int_S \left[k_x \frac{\partial T}{\partial x} \ell_x + k_y \frac{\partial T}{\partial y} \ell_y + k_z \frac{\partial T}{\partial z} \ell_z + q + h(T - T_\infty) + \sigma \epsilon (T^4 - T_\infty^4) \right] \delta T \, dS \qquad (2.4)$$

Eqn. (2.4) can be rearranged as

$$\delta\chi = \int_S k_x \frac{\partial T}{\partial x} \ell_x \, \delta T \, dS - \int_V k_x \frac{\partial^2 T}{\partial x^2} \delta T \, dV + \int_S k_y \frac{\partial T}{\partial y} \ell_y \, \delta T \, dS - \int_V k_y \frac{\partial^2 T}{\partial y^2} \delta T \, dV + \int_S k_z \frac{\partial T}{\partial z} \ell_z \, \delta T \, dS - \int_V k_z \frac{\partial^2 T}{\partial z^2} \delta T \, dV + \int_S q \, \delta T \, dS - \int_V \left(Q - \rho c \frac{\partial T}{\partial t} \right) \delta T \, dV + \int_S h(T - T_\infty) \, \delta T \, dS + \int_S \sigma \epsilon (T^4 - T_\infty^4) \, \delta T \, dS \qquad (2.5)$$

The surface integrals can be transformed into the volume integrals by using Green's divergence theorem. Thus the following integrals in Eqn. (2.5) can be expressed as

$$\int_S k_x \frac{\partial T}{\partial x} \ell_x \, \delta T \, dS = \int_V k_x \frac{\partial^2 T}{\partial x^2} \delta T \, dV + \int_V \frac{k_x}{2} \delta \left(\frac{\partial T}{\partial x}\right)^2 dV \qquad (2.6)$$

$$\int_S k_y \frac{\partial T}{\partial y} \ell_y \, \delta T \, dS = \int_V k_y \frac{\partial^2 T}{\partial y^2} \delta T \, dV + \int_V \frac{k_y}{2} \delta \left(\frac{\partial T}{\partial y}\right)^2 dV \qquad (2.7)$$

and

$$\int_S k_z \frac{\partial T}{\partial z} \ell_z \, \delta T \, dS = \int_V k_z \frac{\partial^2 T}{\partial z^2} \delta T \, dV + \int_V \frac{k_z}{2} \delta \left(\frac{\partial T}{\partial z}\right)^2 dV \qquad (2.8)$$

Substituting Eqns. (2.6) to (2.8) in Eqn. (2.5), we get

$$\begin{aligned} \delta\chi = & \int_V \frac{k_x}{2} \delta \left(\frac{\partial T}{\partial x}\right)^2 dV + \int_V \frac{k_y}{2} \delta \left(\frac{\partial T}{\partial y}\right)^2 dV \\ & + \int_V \frac{k_z}{2} \delta \left(\frac{\partial T}{\partial z}\right)^2 dV - \int_V Q \, \delta T \, dV + \int_V \rho c \frac{\partial T}{\partial t} \delta T \, dV \\ & + \int_S q \, \delta T \, dS + \int_S \frac{h}{2} \delta (T - T_\infty)^2 \, dS \\ & + \int_S \sigma \in \delta \left(\frac{T^5}{5} - T_\infty^4 T\right) dS \end{aligned} \qquad (2.9)$$

Rewriting Eqn. (2.9) by removing the variational operator δ from both sides we get

$$\begin{aligned} \chi = & \int_V \frac{1}{2} \left[k_x \left(\frac{\partial T}{\partial x}\right)^2 + k_y \left(\frac{\partial T}{\partial y}\right)^2 + k_z \left(\frac{\partial T}{\partial z}\right)^2 \right. \\ & \left. - 2QT + 2\rho c \, T \frac{\partial T}{\partial t} \right] dV + \int_{S_1} qT \, dS \\ & + \int_{S_2} \left[\frac{h}{2} (T - T_\infty)^2 + \sigma \in \left(\frac{T^5}{5} - T_\infty^4 T\right) \right] dS \end{aligned} \qquad (2.10)$$

where

S_1 is the surface experiencing heat flux

and S_2 is the surface experiencing convection and radiation boundary conditions.

For finite element analysis we assume that the temperature T is not continuous over the whole domain but it is defined over an individual element. In order to formulate the finite element equations from Eqn (2.10) we make use of the following finite element equalities:

$$T^e = \begin{bmatrix} N_i^e & N_j^e & N_k^e \end{bmatrix} \begin{Bmatrix} T_i \\ T_j \\ T_k \end{Bmatrix} \tag{2.11a}$$

where T_i, T_j and T_k are nodal temperatures of a triangular finite element taken in the counter-clockwise sense from node i,

$$\left[D^e\right] = \begin{bmatrix} k_x^e & 0 \\ 0 & k_y^e \end{bmatrix}, \tag{2.11b}$$

$$\left[B^e\right] = \begin{bmatrix} \frac{\partial N_i^e}{\partial x} & \frac{\partial N_j^e}{\partial x} & \frac{\partial N_k^e}{\partial x} \\ \frac{\partial N_i^e}{\partial y} & \frac{\partial N_j^e}{\partial y} & \frac{\partial N_k^e}{\partial y} \end{bmatrix} \tag{2.11c}$$

$$\left\{g^e\right\} = \begin{Bmatrix} \frac{\partial T}{\partial x} \\ \frac{\partial T}{\partial y} \end{Bmatrix} = \left[B^e\right] \begin{Bmatrix} T_i \\ T_j \\ T_k \end{Bmatrix}, \tag{2.11d}$$

and

$$\frac{\partial T^e}{\partial t} = \begin{bmatrix} N_i^e & N_j^e & N_k^e \end{bmatrix} \begin{Bmatrix} \frac{\partial T_i}{\partial t} \\ \frac{\partial T_j}{\partial t} \\ \frac{\partial T_k}{\partial t} \end{Bmatrix} \tag{2.11e}$$

Since in the present investigation of the transient heat transfer in the turbine blades, there is no heat generation and there are no specified heat fluxes, therefore the terms Q and q in Eqn. (2.10) are respectively equal to zero. Also, because we have modelled our problem as a two-dimensional heat-flow problem, the term $\frac{\partial T}{\partial z}$ in Eqn. (2.10) is equal to zero. Thus, substituting the above finite element equalities into Eqn. (2.10) one can express the functional for an element as

$$\chi^e = \int_{V^e} \frac{1}{2} \left\{T^e\right\}^T \left[B^e\right]^T \left[D^e\right] \left[B^e\right] \left\{T^e\right\} dV + \int_{V^e} \rho c^e \left[N^e\right] \frac{\partial \left\{T^e\right\}}{\partial t} \left[N^e\right] \left\{T^e\right\} dV + \int_{S_2^e} \frac{h^e}{2} \left(\left[N^e\right] \left\{T^e\right\}\right)^2 dS - \int_{S_2^e} h^e T_\infty \left[N^e\right] \left\{T^e\right\} dS + \int_{S_2^e} \frac{h^e}{2} T_\infty^2 \, dS + \int_{S_2^e} \frac{\sigma\epsilon}{5} \left(\left[N^e\right] \left\{T^e\right\}\right)^5 dS - \int_{S_2^e} \sigma\epsilon T_\infty^4 \left[N^e\right] \left\{T^e\right\} dS \qquad (2.12)$$

The functional χ is defined for individual triangular elements. So, minimizing χ with respect to the nodal temperature vector, $\left\{T^e\right\}$, will yield a stationary value of χ which will satisfy Eqn. (2.1) and its boundary condition Eqn. (2.2). This can be expressed as

$$\frac{\partial \chi}{\partial \left\{T^e\right\}} = \frac{\partial \chi^1}{\partial \left\{T^e\right\}} + \frac{\partial \chi^2}{\partial \left\{T^e\right\}} + \ldots + \frac{\partial \chi^n}{\partial \left\{T^e\right\}} = 0 \qquad (2.13)$$

where n denotes the total number of elements.

In order to differentiate Eqn. (2.12) with respect to $\left\{T^e\right\}$ we make use of the following relationships given in [24]:

$$\frac{\partial}{\partial\left\{T^e\right\}} \int_{V^e} \frac{1}{2} \left\{T^e\right\}^T \left[B^e\right]^T \left[D^e\right] \left[B^e\right] \left\{T^e\right\} dV$$

$$= \int_{V^e} \left[B^e\right]^T \left[D^e\right] \left[B^e\right] \left\{T^e\right\} dV \qquad (2.14a)$$

$$\frac{\partial}{\partial\left\{T^e\right\}} \int_{V^e} \rho c^e \left[N^e\right] \frac{\partial\left\{T^e\right\}}{\partial t} \left[N^e\right] \left\{T^e\right\} dV$$

$$= \int_{V^e} \rho c^e \left[N^e\right] \frac{\partial\left\{T^e\right\}}{\partial t} \left[N^e\right]^T dV \qquad (2.14b)$$

$$\frac{\partial}{\partial\left\{T^e\right\}} \int_{S_2^e} \frac{h^e}{2} \left(\left[N^e\right] \left\{T^e\right\}\right)^2 dS = \int_{S_2^e} h^e \left[N^e\right]^T \left[N^e\right] \left\{T^e\right\} dS \qquad (2.14c)$$

$$\frac{\partial}{\partial\left\{T^e\right\}} \int_{S_2^e} h^e T_\infty \left[N^e\right] \left\{T^e\right\} dS = \int_{S_2^e} h^e T_\infty \left[N^e\right]^T dS \qquad (2.14d)$$

$$\frac{\partial}{\partial\left\{T^e\right\}} \int_{S_2^e} \frac{\sigma\epsilon}{5} \left(\left[N^e\right] \left\{T^e\right\}\right)^5 dS = \int_{S_2^e} \sigma\epsilon \left[N^e\right]^T \left(\left[N^e\right] \left\{T^e\right\}\right)^4 dS \qquad (2.14e)$$

$$\frac{\partial}{\partial\left\{T^e\right\}} \int_{S_2^e} \frac{h^e}{2} T_\infty^2 \, dS = 0 \qquad (2.14f)$$

and

$$\frac{\partial}{\partial\left\{T^e\right\}} \int_{S^2} \sigma\epsilon \, T_\infty^4 \left[N^e\right] \left\{T^e\right\} dS = \int_{S_2^e} \sigma\epsilon \, T_\infty^4 \left[N^e\right]^T dS \qquad (2.14g)$$

Substituting these relationships into Eqn. (2.12) and adding up the contributions of each element as per Eqn. (2.13), we get

$$\frac{\partial \chi}{\partial \{T^e\}} = \sum_{e=1}^{n} \left[\int_{V^e} [B^e]^T [D^e] [B^e] \{T^e\} \, dV + \int_{V^e} \rho c^e [N^e] \frac{\partial \{T^e\}}{\partial t} [N^e]^T \, dV + \int_{S_2^e} h^e [N^e]^T [N^e] \{T^e\} \, dS - \int_{S_2^e} h^e T_\infty [N^e]^T \, dS + \int_{S_2^e} \sigma \epsilon [N^e]^T \left([N^e] \{T^e\} \right)^4 dS - \int_{S_2^e} \sigma \epsilon T_\infty^4 [N^e]^T \, dS \right] = 0 . \quad (2.15)$$

The expression for the elemental capacitance matrix $[CP^e]$ can be expressed as [24]

$$[CP^e] = \int_{V^e} \rho c^e [N^e]^T [N^e] \, dV . \quad (2.16a)$$

The elemental conduction matrix $[K^e]$ can be expressed as

$$[K^e] = \int_{V^e} [B^e]^T [D^e] [B^e] \, dV + \int_{S_2^e} h^e [N^e]^T [N^e] \, dS \quad (2.16b)$$

The force vector due to convection can be expressed as

$$\{F_c^e\} = \int_{S_2^e} h^e T_\infty [N^e]^T \, dS \quad (2.16c)$$

and the force vector due to radiation can be written as

$$\left\{F_r^e\right\} = \int_{S_2^e} \sigma\epsilon\, T_\infty^4 \left[N^e\right]^T dS - \int_{S_2^e} \sigma\epsilon \left[N^e\right] \left(\left[N^e\right]\left\{T^e\right\}^4\right) dS \quad (2.16d)$$

Substituting these expressions for the elemental matrices into Eqn. (2.15) and summing up for all the elements we arrive at the following equation for the global matrices

$$\left[CP^G\right] \frac{\partial\left\{T^G\right\}}{\partial t} + \left[K^G\right]\left\{T^G\right\} = \left\{F_c^G\right\} + \left\{F_r^G\right\} \quad (2.17)$$

The expressions for the elemental matrices $\left[CP^e\right]$, $\left[K^e\right]$, $\left\{F_c^e\right\}$ and $\left\{F_r^e\right\}$ for the case of a triangular element are given in Appendix A.

From Appendix A, one can clearly see that upon assembling the elemental matrices, the resultant global system of equations, Eqn. (2.17), is a non-linear set of partial differential equations because of the radiation term which introduces non-linearity in this system. To solve such a system of equations, one of the ways would be to transform these equations into a system of non-linear algebraic equations using the Crank-Nicolson finite difference method which is unconditionally stable and is widely used by researchers.

Thus the first derivative of the nodal temperature vector between the points using this method in the time domain can be expressed as

$$\frac{d\left\{T^G\right\}_t}{dt} = \frac{\left\{T^G\right\}_{t+\frac{\Delta t}{2}} - \left\{T^G\right\}_{t-\frac{\Delta t}{2}}}{\Delta t}, \quad (2.18)$$

here Δt is the time step.

The expressions for $\left\{T^G\right\}_t$ and $\left\{F^G\right\}_t$ can also be written as

$$\left\{T^G\right\}_t = \frac{\left\{T^G\right\}_{t+\frac{\Delta t}{2}} + \left\{T^G\right\}_{t-\frac{\Delta t}{2}}}{2} \tag{2.19}$$

and

$$\left\{F^G\right\}_t = \frac{\left\{F^G\right\}_{t+\frac{\Delta t}{2}} + \left\{F^G\right\}_{t-\frac{\Delta t}{2}}}{2} \tag{2.20}$$

Substitution of Eqns. (2.18), (2.19) and (2.20) into Eqn. (2.17) results in the following equation

$$\begin{aligned}
&\frac{1}{\Delta t}\left[CP^G\right]\left\{T^G\right\}_{t+\frac{\Delta t}{2}} - \frac{1}{\Delta t}\left[CP^G\right]\left\{T^G\right\}_{t-\frac{\Delta t}{2}} \\
&+ \frac{1}{2}\left[K^G\right]\left\{T^G\right\}_{t+\frac{\Delta t}{2}} + \frac{1}{2}\left[K^G\right]\left\{T^G\right\}_{t-\frac{\Delta t}{2}} \\
&= \frac{1}{2}\left\{F_c^G\right\}_{t+\frac{\Delta t}{2}} + \frac{1}{2}\left\{F_c^G\right\}_{t-\frac{\Delta t}{2}} + \frac{1}{2}\left\{F_r^G\right\}_{t+\frac{\Delta t}{2}} \\
&+ \frac{1}{2}\left\{F_r^G\right\}_{t-\frac{\Delta t}{2}}
\end{aligned} \tag{2.21}$$

In the above equation, the unknown terms are the nodal temperature vector $\left\{T^G\right\}$ and the vectors $\left\{F_c^G\right\}$ and $\left\{F_r^G\right\}$ at time $t + \frac{\Delta t}{2}$. All other vectors and matrices for the previous time instant are known. Thus, Eqn. (2.21) can be arranged as

$$\begin{aligned}
&\left(\left[K^G\right] + \frac{2}{\Delta t}\left[CP^G\right]\right)\left\{T^G\right\}_{t+\frac{\Delta t}{2}} = \left(\frac{2}{\Delta t}\left[CP^G\right] - \left[K^G\right]\right) \\
&\left\{T^G\right\}_{t-\frac{\Delta t}{2}} + \left\{F_c^G\right\}_{t+\frac{\Delta t}{2}} + \left\{F_c^G\right\}_{t-\frac{\Delta t}{2}} + \left\{F_r^G\right\}_{t+\frac{\Delta t}{2}} + \left\{F_r^G\right\}_{t-\frac{\Delta t}{2}}
\end{aligned} \tag{2.22}$$

Since the nodal temperature vector $\left\{T^G\right\}$ and the force vectors due to convection and radiation at time $t - \frac{\Delta t}{2}$ are known, Eqn. (2.22)

can be rewritten as

$$\left(\left[K^G\right] + \frac{2}{\Delta t}\left[CP^G\right]\right)\left\{T^G\right\}_{t+\frac{\Delta t}{2}} = \left\{A_1\right\} + \left\{F_c^G\right\}_{t+\frac{\Delta t}{2}} + \left\{F_r^G\right\}_{t+\frac{\Delta t}{2}} \quad (2.23)$$

The vector $\left\{A_1\right\}$ is known at this stage. On the right hand side of Eqn. (2.23) the vectors $\left\{F_c^G\right\}_{t+\frac{\Delta t}{2}}$ and $\left\{F_r^G\right\}_{t+\frac{\Delta t}{2}}$ are to be evaluated using the nodal temperatures at time $t + \frac{\Delta t}{2}$. One of the ways to solve Eqn. (2.23) for the nodal temperatures would be by making use of an iteration scheme. In this scheme, one assumes a nodal temperature vector $\left\{T^G\right\}$ at time $t + \frac{\Delta t}{2}$, which can be same as the nodal temperature vector at time $t - \frac{\Delta t}{2}$, and substitute this on the right hand side of Eqn. (2.23). This results in the evaluation of the vectors $\left\{F_c^G\right\}_{t+\frac{\Delta t}{2}}$ and $\left\{F_r^G\right\}_{t+\frac{\Delta t}{2}}$ at these assumed temperatures.

At this stage Eqn. (2.23) reduces to

$$\left(\left[K^G\right] + \frac{2}{\Delta t}\left[CP^G\right]\right)\left\{T^G\right\}_{t+\frac{\Delta t}{2}} = \left\{A_2\right\} \quad (2.24)$$

where $\left\{A_2\right\}$ is now known.

This system of algebraic equations, Eqn. (2.24), can now be solved for the unknown nodal temperature vector $\left\{T^G\right\}_{t+\frac{\Delta t}{2}}$. The calculated nodal temperatures are now compared to the assumed nodal temperatures and if they do not meet the convergence criteria, then the calculated nodal temperature vector becomes the assumed nodal temperature vector for the next iteration. In this way the transient nodal temperatures in the airfoil cross-section of the turbine blade can be determined.

Once the transient temperature distribution is known, the transient temperature gradients along the x and y directions can be calculated by making use of Eqn. (2.11d) for a triangular element.

2.2.2 The Transient Thermal Stress Determination

The variation of temperature across the cross-section of a blade causes thermal stresses along the x, y and z directions respectively. It has been established in [6] that all stress components other than σ_z are negligible in such situations. The relationship between σ_z and the elemental temperature, T_{av} (the average temperature of the three nodes of an element), can be written in the form [25]

$$\sigma_z = E \left[x_c \frac{\int_{A^e} E\, x_c\, \Delta T_{av}\, dA^e}{\int_{A^e} E\, x_c^2\, dA^e} + y_c \frac{\int_{A^e} E\, \alpha\, \Delta T_{av}\, dA^e}{\int_{A^e} E\, y_c^2\, dA^e} + \frac{\int_{A^e} E\, \alpha\, \Delta T_{av}\, dA^e}{\int_{A^e} E\, dA^e} - \alpha\, \Delta T_{av} \right] \qquad (2.25)$$

This equation can be expressed in the summation form as

$$\sigma_z = E(T) \left[\frac{\sum_{e=1}^{n} A^e\, E(T)\, \alpha(T)\, \Delta T_{av}}{\sum_{e=1}^{n} A^e\, E(T)} \right.$$

$$+ x_c \frac{\sum_{e=1}^{n} A^e E(T)\ \alpha(T)\ \Delta T_{av}\ x_c^e}{\sum_{e=1}^{n} A^e E(T)\ (x_c^e)^2}$$

$$+ y_c \frac{\sum_{e=1}^{n} A^e E(T)\ \alpha(T)\ \Delta T_{av}\ y_c^e}{\sum_{e=1}^{n} E(T)\ (y_c^e)^2} - \alpha(T)\ \Delta T_{av} \Bigg] \qquad (2.26)$$

In this equation, the modulus of elasticity, $E(T)$, and the coefficient of thermal expansion $\alpha(T)$, are evaluated at the average temperature of the element. ΔT_{av} for an element is the difference in T_{av} at any instant of time and T_{av} initially when there is no stress; in other words, the stress is induced in the material due to the rise in temperature from the stress free state. In this way the thermal stress, σ_z, can be calculated at different instants of time.

2.3 Numerical Example

To illustrate the theory developed in Section 2.2, the heat transfer process within a turbine blade was studied on a blade made of MAR-M200, which is a superalloy of nickel, and widely used in the manufacturing of aircraft gas turbine blades. A cross-section of this blade is shown in the Fig. 2.1. In order to carry out the finite element analysis of this blade, the airfoil cross-section was divided into 174 linear triangular elements. This discretization was finer near both the pressure and suction surfaces and the convergence in the nodal temperatures was achieved by refining both the mesh size and the time increment. A computer program for automatic mesh

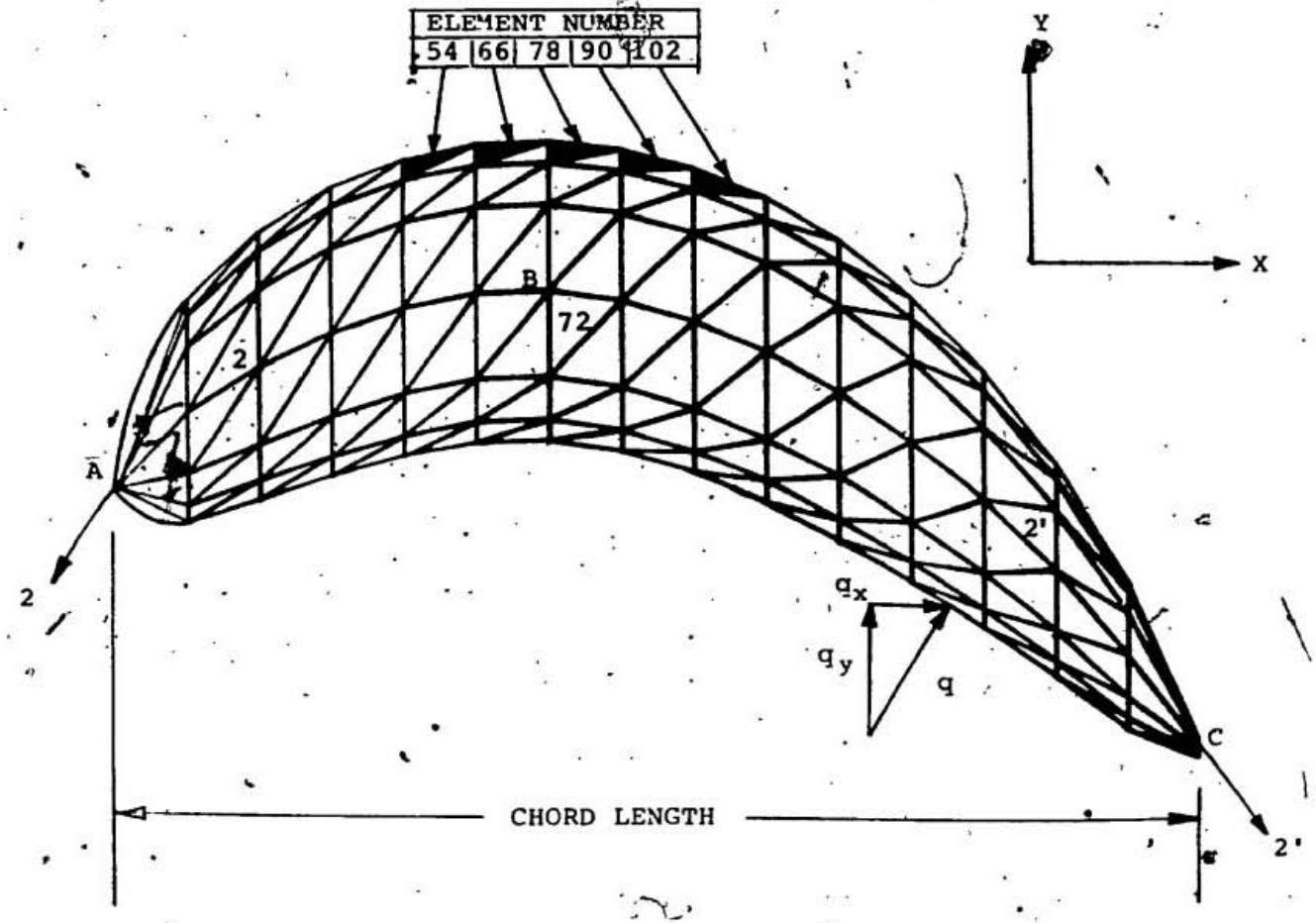

FIG.2.1 THE FINITE ELEMENT DISCRETIZATION OF THE TURBINE BLADE CROSS-SECTION.

generation for this blade was written in order to carry out the convergence studies. The convective heat transfer coefficients were assumed to vary along the pressure and suction surfaces of the blade and these were obtained from [7]. In addition to the variation of the convective heat transfer coefficients along the surface, it was also assumed that they varied with temperature of the surface. The values for these variations were also obtained from [7]. These two variations of the convective heat transfer coefficient are shown in Figs. 2.2 and 2.3. In the present analysis, all the material properties of the blade such as α, E, c, k, etc. were a function of temperature and were obtained from [26]. Table 2.1 shows the values of these parameters at different temperatures.

2.4 The Transient Thermal and Thermoelastic Studies of the Turbine Blade

2.4.1 The Effect of the Radiative Heat Flux on the Temperature Distribution [27]

As we have seen earlier, the radiative heat flux includes terms made up of higher powers of the nodal temperatures, hence its effect would be quite considerable at elevated temperatures. The effect of including the radiative term can be seen in Fig. 2.4 where the hot gases are maintained at 1143°K (870°C). Hence, the time-temperature paths of several points which include the leading edge, the trailing edge and one of the inside nodes (the location of these nodes are shown in Fig. 2.1) are shown. The difference in the temperature values, with and without radiative terms, at any instant of time can be seen in the Fig. 2.4. This figure clearly shows that

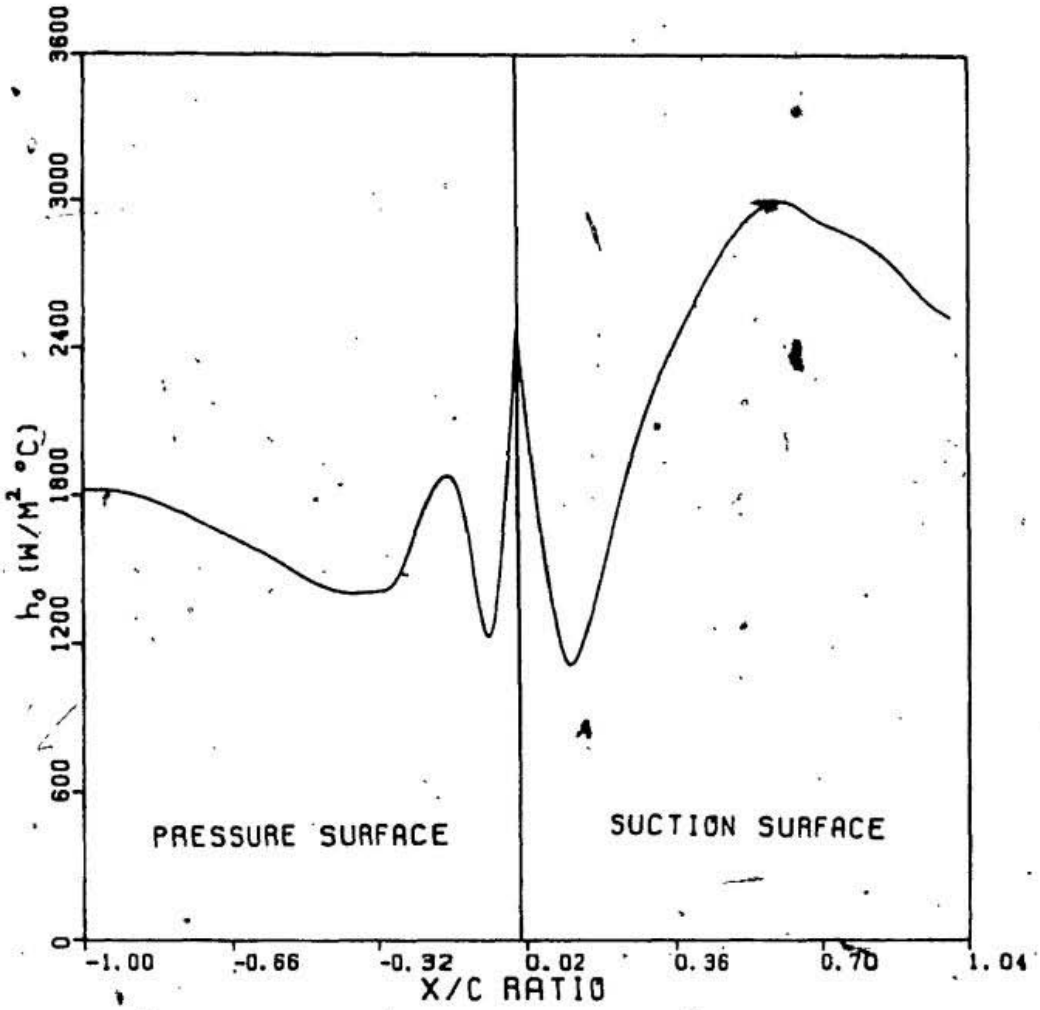

FIG.2.2 HEAT TRANSFER DISTRIBUTION AROUND THE BLADE SURFACE AT FULL LOAD OPERATION. [7]

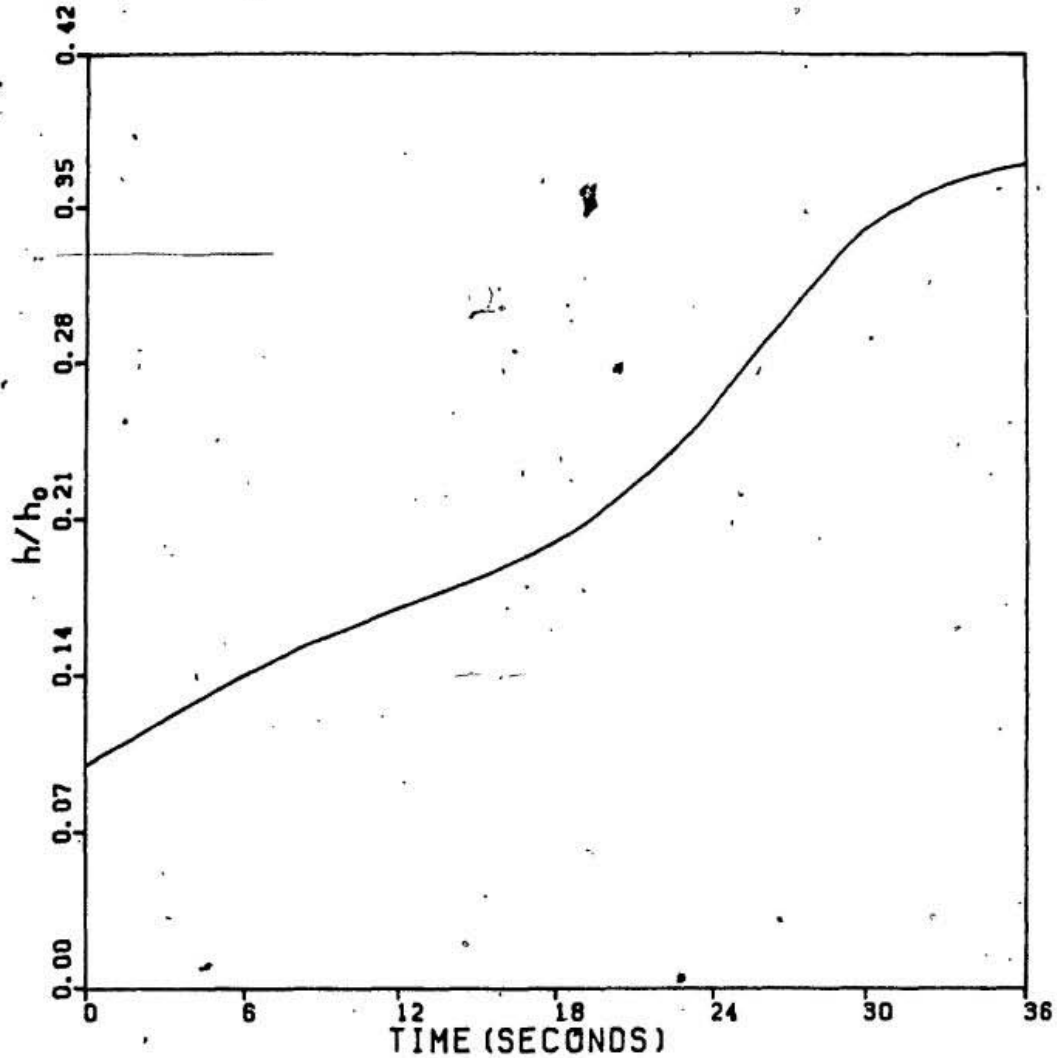

FIG.2.3 HEAT TRANSFER COEFFICIENT DURING QUICK START AS A FUNCTION OF TIME.[7]

Table 2.1

The Variation of the Material Properties of the Blade with Temperature

(ρ = 8526 Kg/m^3)

Temperature (^{o}C)	E (GPa)	σ yield (MPa)	α (μm/m^{o}k)	c (J/kg)	K (W/m^{o}k)
21	220	840	11.9	400	12.7
93	215	842	12.07	400	13.0
205	215	844	12.07	395	13.5
315	195	846.3	12.4	420	13.8
425	190	848.4	12.8	440	15.1
540	185	850	13.1	420	15.2
650	175	855	13.5	460	17.3
760	170	840	14.0	480	14.0
870	160	760	14.8	500	21.6
980	145	470	15.8	525	24.9

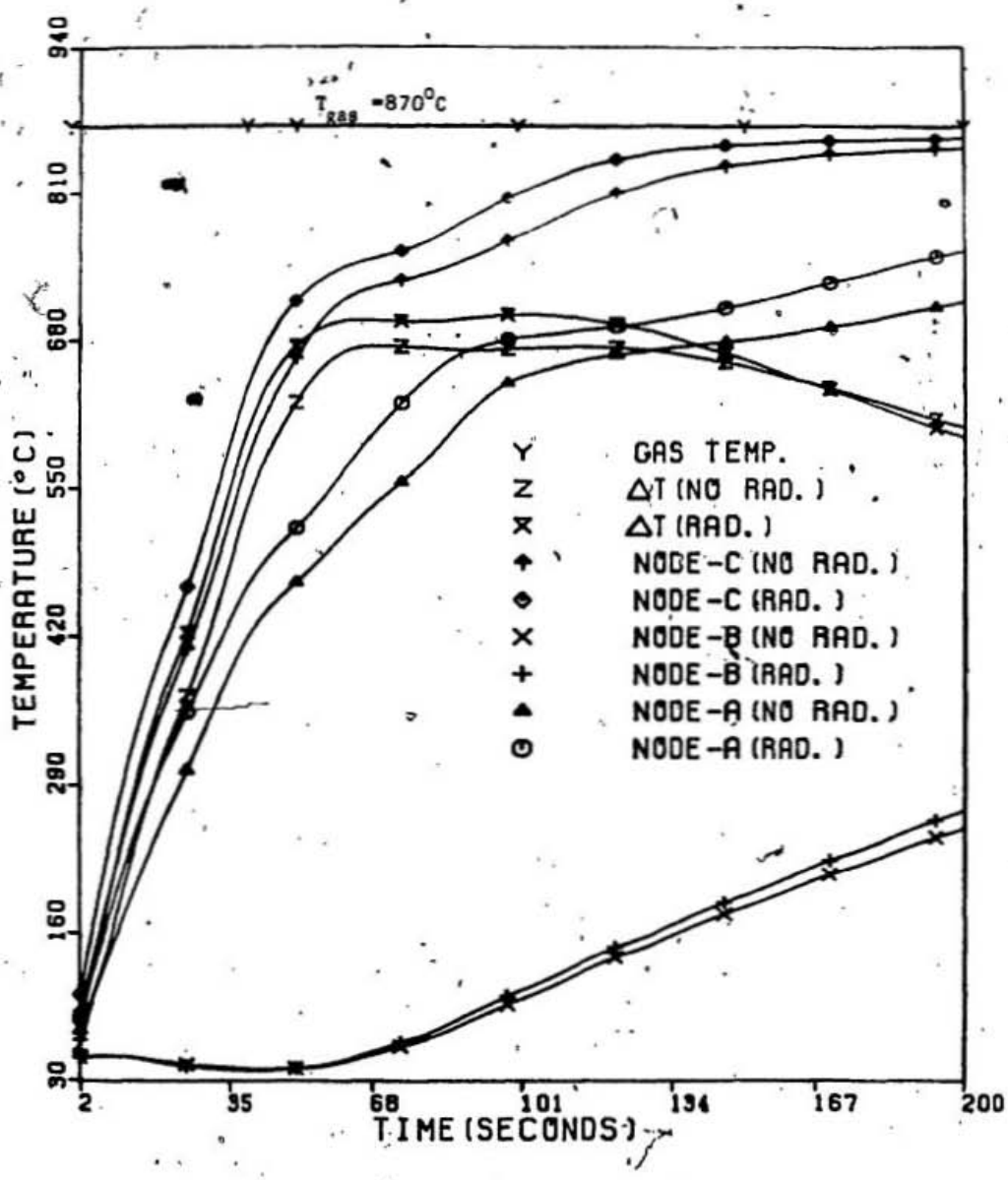

FIG.2.4 THE TRANSIENT TEMPERATURE DISTRIBUTION WITH AND WITHOUT RADIATION (T_g = 870°C).

one has to include the nonlinear radiative term in the Eqn. (2.2). This figure also shows the variation of ΔT versus time. Here, ΔT corresponds to the maximum difference in temperature between the various nodes at a given instant of time. This was obtained by searching for the maximum and the minimum nodal temperatures at a given instant of time. The ΔT curve reaches a maximum value and then drops down and is an indicator of the differential heating process taking place at various nodes. Further significance of this curve is discussed later on in the Sec. 2.4.3. Furthermore, it is quite clear in this figure that the surface nodes are affected much more by the radiation process than the inner nodes. Since it is established here that radiation plays a very significant role in the transient temperature distribution analysis, hereafter, all further results include the radiative terms.

2.4.2 The Temperature Gradient Distribution across the Airfoil Cross-section of the Turbine Blade [28]

For the two dimensional variation of temperature, the spatial gradients along the x and y directions were also calculated at various instants of time. The study of these gradients give us an idea of the dynamics of the heat transfer process. The variations of the gradients in the x-direction along the pressure surface at six instants of time are shown in Fig. 2.5. Referring to Figs. 2.1 and 2.5, one can see that this gradient changes sign twice (in Fig. 2.5) as we move from the left to the right along the pressure surface. The reason for this change of sign can be understood from the Fig.

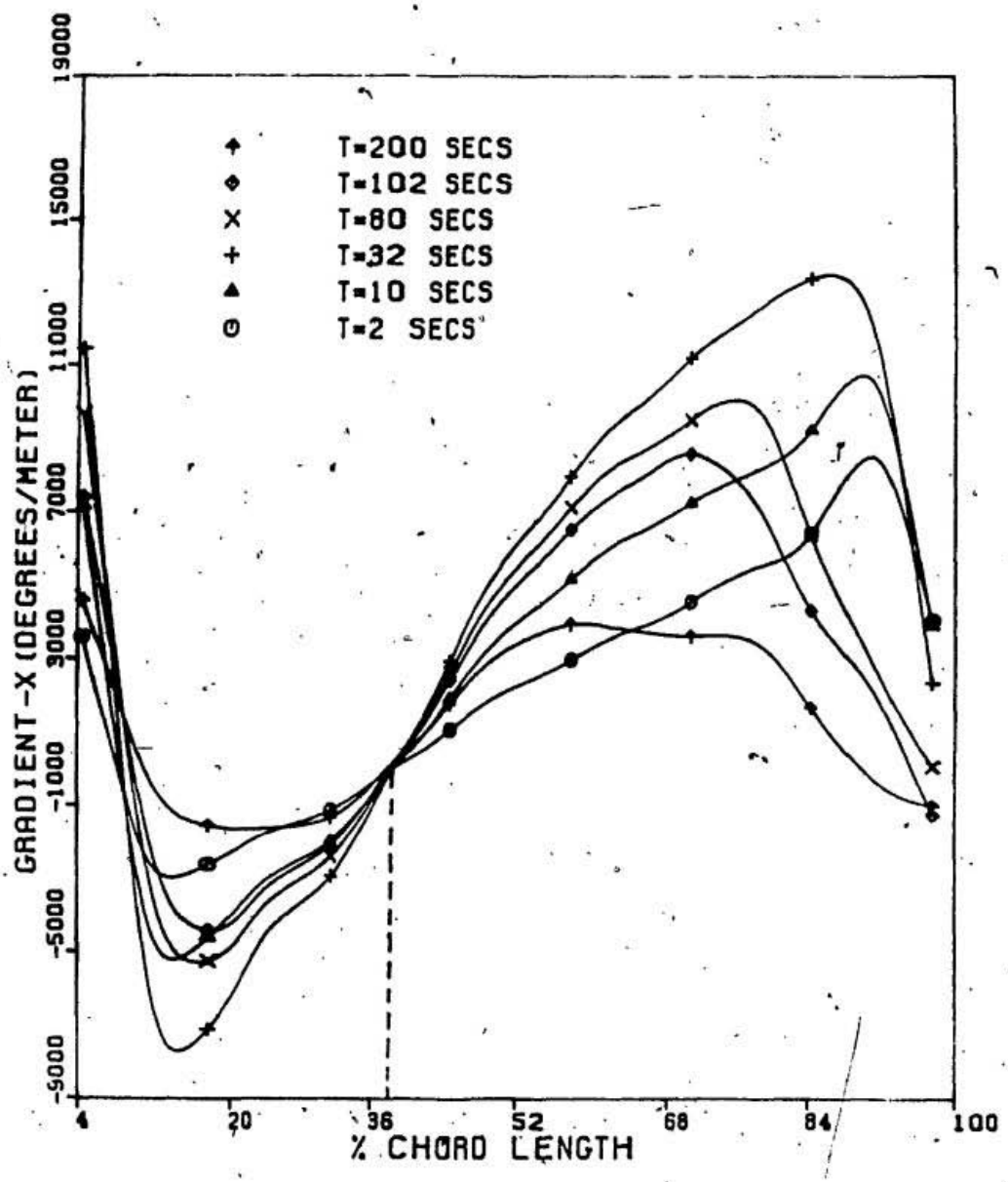

FIG.2.5 THE VARIATION OF THE TEMPERATURE GRADIENT-X ALONG THE PRESSURE SURFACE (Tg = 870°C).

2.1 where the direction of the heat flux at a point is shown normal to the pressure surface. This q can be resolved along the x and y axes as q_x and q_y respectively. The heat flux q_x would correspond to the first term in Eqn. (2.2), and, similarly q_y would correspond to the second term. Whenever q_x is positive the gradient in the x-direction will also be positive; same reasoning holds for the gradient in the y-direction. Since in the Fig. 2.1, q is along the normal to the surface, the points which have positive q_x values would have positive gradients in the x-direction. Similar would be the case for the gradient in the y-direction. This explains the change in sign for these gradients as we go along the surface of the blade.. The magnitudes and directions of these gradients depend on the direction cosines ℓ_x and ℓ_y. Therefore, the maximum value of these gradients would correspond to the points where these direction cosines correspondingly reach their maxima. This figure also shows that this gradient increases in magnitude with time upto t = 32 seconds and then starts decreasing. The peak values of this gradient shift towards the left on the right hand side of this figure and to the right on the left-hand side of this figure. This is because of the finite rate at which the heat flux diffuses into the system. The points near the extreme edges would experience the effect first and this effect will be experienced by the points removed from the ends at later stages. An interesting observation can be made in this figure that the point corresponding to 30% chord length has always zero gradient. This is because the heat flux q is parallel to the y-axis here.

The gradients in the y-direction are shown in Fig. 2.6 at various instants of time on the pressure surface. All along this surface these gradients are positive because the direction cosine ℓ_y is positive. Similar to our earlier discussion, the magnitudes of this gradient at a given point on this surface increase upto t = 32 seconds and then decrease. Figs. 2.7 and 2.8 show the gradients along the mid-section 2-2' (shown in Fig. 2.1). Fig. 2.7 shows that the x-direction gradients are not severe between 25% and 55% chord length. Between 0 and 25% chord length, the gradients are positive indicating that heat is entering along x-axis and negative between 55% and 100% chord length indicating that heat is entering the blade in the negative x-direction. In Fig. 2.8 at t = 2 seconds, the y-gradients are negative for all elements indicating that the heat flux, q_y, is entering from the suction surface, but with the passage of time at elements away from the leading edge this gradient changes its sign. We also see that the global maximum value of the gradient occurs at t = 102 seconds at 15% chord length. This indicates that there is a delayed response in the occurance of the peak gradients between surface nodes and the internal nodes of the blade due to the effect of the thermal diffusivity.

The Figs. 2.9 and 2.10 show the gradients in the x and y directions respectively at the suction surface. The results shown in these figures are very similar to those discussed earlier.

The above discussion deals with the local gradients at various thicknesses of the airfoil. But there is another gradient called the overall gradient at a particular time instant. This

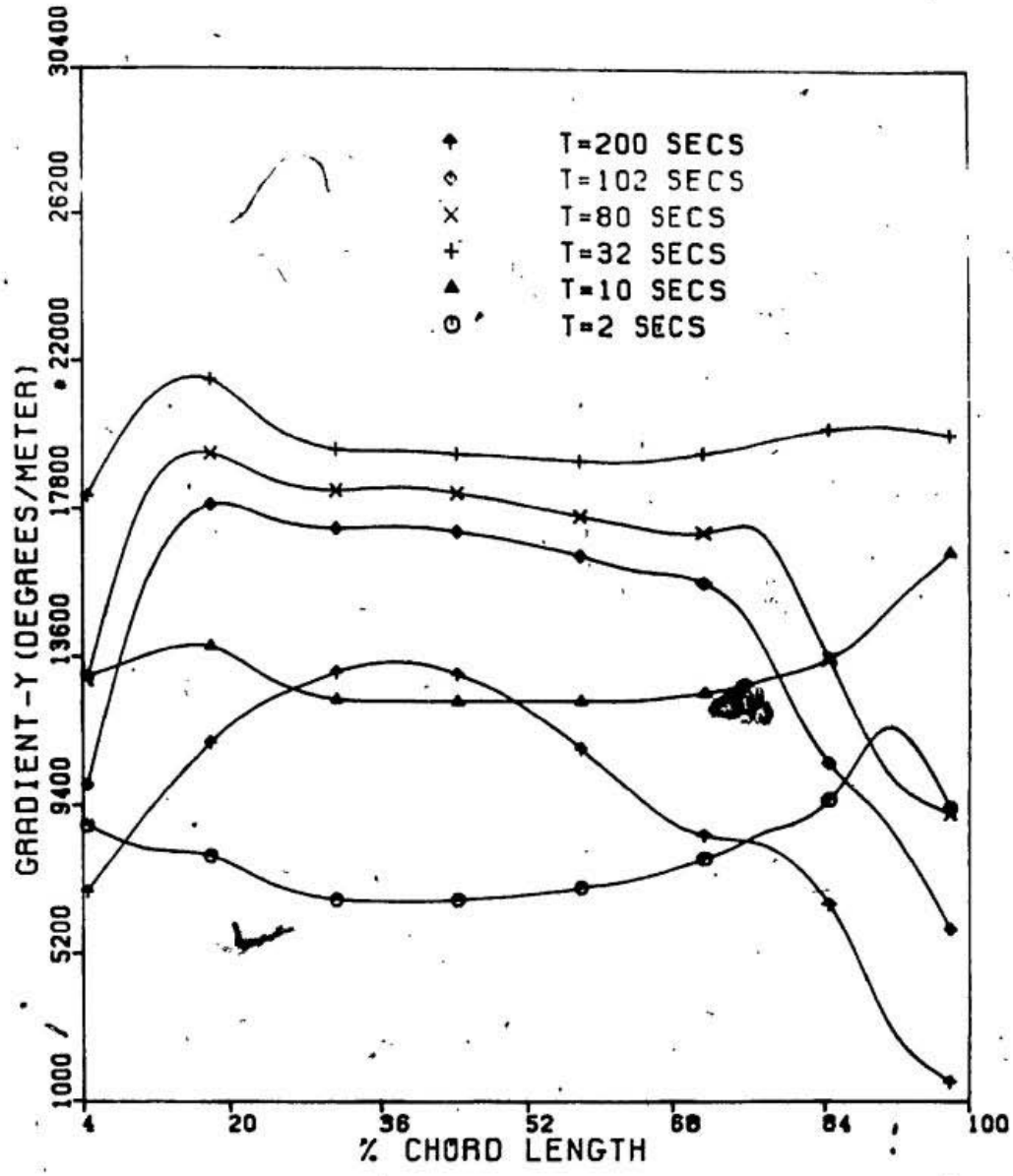

FIG.2.6 THE VARIATION OF THE TEMPERATURE GRADIENT-Y ALONG THE PRESSURE SURFACE (Tg = 870°C).

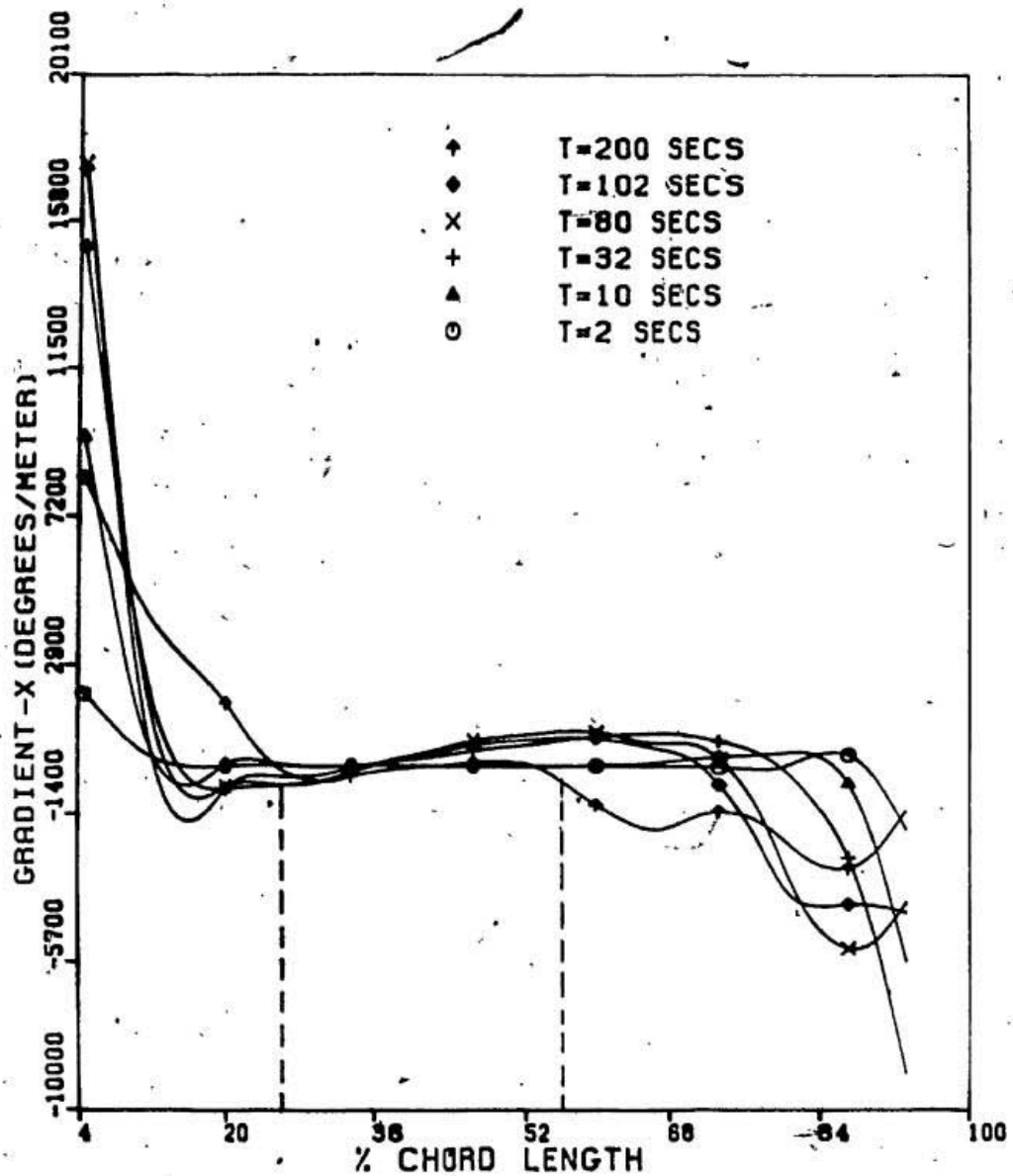

FIG.2.7 THE VARIATION OF THE TEMPERATURE GRADIENT-X ALONG THE MID-SECTION (2-2') AT Tg = 870°C.

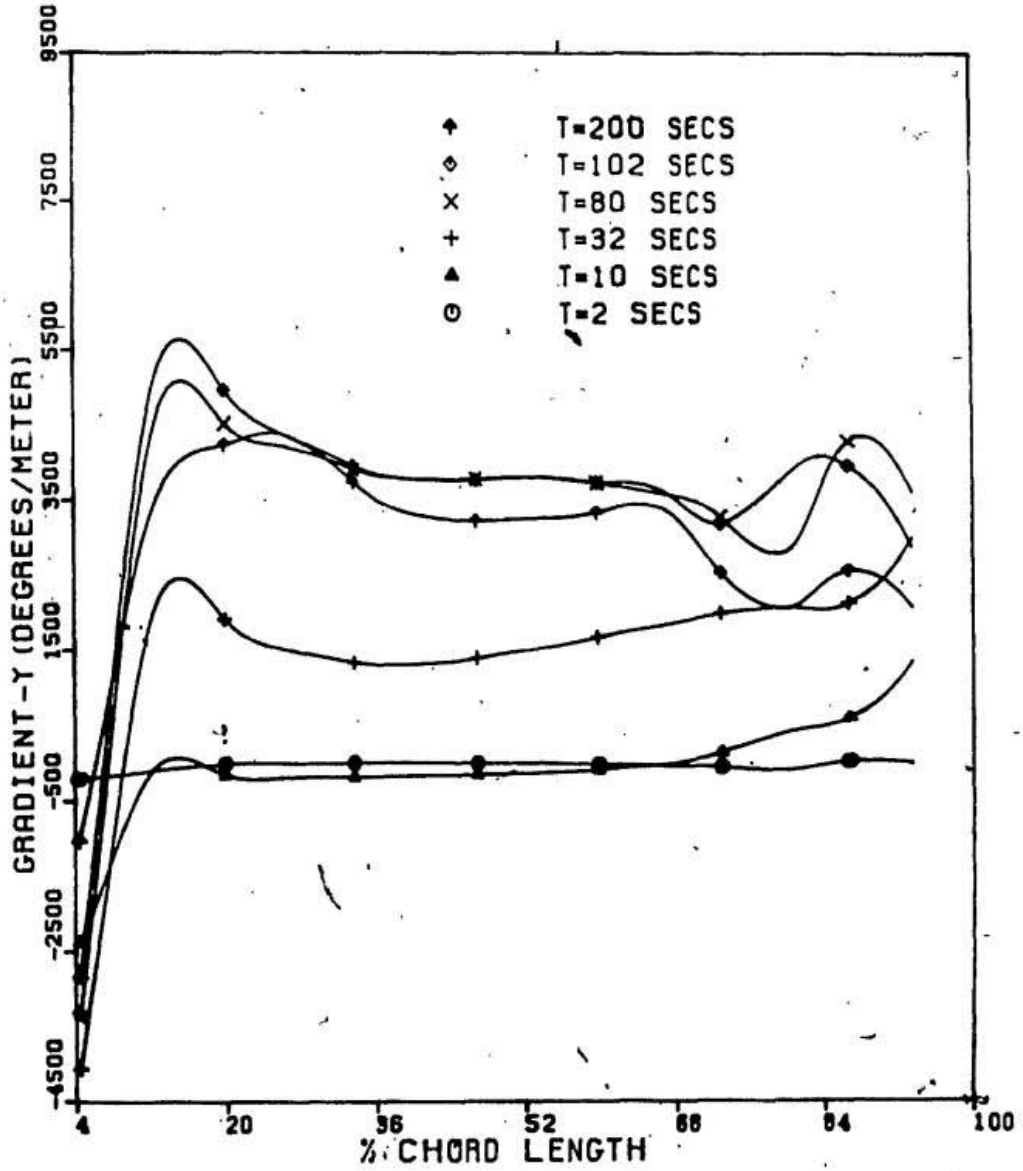

FIG.2.8 THE VARIATION OF THE TEMPERATURE GRADIENT-Y ALONG THE MID-SECTION (2-2') AT T_g = 870°C.

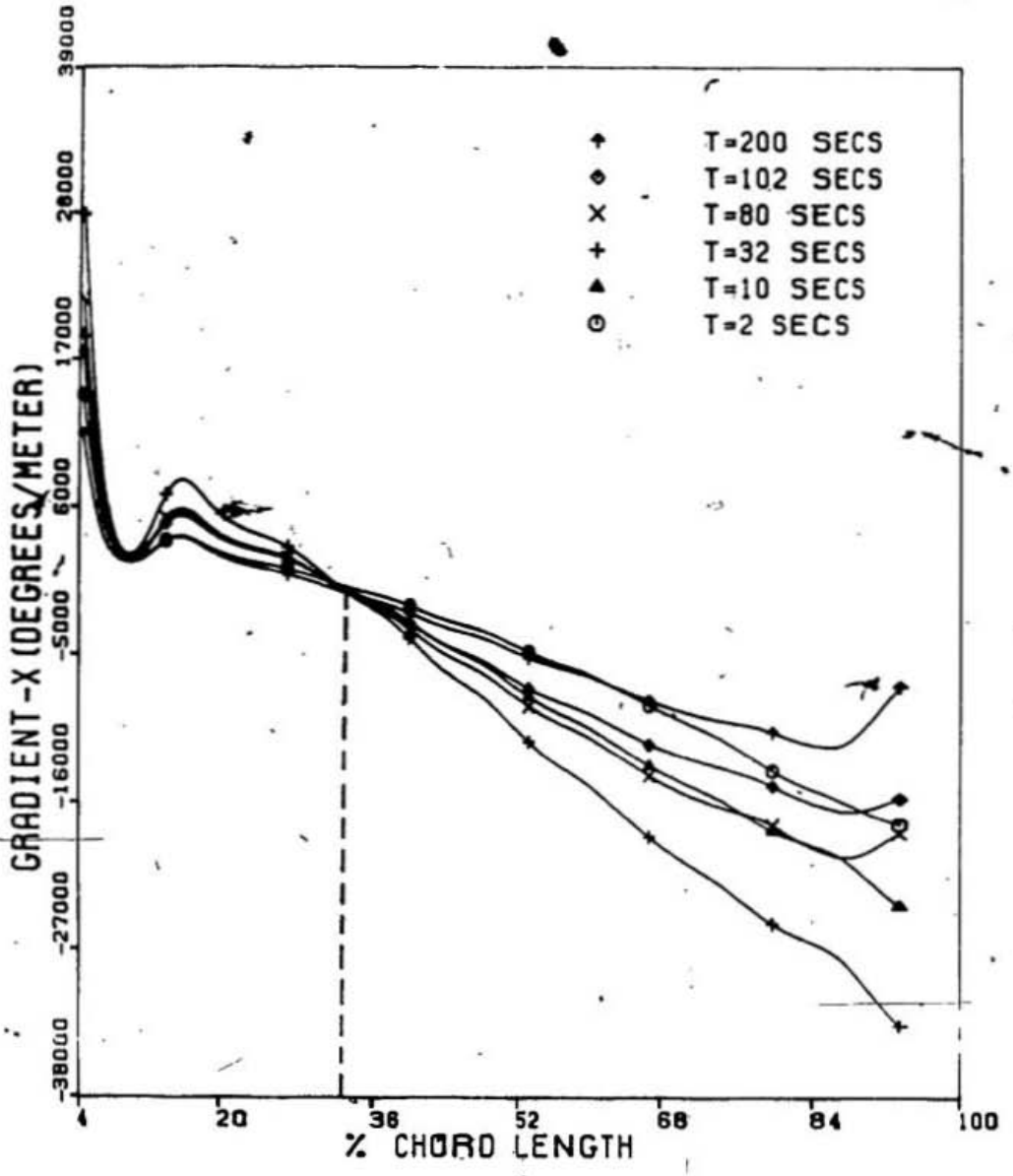

FIG.2.9 THE VARIATION OF THE TEMPERATURE GRADIENT-X ALONG THE SUCTION SURFACE (T_g = 870°C).

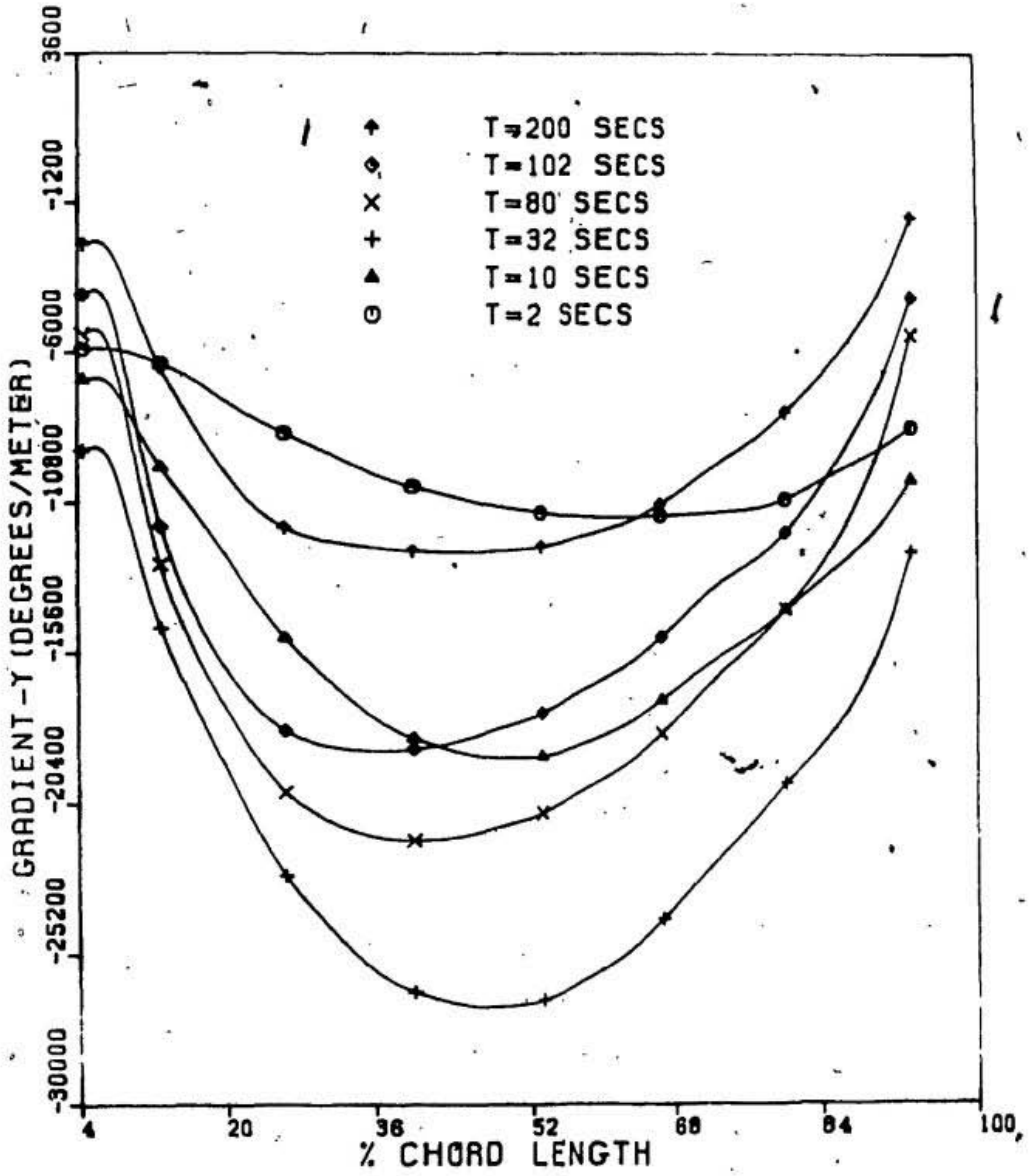

FIG.2.10 THE VARIATION OF THE TEMPERATURE GRADIENT-Y ALONG THE SUCTION SURFACE (Tg = 870°C).

gradient is due to the difference between the maximum and minimum value of the temperature field across the blade section. It is related to ΔT and its significance is discussed in the next subsection.

2.4.3 The Thermal Stress Distribution [27]

As discussed in Section 2.2.2, σ_z is the most important component of the stress vector. These thermal stresses were calculated using Eqn. (2.26). In this equation T_{av} was calculated as the average of the nodal temperature values of individual elements at a time t. The material properties were calculated at this T_{av}. The variations of these normal stresses with time at the leading edge, the trailing edge and at an internal node B (refer to Fig. 2.1) are shown in Fig. 2.11. These stresses have been normalized with respect to the yield stress, $\sigma_{yield}(T)$. This yield stress is a function of temperature; therefore the normalizing values would be different for different elements at a given instant of time. For example, if the elemental temperature at the trailing edge at a given instant of time is different from that at the other two locations, then the normalizing values of the yield stress for these three locations would be different. It was found that the core of the section was in tension and the outside was under compression throughout the heating period. Here, in this figure, the absolute value of the normalized stresses have been plotted as a function of time. Thus, the stress at the location B was tensile and the other two were compressive in nature.

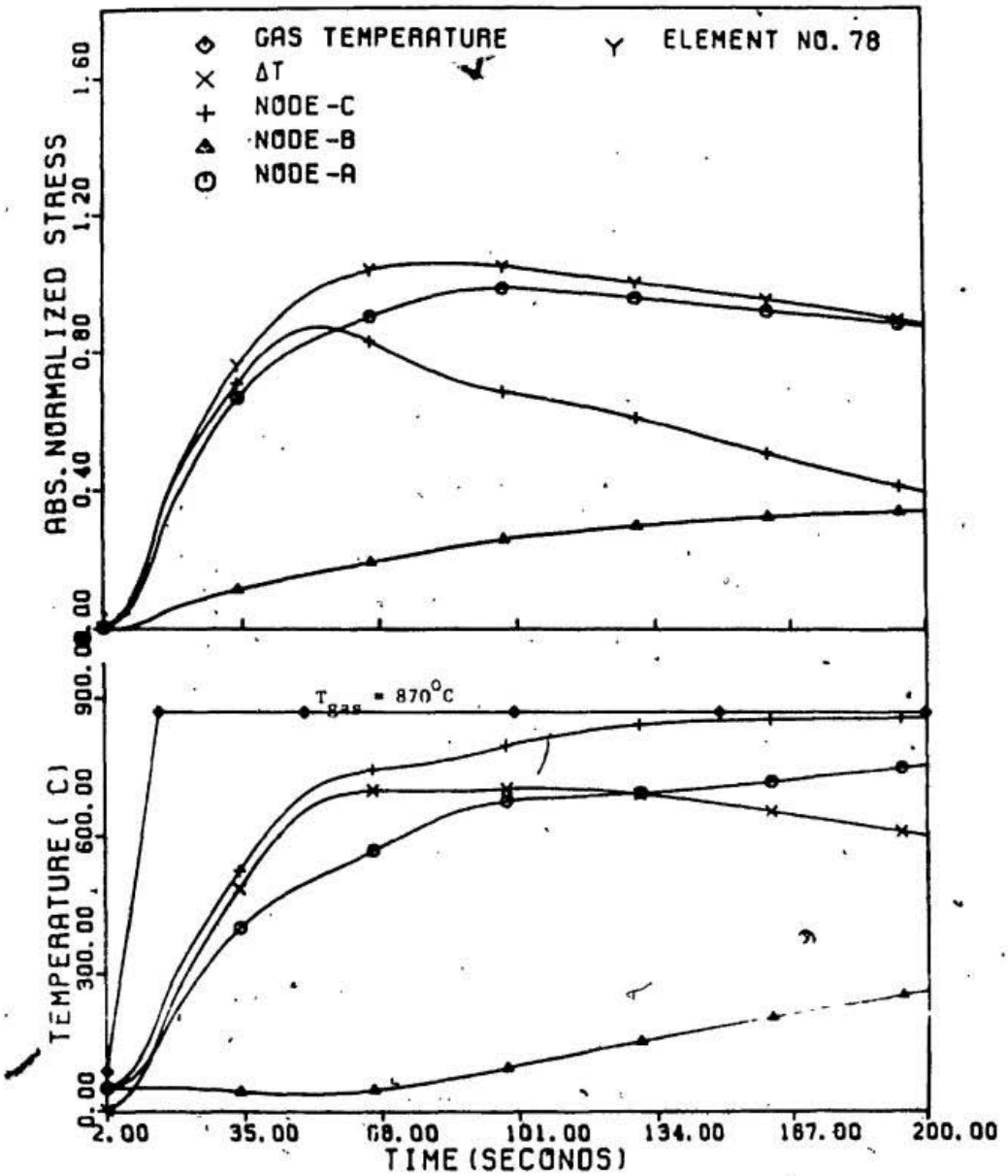

FIG.2.11 THE VARIATION OF THE NORMALIZED STRESSES AND ΔT AS A FUNCTION OF TIME CORRESPONDING TO THE TURBINE HEATING RATE OF 56°C/SEC & FINAL Tg = 870°C.

It is very clear from Fig. 2.11 that the peak value of the stress at the trailing edge occurs at a different instant of time than that of the leading edge. The absolute magnitude of the peak stress is larger for the leading edge as compared to the trailing edge (refer to Fig. 2.11). The results as reported by [7] are similar to those shown here but the calculations do not extend to include the peak occurence at the leading edge (refer to Fig. 2.12). So the maximum stress reported by [7] corresponded to that of the trailing edge. In fact the calculations should have been extended to observe the occurence of the peak at the leading edge because the magnitude of the stress here is more than that at the trailing edge. Secondly, in this Fig. 2.11 there is another curve indicating the maximum stress at any given instant of time. This maximum stress curve was obtained by searching for the absolute maximum value of σ_z among all the elements. It is quite obvious that any design of turbine blades based on the thermal stress analysis should be carried out considering this curve in mind rather than those of the leading or trailing edge as suggested by [6] and [7]. It should be added here that the maximum stress curve in Fig. 2.11 exceeds the value of unity, therefore, this heating path would be an infeasible path. One has to, in this case, modify the T_{gas} versus time curve so that the maximum stresses remain below the yield stress throughout the heating period.

This figure also shows the variation of ΔT versus time. In this figure one can see that the peak stress occurs at time $t = 88$ seconds. At this instant of time a search was made for the element

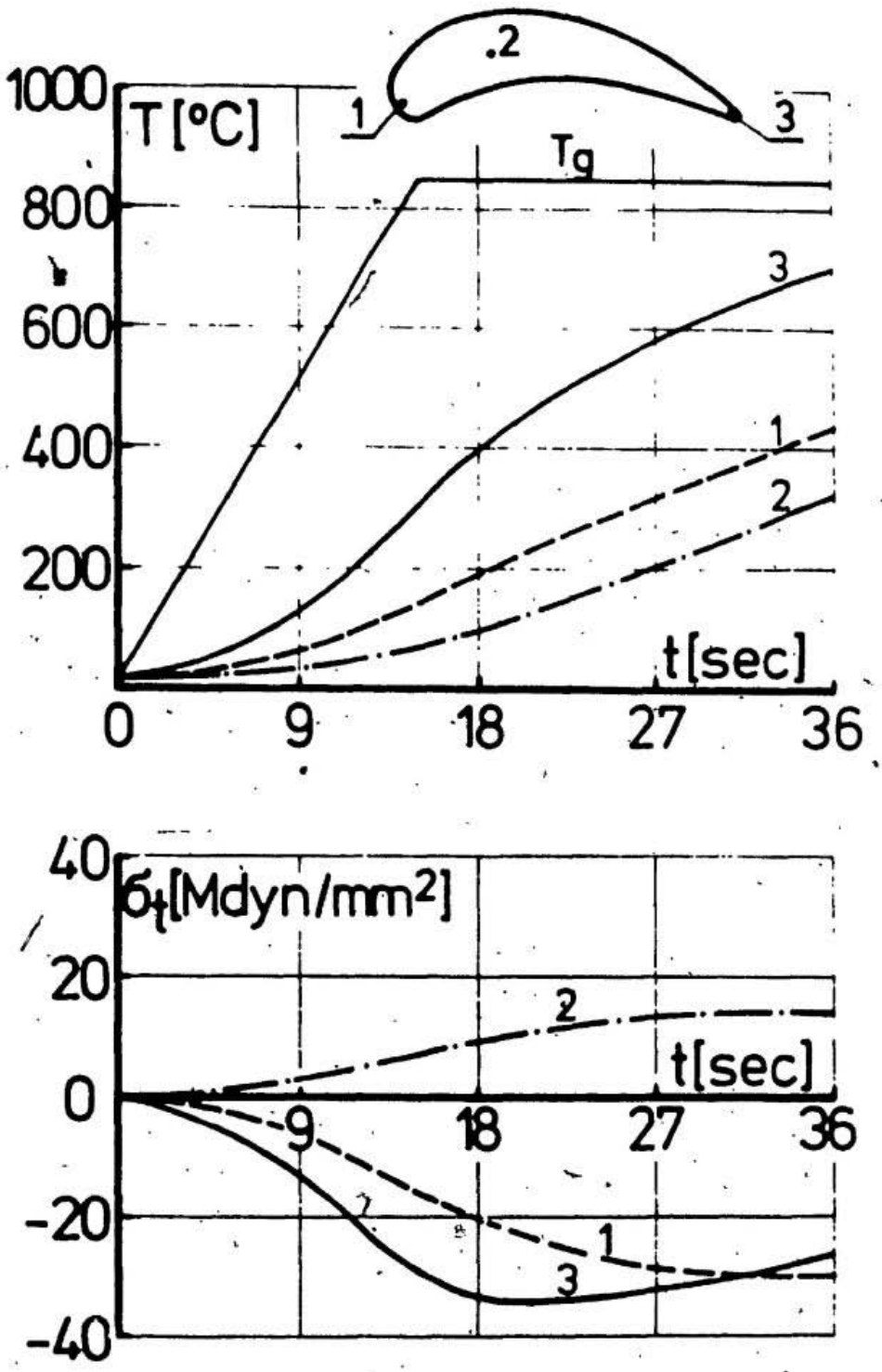

FIG.2.12 CALCULATED TEMPERATURE AND STRESS DISTRIBUTION DURING START FOR LEADING EDGE, MID-PART AND TRAILING EDGE [7]

having the minimum temperature and it was found to be the element number 72 (the locations of this and some other elements are shown in Fig. 2.1). At this instant of time element numbers 54, 66, 78, 90 and 102 were showing high values of σ_z. Table 2.2 shows the parameter ΔT^* which is the difference of temperature between an element having very high stress value and the element no. 72. Similarly, s, is the distance between the centroids of the elements having high stress value and element 72. Obviously $\Delta T^*/s$ would be the temperature gradient between these centroids. From this table one can see that the maximum value of the gradient occurs between the elements 78 and 72. A search was carried out to find the element experiencing maximum σ_z at this instant of time and it was found to be the element no. 78. This shows that it is possible to find the location of the element having maximum stress just from the transient temperature analysis of the solid without doing stress analysis. It is obviously understood that the cause of the stress being discussed here is due to the thermal loading only.

A table similar to Table 2.2 was analysed at time $t = 104$ seconds where the ΔT curve shown in Fig. 2.11, reaches the peak value. The maximum value of gradient $\Delta T^*/s$ at this instant of time was less than at time $t = 88$ seconds when the stress curve had a maximum value. Since the calculation of $\Delta T^*/s$ for every instant of time requires very large number of computations, it would be helpful to roughly have an idea about the instant of time at which the stress curve will have a peak value. This rough approximation can be made from ΔT versus time curve. But the exact instant of time when the

Table 2.2

The Calculation of Overall Temperature Gradient of Elements Having High Stress State (t = 88 seconds)

Parameters	Element Numbers				
	54	66	78	90	102
ΔT^*	406.83	431.28	445.813	454.95	462.36
S (m)	0.005867	0.005434	0.004955	0.005507	0.005776
$\Delta T^*/s$	68990.0	79360.0	89960.0	89700.0	80050.0

stress will reach the peak value can be known only from $\Delta T^*/s$ versus time curve.

The temperature and stress distributions at $t = 88$ seconds are shown in Figs. 2.13 and 2.14. In the Fig. 2.14, the stresses are high at the leading and trailing edges but the highest stresses occur at the suction surface on elements shown in the Fig. 2.1.

2.5 Conclusion

In this chapter calculations were carried out to determine the transient temperature and temperature gradient distributions in a turbine blade using the non-linear finite element analysis. It was shown in this chapter that the temperature gradient analysis helps in better understanding the dynamics of the heat transfer problem. In this chapter the thermoelastic analysis was also carried out to calculate the maximum thermal stress path. The approximate occurence of the peak thermal stress was estimated from ΔT versus time curve. It is also shown that the instant of time when the peak stress will occur can be known from the transient temperature analysis only. However, the magnitude of the peak stress can be known only by carrying out the thermal stress calculation. Thus, the following conclusions can be drawn from this chapter:

1. The radiation effects are quite significant in the transient temperature analysis.
2. The design of the blades based on thermal analysis should be carried out using the transient maximum stress curve.

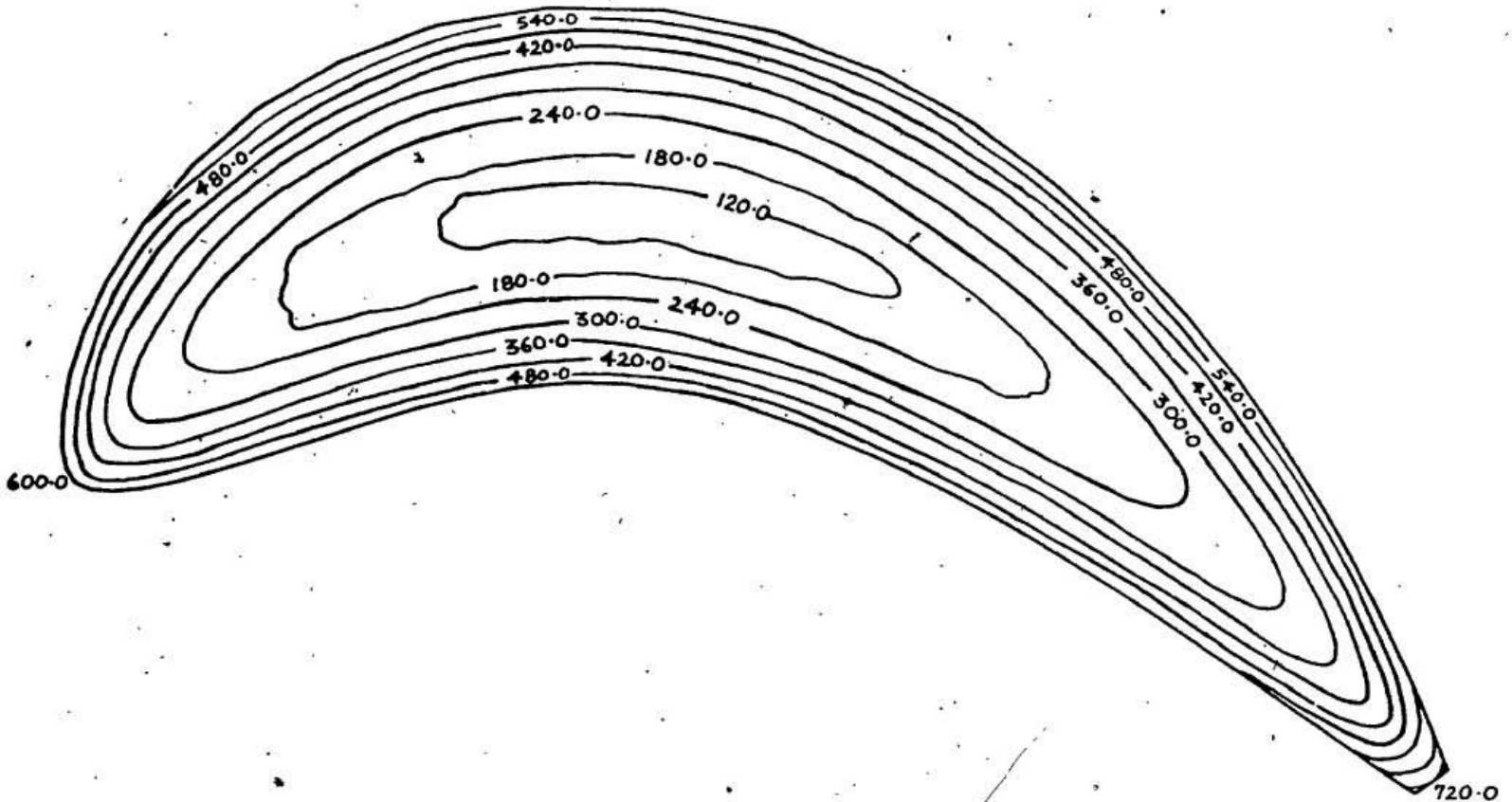

FIG.2.13 THE TEMPERATURE CONTOURS ACROSS THE AIRFOIL SECTION AT t=88 SECONDS.

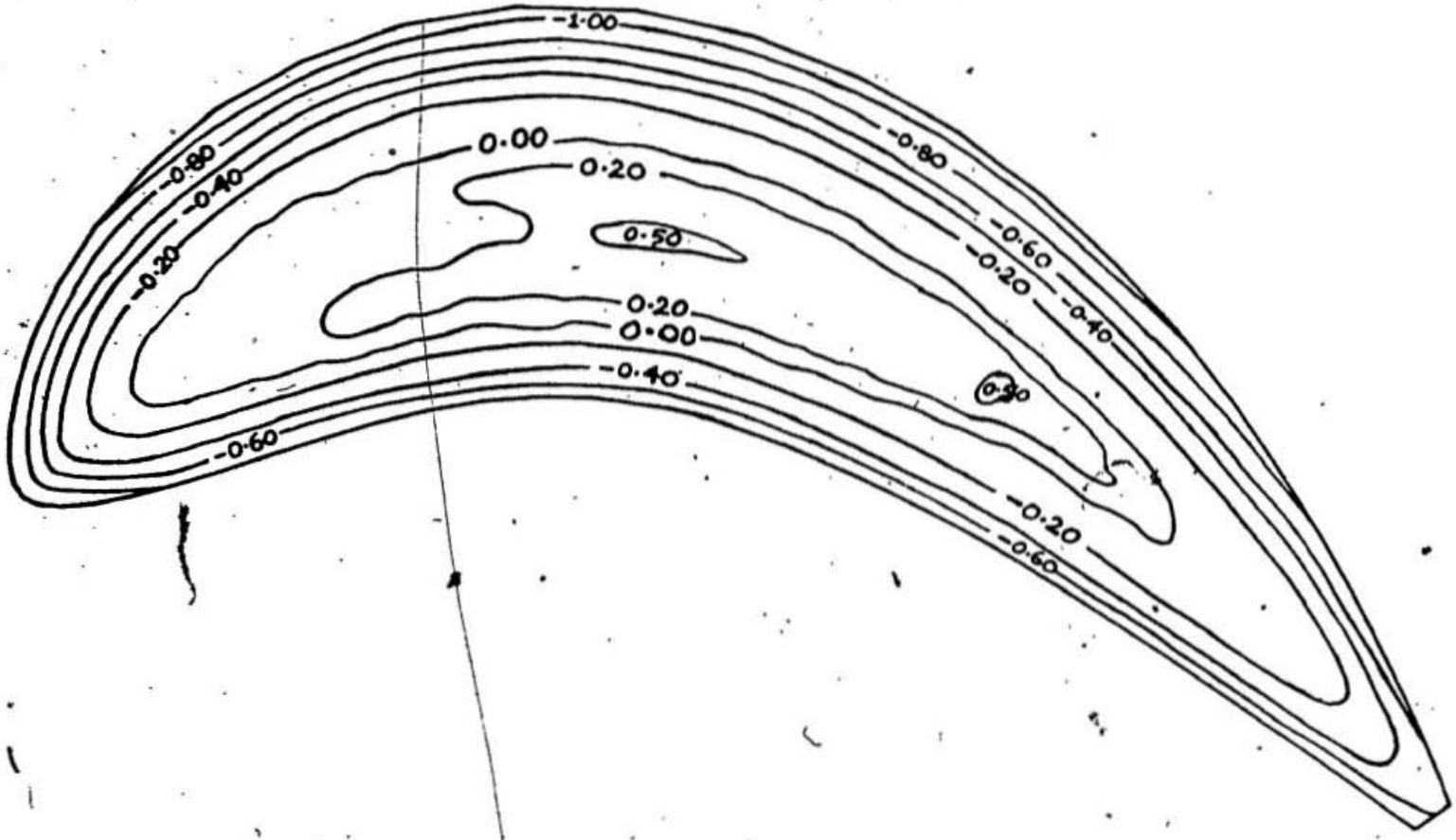

FIG.2.14 THE STRESS CONTOURS ACROSS THE AIRFOIL SECTION AT t=88 SECONDS.

CHAPTER 3

THE FREE VIBRATION ANALYSIS OF THE TURBINE BLADE

3.1 Introduction

The determination of the undamped natural frequencies of a turbine blade is very important in order to design a blade. There are two reasons for doing this; the first reason is that during the start-up the rotor goes through the various blade natural frequencies until it comes to a constant operating speed and secondly, the steady state excitation frequencies should not match with the system natural frequencies. These system natural frequencies are known from the free vibration studies. Another advantage of determining the natural frequencies is that one can obtain the matrix of modal vectors which can then be used in the transient as well as steady state analyses.

In this chapter the free vibration analysis is carried out using curved, solid, C° continuity, 'serendipity', 20-noded isoparametric finite elements. This type of element is chosen because of its versatility in accurately mapping the complex geometry of the turbine blade. The geometry of the blade can be described as one having airfoil cross-section, being asymmetric and pre-twisted and having taper along its length. The two sections of the blade along its length can be seen in Fig. 3.1. Since the size of the global matrices, using finite elements, is quite large, a dynamic matrix reduction scheme has also been used to carry out the

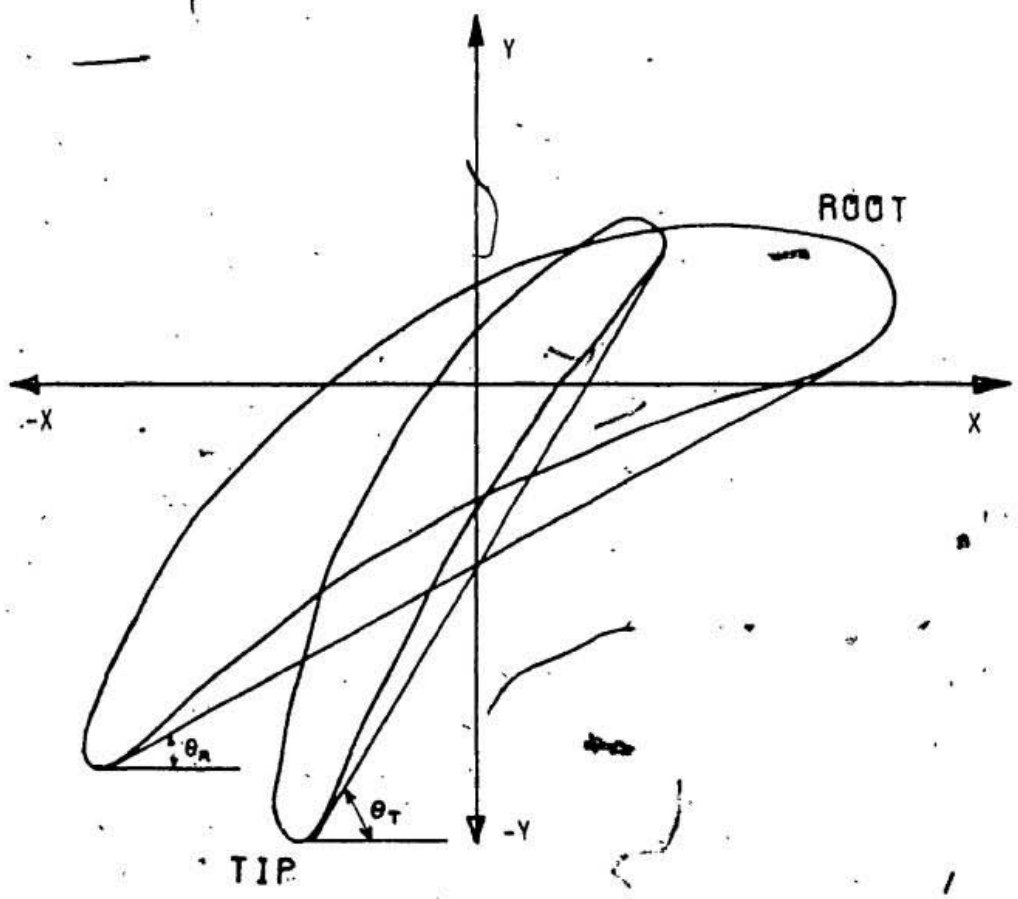

FIG.3.1 THE BLADE AIRFOIL CROSS-SECTIONS AT THE ROOT AND THE TIP.

free vibration analysis. The variation of natural frequencies of the blade with temperature over the entire transient heating period has also been studied in this chapter. In addition, the effect of pre-twist on the natural frequencies has also been studied.

3.2 Mathematical Formulation

3.2.1 The Isoparametric Finite Element Formulation

The most apparent features of isoparametric elements are that their sides may be curved and that they make use of a special coordinate system (ξ, η, ζ) as shown in Fig. 3.2. These features can be understood in the following manner:

1. Nodal degrees of freedom, $\{d\}$, dictate displacements $\{u\ v\ w\}$ of a point in the element. This can be symbolically shown as

$$\begin{Bmatrix} u \\ v \\ w \end{Bmatrix} = [N]\ \{d\} \tag{3.1}$$

2. Nodal local coordinates, $\{c\}$, define global coordinates $\{x\ y\ z\}$ of a point in the element. This can be symbolically shown as

$$\begin{Bmatrix} x \\ y \\ z \end{Bmatrix} = [\bar{N}]\ \{c\} \tag{3.2}$$

The matrices $[N]$ and $[\bar{N}]$ are functions of ξ, η and ζ. An element is isoparametric if for the same node $[N]$ and $[\bar{N}]$ are identical.

The interpolation functions, $[N]$, for the twenty-noded isoparametric element were obtained from [29] and can be expressed as:

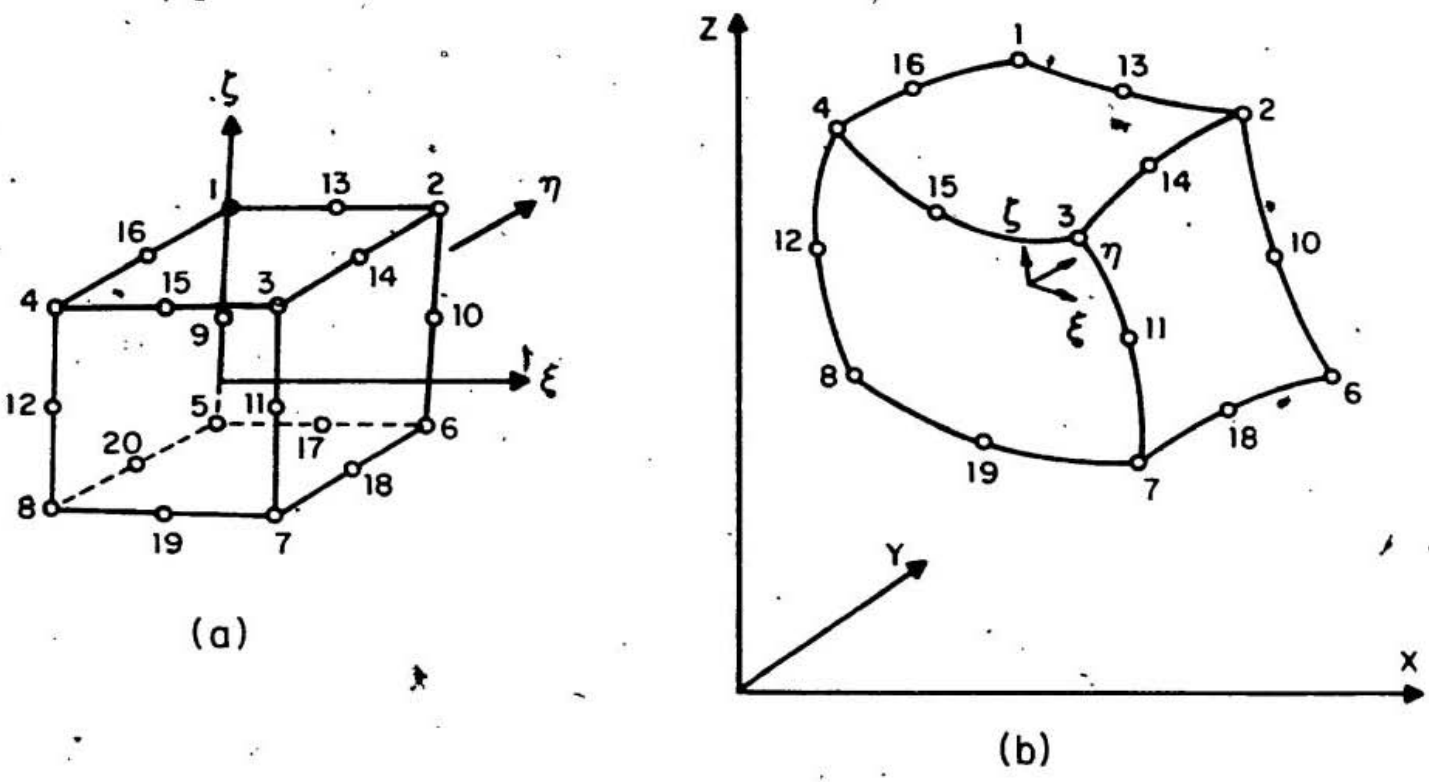

FIG.3.2 The solid isoparametric 'serendipity' 20-noded element (a) Local coordinate system, (b) Global cartesian coordinate system

Corner Nodes:

$$N_i = \frac{1}{8}(1 + \xi\,\xi_i)(1 + \eta\,\eta_i)(1 + \zeta\,\zeta_i)(\xi\,\xi_i + \eta\,\eta_i + \zeta\,\zeta_i - 2) \quad (3.3)$$

Typical Mid-side Node:

$$N_i = \frac{1}{4}(1 - \xi^2)(1 + \eta\,\eta_i)(1 + \zeta\,\zeta_i) \quad (3.4)$$

for the case when $\xi_i = 0$, $\eta_i = \pm 1$ and $\zeta_i = \pm 1$. Here subscript i represent the ith node of the 20-noded element.

In order to evaluate the element stiffness matrix $\left[\dot{K}S^e\right]$ we need to know the matrix $\left[B^e\right]$ which relates the strain in the element to the nodal displacements. The matrix $\left[B^e\right]$ can be evaluated in the following four steps [30]:

1. The strain vector in the global coordinate system can be related to the derivatives of the displacement field as

$$\begin{Bmatrix} \epsilon_x \\ \epsilon_y \\ \epsilon_z \\ \gamma_{xy} \\ \gamma_{xz} \\ \gamma_{yz} \end{Bmatrix} = [P] \begin{Bmatrix} u_{,x} \\ u_{,y} \\ u_{,z} \\ v_{,x} \\ v_{,y} \\ v_{,z} \\ w_{,x} \\ w_{,y} \\ w_{,z} \end{Bmatrix} \quad (3.5)$$

where $u_{,x}$, $u_{,y}$ and $u_{,z}$ represents $\frac{\partial u}{\partial x}$, $\frac{\partial u}{\partial y}$ and $\frac{\partial u}{\partial z}$ respectively. The matrix $[P]$ is given as

$$[P]_{6\times 9} = \begin{bmatrix} 1 & 0 & 0 & 0 & 0 & 0 & 0 & 0 & 0 \\ 0 & 0 & 0 & 0 & 1 & 0 & 0 & 0 & 0 \\ 0 & 0 & 0 & 0 & 0 & 0 & 0 & 0 & 1 \\ 0 & 1 & 0 & 1 & 0 & 0 & 0 & 0 & 0 \\ 0 & 0 & 1 & 0 & 0 & 0 & 1 & 0 & 0 \\ 0 & 0 & 0 & 0 & 0 & 1 & 0 & 1 & 0 \end{bmatrix} \tag{3.6}$$

2. The vector containing derivatives of the displacement field in the global coordinate system can be transformed to the vector containing derivatives of the displacement field in the local coordinate system as

$$\begin{Bmatrix} u_{,x} \\ u_{,y} \\ u_{,z} \\ v_{,x} \\ v_{,y} \\ v_{,z} \\ w_{,x} \\ w_{,y} \\ w_{,z} \end{Bmatrix} = [Q] \begin{Bmatrix} u_{,\xi} \\ u_{,\eta} \\ u_{,\zeta} \\ v_{,\xi} \\ v_{,\eta} \\ v_{,\zeta} \\ w_{,\xi} \\ w_{,\eta} \\ w_{,\zeta} \end{Bmatrix} \tag{3.7}$$

here $u_{,\xi}$, $u_{,\eta}$ and $u_{,\zeta}$ represent $\frac{\partial u}{\partial \xi}$, $\frac{\partial u}{\partial \eta}$ and $\frac{\partial u}{\partial \zeta}$ respectively. The matrix [Q] contains terms of the inverse of the Jacobian matrix [J] and can be shown as

$$
[Q]_{9\times 9} = \begin{bmatrix}
J_{11}^{-1} & J_{12}^{-1} & J_{13}^{-1} & 0 & 0 & 0 & 0 & 0 & 0 \\
J_{21}^{-1} & J_{22}^{-1} & J_{23}^{-1} & 0 & 0 & 0 & 0 & 0 & 0 \\
J_{31}^{-1} & J_{32}^{-1} & J_{33}^{-1} & 0 & 0 & 0 & 0 & 0 & 0 \\
0 & 0 & 0 & J_{11}^{-1} & J_{12}^{-1} & J_{13}^{-1} & 0 & 0 & 0 \\
0 & 0 & 0 & J_{21}^{-1} & J_{22}^{-1} & J_{23}^{-1} & 0 & 0 & 0 \\
0 & 0 & 0 & J_{31}^{-1} & J_{32}^{-1} & J_{33}^{-1} & 0 & 0 & 0 \\
0 & 0 & 0 & 0 & 0 & 0 & J_{11}^{-1} & J_{12}^{-1} & J_{13}^{-1} \\
0 & 0 & 0 & 0 & 0 & 0 & J_{21}^{-1} & J_{22}^{-1} & J_{23}^{-1} \\
0 & 0 & 0 & 0 & 0 & 0 & J_{31}^{-1} & J_{32}^{-1} & J_{33}^{-1}
\end{bmatrix} \qquad (3.8)
$$

The details regarding [J] are given later on in this section (see Eqns. 3.17-3.19)

3. Now, the vector containing derivatives of the displacement field in the local coordinate system can be related to the nodal displacement vector as

$$
\begin{Bmatrix}
u_{,\xi} \\ u_{,\eta} \\ u_{,\zeta} \\ v_{,\xi} \\ v_{,\eta} \\ v_{,\zeta} \\ w_{,\xi} \\ w_{,\eta} \\ w_{,\zeta}
\end{Bmatrix} = [R] \begin{Bmatrix}
d_1 \\ d_2 \\ d_3 \\ . \\ . \\ . \\ . \\ . \\ d_{20}
\end{Bmatrix} \qquad (3.9)
$$

here the matrix [R] contains derivatives of the interpolation functions with respect to the local coordinate system and this matrix can be represented as

$$[R]_{9\times 60} = \begin{bmatrix} \frac{\partial N_1}{\partial \xi} & 0 & 0 & \frac{\partial N_2}{\partial \xi} & 0 & 0 & \frac{\partial N_3}{\partial \xi} & - & - & - & - \\ \frac{\partial N_1}{\partial \eta} & 0 & 0 & \frac{\partial N_2}{\partial \eta} & 0 & 0 & \frac{\partial N_3}{\partial \eta} & - & - & - & - \\ \frac{\partial N_1}{\partial \zeta} & 0 & 0 & \frac{\partial N_2}{\partial \zeta} & 0 & 0 & \frac{\partial N_3}{\partial \zeta} & - & - & - & - \\ 0 & \frac{\partial N_1}{\partial \xi} & 0 & 0 & \frac{\partial N_2}{\partial \xi} & 0 & 0 & - & - & - & - \\ 0 & \frac{\partial N_1}{\partial \eta} & 0 & 0 & \frac{\partial N_2}{\partial \eta} & 0 & 0 & - & - & - & - \\ 0 & \frac{\partial N_1}{\partial \zeta} & 0 & 0 & \frac{\partial N_2}{\partial \zeta} & 0 & 0 & - & - & - & - \\ 0 & 0 & \frac{\partial N_1}{\partial \xi} & 0 & 0 & \frac{\partial N_2}{\partial \xi} & 0 & - & - & - & - \\ 0 & 0 & \frac{\partial N_1}{\partial \eta} & 0 & 0 & \frac{\partial N_2}{\partial \eta} & 0 & - & - & - & - \\ 0 & 0 & \frac{\partial N_1}{\partial \zeta} & 0 & 0 & \frac{\partial N_2}{\partial \zeta} & 0 & - & - & - & - \end{bmatrix} \qquad (3.10)$$

4. Finally the $[B^e]$ matrix for an element can be expressed as

$$[B^e]_{6\times 60} = [P]_{6\times 9}\,[Q]_{9\times 9}\,[R]_{9\times 60} \qquad (3.11)$$

Once the $[B^e]$ matrix is known, the element stiffness matrix $[KS^e]$ can be evaluated as

$$[KS^e] = \int_V [B(x,y,z)]^T\,[D]\,[B(x,y,z)]\,dx\,dy\,dz \qquad (3.12)$$

In case of isoparametric finite elements the shape functions, [N], are defined for the variation of the local coordinate system from +1 to -1. Thus $\xi = \pm 1$, $\eta = \pm 1$ and $\zeta = \pm 1$. For the isoparametric formulation the element stiffness matrix can be expressed as

$$\underset{60\times60}{\left[KS^e\right]} = \int_{-1}^{+1}\int_{-1}^{+1}\int_{-1}^{+1} \underset{60\times6}{[B(\xi,\eta,\zeta)]^T}\ \underset{6\times6}{[D]}\ \underset{6\times60}{[B(\xi,\eta,\zeta)]}\ |J(\xi,\eta,\zeta)|\ d\xi\ d\eta\ d\zeta \qquad (3.13)$$

In Eqn. (3.13) the material property matrix, [D], for a three-dimensional isotropic material can be expressed as

$$[D] = \frac{E(1-\nu)}{(1+\nu)(1-2\nu)} \begin{bmatrix} 1 & \nu/(1-\nu) & \nu/(1-\nu) & 0 & 0 & 0 \\ & 1 & \nu/(1-\nu) & 0 & 0 & 0 \\ & & 1 & 0 & 0 & 0 \\ & & & \frac{1-2\nu}{2(1-\nu)} & 0 & 0 \\ & \text{symmetrical} & & & \frac{1-2\nu}{2(1-\nu)} & 0 \\ & & & & & \frac{1-2\nu}{2(1-\nu)} \end{bmatrix}$$

Similarly, the expression for the consistent mass matrix can be written as

$$\left[M^e\right] = \int_V [N]^T\ \rho\ [N]\ dx\ dy\ dz \qquad (3.14)$$

In case of isoparametric formulation the consistent mass matrix is evaluated as

$$\underset{60\times60}{\left[M^e\right]} = \int_{-1}^{+1}\int_{-1}^{+1}\int_{-1}^{+1} \underset{60\times3}{[N(\xi,\eta,\zeta)]^T}\ \rho\ \underset{3\times60}{[N(\xi,\eta,\zeta)]}\ |J(\xi,\eta,\zeta)|\ d\xi\ d\eta\ d\zeta \qquad (3.15)$$

The shape function matrix used in the evaluation of the elemental consistent mass matrix $[M^e]$ can be expressed as

$$[N]_{3\times 60} = \begin{bmatrix} N_1 & 0 & 0 & N_2 & 0 & 0 & N_3 & 0 & 0 & - & - & - \\ 0 & N_1 & 0 & 0 & N_2 & 0 & 0 & N_3 & 0 & - & - & - \\ 0 & 0 & N_1 & 0 & 0 & N_2 & 0 & 0 & N_3 & - & - & - \end{bmatrix} \quad (3.16)$$

The Jacobian matrix here relates the derivatives of the displacement field $\{u,v,w\}$ with respect to the local coordinate system $\{\xi,\eta,\zeta\}$ to the derivatives of $\{u,v,w\}$ with respect to the global coordinate system $\{x,y,z\}$. The Jacobian matrix is evaluated by making use of the chain rule of calculus, for example,

$$\frac{\partial u}{\partial \xi} = \frac{\partial u}{\partial x}\frac{\partial x}{\partial \xi} + \frac{\partial u}{\partial y}\frac{\partial y}{\partial \xi} + \frac{\partial u}{\partial z}\frac{\partial z}{\partial \xi} \quad (3.17)$$

where u is a function of x, y and z. Hence, the Jacobian matrix $[J]$ can be expressed as

$$[J] = \begin{bmatrix} \frac{\partial x}{\partial \xi} & \frac{\partial y}{\partial \xi} & \frac{\partial z}{\partial \xi} \\ \frac{\partial x}{\partial \eta} & \frac{\partial y}{\partial \eta} & \frac{\partial z}{\partial \eta} \\ \frac{\partial x}{\partial \zeta} & \frac{\partial y}{\partial \zeta} & \frac{\partial z}{\partial \zeta} \end{bmatrix} \quad (3.18)$$

The element J_{11} of $[J]$ can be written as

$$J_{11} = \frac{\partial x}{\partial \xi} = \frac{\partial}{\partial \xi}\underset{1\times 20}{([N_i]^e]} \underset{20\times 1}{\{x\}^e} \quad (3.19)$$

Here the vector $\{x\}^e$ contains cartesian coordinates of the 20- noded element along the x-direction and $e = 1, 2, \ldots, 20$. Similarly, one can evaluate other elements of the matrix $[J]$.

The evaluation of the element stiffness matrix, Eqn. (3.13), and element mass matrix, Eqn. (3.15), can be achieved by numerically evaluating the volume integral in these equations. One of the most widely used techniques in integrating the elemental matrices in case of isoparametric formulation is by making use of Gaussian quadrature [31]. Since in the present investigation a quadratic polynomial is used to describe each side of the 20-noded element, hence there would be 2 Gauss points on each side of the element. In this way a total of 8 Gauss points within the element were sufficient to integrate each element of the matrices $\left[KS^e\right]$ and $\left[M^e\right]$.

The final expressions for the matrices $\left[KS^e\right]$ and $\left[M^e\right]$ can be written using Gaussian quadrature as

$$\left[KS^e\right] = \sum_{i=1}^{NG}\sum_{j=1}^{NG}\sum_{k=1}^{NG} W_i W_j W_k \left[B(\xi,\eta,\zeta)\right]^T [D] \left[B(\xi,\eta,\zeta)\right] |J(\xi,\eta,\zeta)| \tag{3.20}$$

and

$$\left[M^e\right] = \sum_{i=1}^{NG}\sum_{j=1}^{NG}\sum_{k=1}^{NG} W_i W_j W_k \rho \underset{60\times 3}{\left[N(\xi,\eta,\zeta)\right]^T} \underset{3\times 60}{\left[N(\xi,\eta,\zeta)\right]} |J(\xi,\eta,\zeta)| \tag{3.21}$$

where $NG = 2$ for the case of a 20-noded element, and W_i, W_j and W_k are corresponding weighting functions in the ξ, η and ζ directions respectively.

3.2.2 The Free Vibration Analysis

After the elemental matrices $\left[KS^e\right]$ and $\left[M^e\right]$ are evaluated, they are assembled into global matrices and the dynamic equation of motion is written as

$$\left[M^G\right]\{\ddot{U}\} + \left[C^G\right]\{\dot{U}\} + \left[KS^G\right]\{U\} = \left\{F(t)^G\right\} \qquad (3.22)$$

The natural frequencies of the undamped turbine blade can be obtained by solving the eigenvalue problem.

Since the matrices $\left[KS^G\right]$ and $\left[M^G\right]$ for this three-dimensional problem become very large therefore it is desirable that a coordinate reduction scheme be used to reduce the size of these matrices without any significant loss of accuracy in terms of the lower modes. One of these schemes is the Guyan's reduction technique [32] .

In this dynamic matrix reduction scheme, one makes use of the ratios of the diagonal terms of the stiffness and mass matrices by rearranging these in terms of the ratios KS_{ii}/M_{ii}. In this technique certain degrees of freedom are discarded and these are called the slave degrees of freedom. On the other hand the degrees of freedom which are retained in the reduced matrices are called the masters. The degree of freedom which has the largest KS_{ii}/M_{ii} ratio is selected as the first slave. In this way one can rearrange the inertia and the stiffness matrices depending upon the number of masters and write the dynamic equation of motion in the form

$$\left[\begin{array}{c|c} [M_{mm}] & [M_{ms}] \\ \hline [M_{ms}]^T & [M_{ss}] \end{array}\right]\left[\begin{array}{c} \ddot{U}_m(t) \\ \hline \ddot{U}_s(t) \end{array}\right] + \left[\begin{array}{c|c} [C_{mm}] & [C_{ms}] \\ \hline [C_{ms}]^T & [C_{ss}] \end{array}\right]\left[\begin{array}{c} \dot{U}_m(t) \\ \hline \dot{U}_s(t) \end{array}\right]$$

$$+ \left[\begin{array}{c|c} [KS_{mm}] & [KS_{ms}] \\ \hline [KS_{ms}]^T & [KS_{ss}] \end{array}\right]\left[\begin{array}{c} U_m(t) \\ \hline U_s(t) \end{array}\right] = \left\{\begin{array}{c} F_m(t) \\ \hline F_s(t) \end{array}\right\} \qquad (3.23)$$

The reduced system matrices are obtained using the following equations

$$\left[\overline{M}^G\right]_{m\times m} = [\psi]^T_{m\times n} \left[M^G\right]_{n\times n} [\psi]_{n\times m} \tag{3.24a}$$

$$\left[\overline{KS}^G\right]_{m\times m} = [\psi]^T_{m\times n} \left[KS^G\right]_{n\times n} [\psi]_{n\times m} \tag{3.24b}$$

$$\left[\overline{C}^G\right]_{m\times m} = [\psi]^T_{m\times n} \left[C^G\right]_{n\times n} [\psi]_{n\times m} \tag{3.24c}$$

$$\left\{\overline{F}^G\right\}_{m\times 1} = [\psi]^T_{m\times n} \left\{F^G\right\}_{n\times 1} \tag{3.24d}$$

where the transformation matrix $[\psi]$ is given as

$$[\psi] = \begin{bmatrix} [I] \\ \hline -[KS_{ss}]^{-1} [KS_{ms}]^T \end{bmatrix} \tag{3.25}$$

The variation of the undamped natural frequencies with temperature can be calculated by updating the material property matrix, [D], in Eqn. (3.13) at every time instant and thus calculating the element stiffness matrix, $\left[KS^e\right]$, at every time instant. This $\left[KS^e\right]$ matrix can then be used to solve the characteristic equation and the undamped natural frequencies can be obtained at every time instant.

3.3 Numerical Example

3.3.1 Verification of the Formulation and the Computer Software

In order to test our formulation, an example problem of determining the undamped natural frequencies of a cantilever beam was taken up. The cantilever beam has its boundary conditions as: one end fixed and the other end free. The geometric and material

property details of this cantilever beam were:

Length of the beam (ℓ) = 10.0 cms

Moment of inertia (I_{xx}) = 675.0×10^{-6} cm^4

Modulus of elasticity (E) = 2.11×10^{11} Pa

Area of cross-section (A) = 0.09 cm^2

Width (b) = 0.30 cm

Mass density (ρ) = 7860 Kg/m^3

The blade was discretized into 36 curved 20-noded isoparametric finite elements. There were in all 317 nodes therefore 951 degrees of freedom. Using the formulation discussed in Section 3.2, the natural frequencies were obtained by using the homogeneous part of the Eqn. (3.22). The exact values of the natural frequencies were obtained by solving the Eqn. (3.26) given below, and the values of the constants, $\beta_i \ell$, were obtained from [33].

$$w_{n_i} = (\beta_i \ell)^2 \sqrt{\frac{EI_{xx}}{\rho A (\ell)^4}} \qquad (3.26)$$

where i represents the mode.

The results of the calculation of first five natural frequencies are shown in the Table 3.1. It can be seen from this table that the natural frequencies obtained using isoparametric finite element formulation agree very well with the exact values. This table also shows the results obtained by other researchers [34] who used Reissner energy formulation for this particular problem.

Table 3.1

A Comparison of the Natural Freqencies of a Cantilever Beam

FREQUENCY NUMBER	EXACT VALUE (HZ.)	REISSNER FORMULATION (HZ.)	FEM (Present Work) (HZ.)	% error (REISSNER)	% error (FEM)
I	251.089	248.68	252.02	-0.959	+0.37
II	1573.55	1558.40	1577.24	-0.963	+0.235
III	4405.984	4365.0	4407.58	-0.930	+0.036
IV	8633.95	8563.30	8648.41	-0.818	+0.167
V	14273.65	14468.00	14389.5	+1.36	+0.812

3.3.2 The Description and Details of the Turbine Blade

The discretization of the turbine blade into finite elements can be seen in the Fig. 3.3. The height of the blade was 0.11 m, and its geometric details, as shown in Table 3.2, were obtained from [35]. As discussed earlier in Section 2.3, the material of the blade was MAR-M200 which is a superalloy of Nickel. The variation of the material properties of the blade with temperature, as shown in Table 2.1, were obtained from [26]. The angle of twist of this blade can be obtained as the difference between θ_T and θ_R shown in Fig. 3.1.

Fig. 3.3 is only a representative diagram of the turbine blade and does not take into account pre-twist, asymmetry and taper of the blade. This figure only gives a general idea of how the various elements were fitted into the turbine blade. A total of 35 elements were used to describe the blade with 7 elements across the cross-section and 5 layers along the height. There were 308 nodes, therefore 924 degrees of freedom to represent the dynamics of the system.

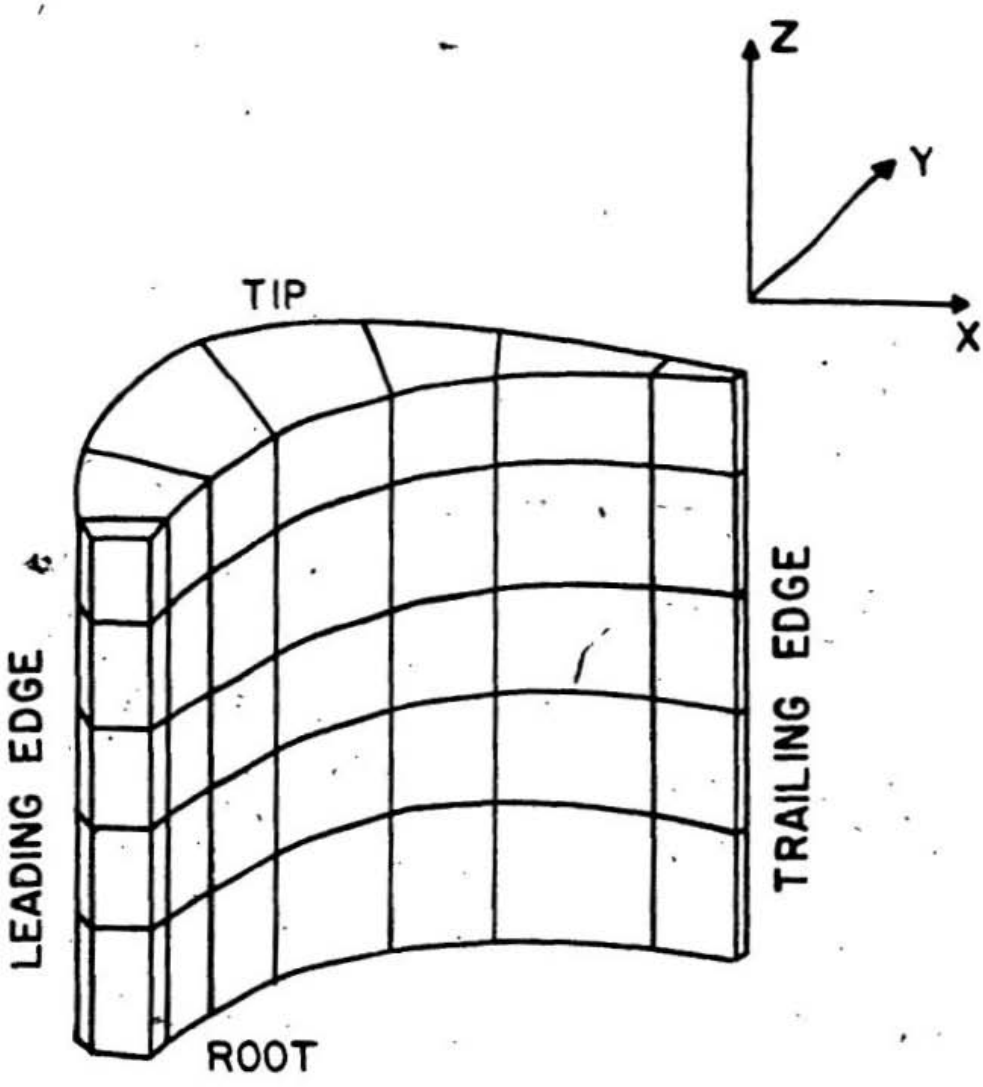

FIG.3.3 The turbine blade finite element model

Table 3.2

The Geometric Properties of the Blade

($R = 0.5m$, $\theta = 30^\circ$, $\theta_N = 7.5^\circ$)

Section	Distance From Root $\times 10^2$, (m)	A $\times 10^4$, (m^2)	I_{xx} $\times 10^8$, (m^4)	I_{yy} $\times 10^8$, (m^4)	Θ_p (DEGREES)
1	0.0	2.127	0.3447	0.9489	0.0
2	2.5	1.738	0.3651	0.6717	10.2
3	5.0	1.647	0.4927	0.5174	21.6
4	7.5	1.263	0.5054	0.3097	33.8
5	10.0	1.008	0.4356	0.1543	38.2
6	11.0	0.736	0.3258	0.0858	42.0

3.4 A Study of the Undampled Natural Frequencies of the Blade

3.4.1 The Variation of the Undamped Natural Frequencies with Temperature

The natural frequencies were obtained by solving the homogeneous part of the Eqn. (3.22). As the temperature of the turbine blade changed with time (refer to Fig. 2.11), the stiffness matrix changed and it resulted in the variation of the natural frequencies. The results obtained during the heating process at various instants of time are shown in the Table 3.3. In this table, the first eleven natural frequencies are shown. At t equal to 1 second, there is no significant change in the material temperature, therefore the frequencies in the first column would be at ordinary temperatures. But as the material gets heated, each of these frequencies start decreasing due to the decrease in the value of the modulus of elasticity. Clearly there is a very significant change in the natural frequencies in the transient phase. This fact must be included in the design of the turbomachinery. Once the blade has reached the steady state temperature, then these frequencies would not change anymore. In summary, to calculate these natural frequencies one has to take into account two types of non-linearities in the analysis; the first one arises due to the non-linear radiative boundary conditions and the second one due to the non-linear variations of the material properties of the blade.

Table 3.3

The Variation of Natural Frequncies (Hz.) with Time

Mode Number	The Natural Frequencies After					
	1 (sec)	30 (sec)	50 (sec)	100 (sec)	120 (sec)	Steady State
I	661.08	651.74	648.48	613.65	603.35	564.58
II	2081.02	2047.43	2001.58	1929.53	1912.24	1784.95
III	3371.59	3310.57	3230.26	3116.24	3094.99	2888.35
IV	4230.02	4171.99	4077.06	3928.37	3900.07	3623.50
V	7159.01	7040.37	6865.78	6629.0	6588.2	6134.51
VI	8891.83	8762.97	8592.89	8261.54	8205.29	7618.53
VII	10956.95	10731.32	10486.71	10118.61	10054.18	9385.74
VIII	13301.75	13118.97	12829.29	12359.61	12280.01	11395.4
IX	15014.76	14777.74	14488.46	13942.27	13848.89	12861.76
X	14232.5	14011.57	13695.39	13198.16	13118.21	12192.42
XI	21803.25	21463.58	21048.37	20259.3	20122.5	18680.02

3.4.2 The Coordinate Reduction Using the Dynamic Matrix Reduction Scheme

As discussed earlier, it almost becomes a necessity to reduce the size of the stiffness and the mass matrices if one uses finite element analysis. In order to establish the reduced size of these matrices, the error in the first five undamped natural frequencies was used as the selection criteria. Fig. 3.4 shows the percentage error versus the number of master degrees of freedom. From this figure one can see that as the number of master degrees of freedom are increased, the errors reduce for all the modes. The higher the mode, the greater is the rate of convergence. The error is less than 1% for all the five modes if 200 master degrees of freedom are selected.. Therefore, the reduced system containing 200 master degrees of freedom would be adequate to represent the uncondensed system. The presence of large number of master degrees of freedom can be attributed to the asymmetric and twisted geometry of the blade.

3.4.3 The Effect of Pre-Twist on the Undamped Natural Frequencies

It is well known that the pre-twist angle has a very significant influence on the natural frequencies of the turbine blade. The amount of pre-twist can be changed in a turbine blade by keeping the root fixed and then twisting the blade about an axis parallel to the z-direction and passing through the geometrical centre of the cross-section at the root. In this way, the amount of pre-twist was varied and the corresponding natural frequencies were

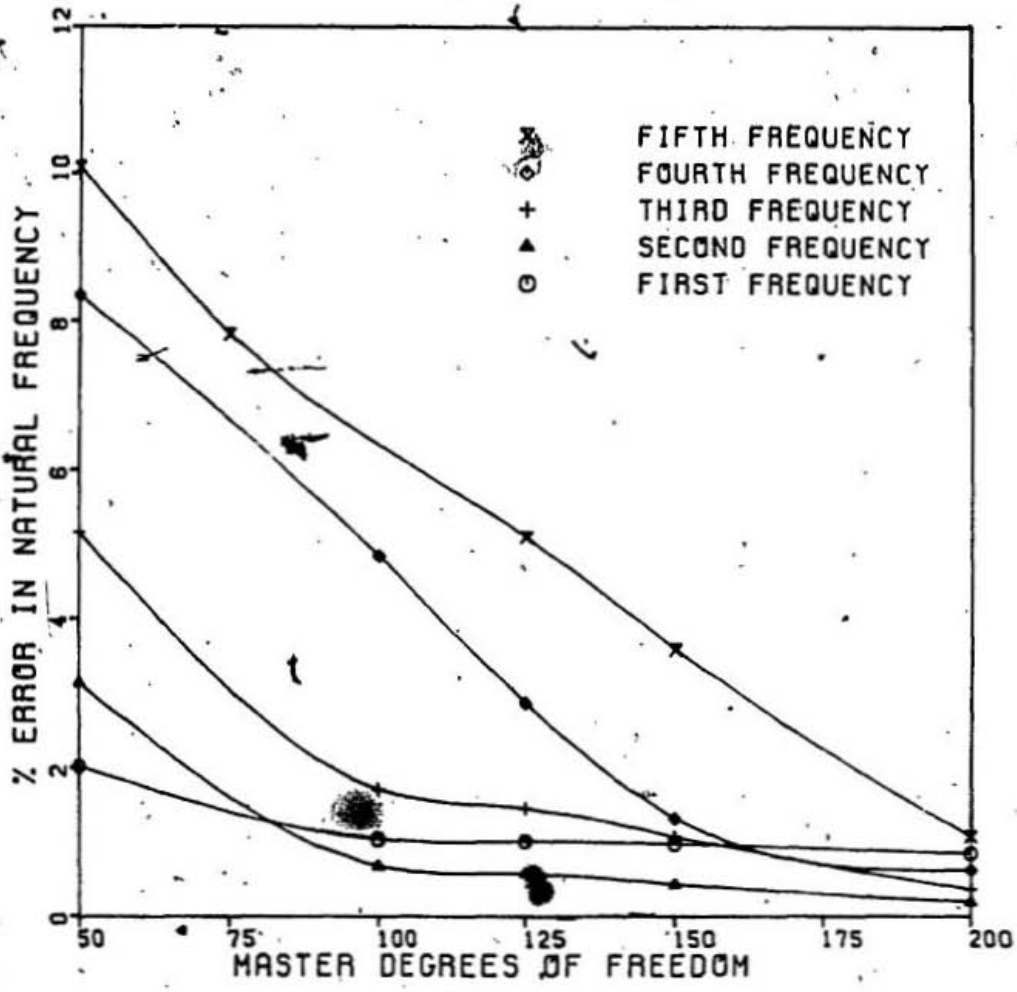

FIG.3.4 PLOT SHOWING THE EFFECT OF GUYAN'S REDUCTION ON THE FIRST FIVE BLADE NATURAL FREQUENCIES.

obtained. The Fig. 3.5 shows the variation of the various modes due to the change in the amount of pre-twist. In this figure all the bending modes decrease as the pre-twist angle is increased. The rate of decrease of these frequencies per degree change in the twist angle is greater for the higher modes. The torsional modes show just the opposite behaviour, i.e. the frequencies increase with the increase in the angle of pre-twist. Similar results were obtained by other researchers [18].

3.5 Conclusion

In this chapter the dynamic equation of motion was formulated using 20-noded solid isoparametric finite elements. The natural frequencies of this system were calculated by taking into account the effect of the variation of stiffness properties with temperature. In order to reduce the size of the system matrices, a dynamic matrix reduction scheme was used. In addition, the effect of pre-twist on the natural frequencies was also studied. From the studies carried out in this chapter, the following conclusions can be drawn:

1. The solid isoparametric finite elements can be successfully used to accurately predict the natural frequencies of the rotor blade.
2. The blade natural frequenices vary quite significantly during the transient heating period.
3. The variation of the pre-twist angle has a significant influence on the natural frequencies. The bending natural frequencies

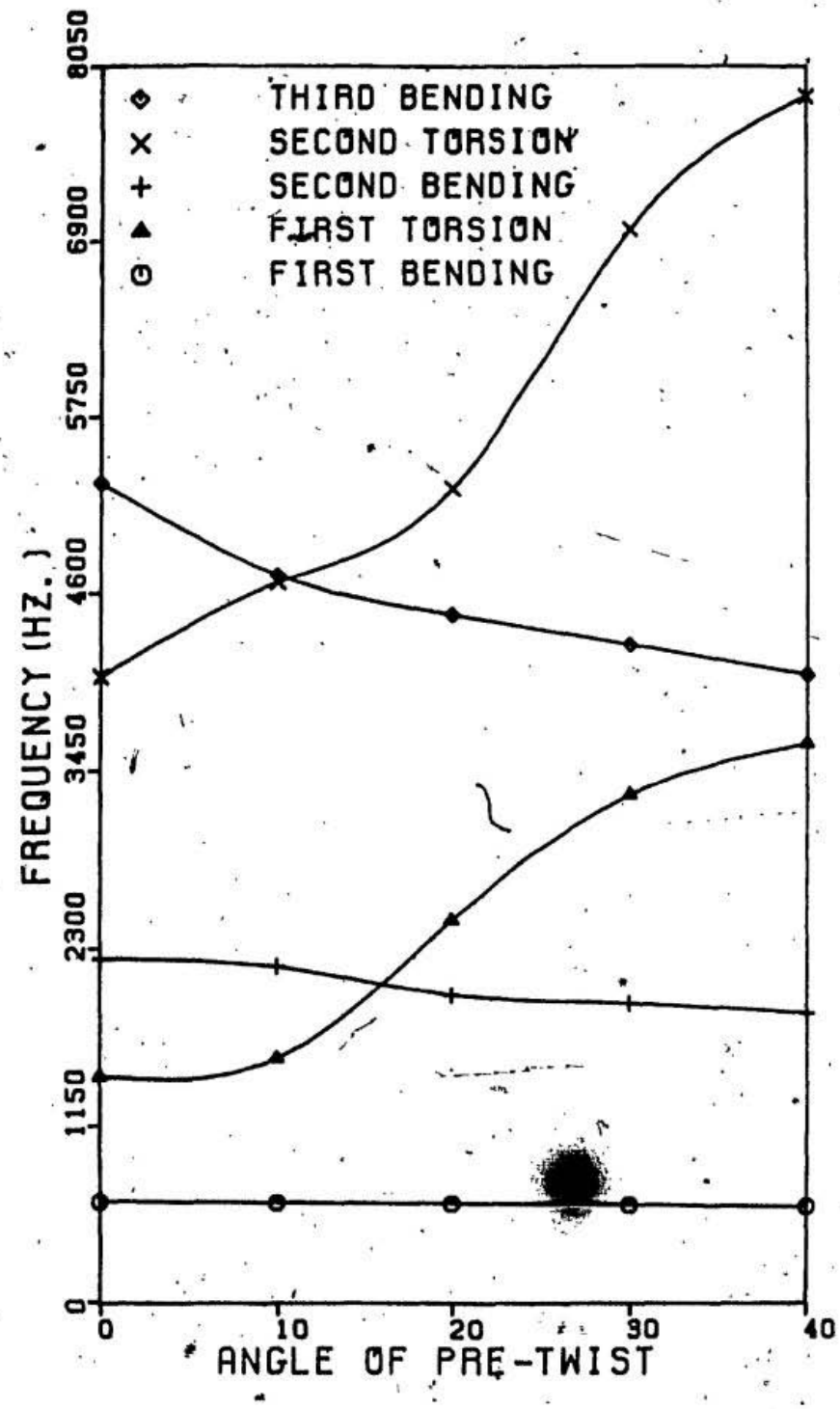

FIG.3.5 THE VARIATION OF NATURAL FREQUENCY WITH PRETWIST.

decrease with the increase in the angle of pre-twist but the effect is just the opposite on the torsional modes.

4. The dynamic matrix reduction scheme can be very fruitfully utilized in the case of rotor blades.

The study of the transient behaviour of the system is quite important as stated in the introduction to this chapter. The transient behaviour can be analysed easily if the modal matrices are known. These matrices were obtained while determining the natural frequencies of the system in this chapter. In the next chapter, the dynamic behaviour of the system under nozzle and centrifugal force excitation is studied.

CHAPTER 4

THE TRANSIENT STRESS ANALYSIS DUE TO THE VIBRATORY AND THERMAL LOADING

4.1 Introduction

In order to get an overall view of the state of stress, the vibratory stresses also have to be calculated. The variation of E at various points due to the temperature change across the cross section of the blade can be calculated from the results of Chapter 2. But, as a first approximation to economize on the CPU time, one can keep E constant for the vibratory stresses only and this approximation has been used here.

4.2 The Mathematical Formulation

4.2.1 The Modelling of Transient Nozzle Excitation Forces

The nozzle excitation force on the blade is modelled as a series of impulses (refer to Fig. 4.1b). As and when the blade approaches a nozzle through which the gases enter the turbine chamber, it is impinged upon by the gases at high pressure. This momentary impingement of the gases can be modelled as an impulse excitation. Thus, as the speed of the rotor increases, the time delay between two impulses on the turbine blade would decrease.

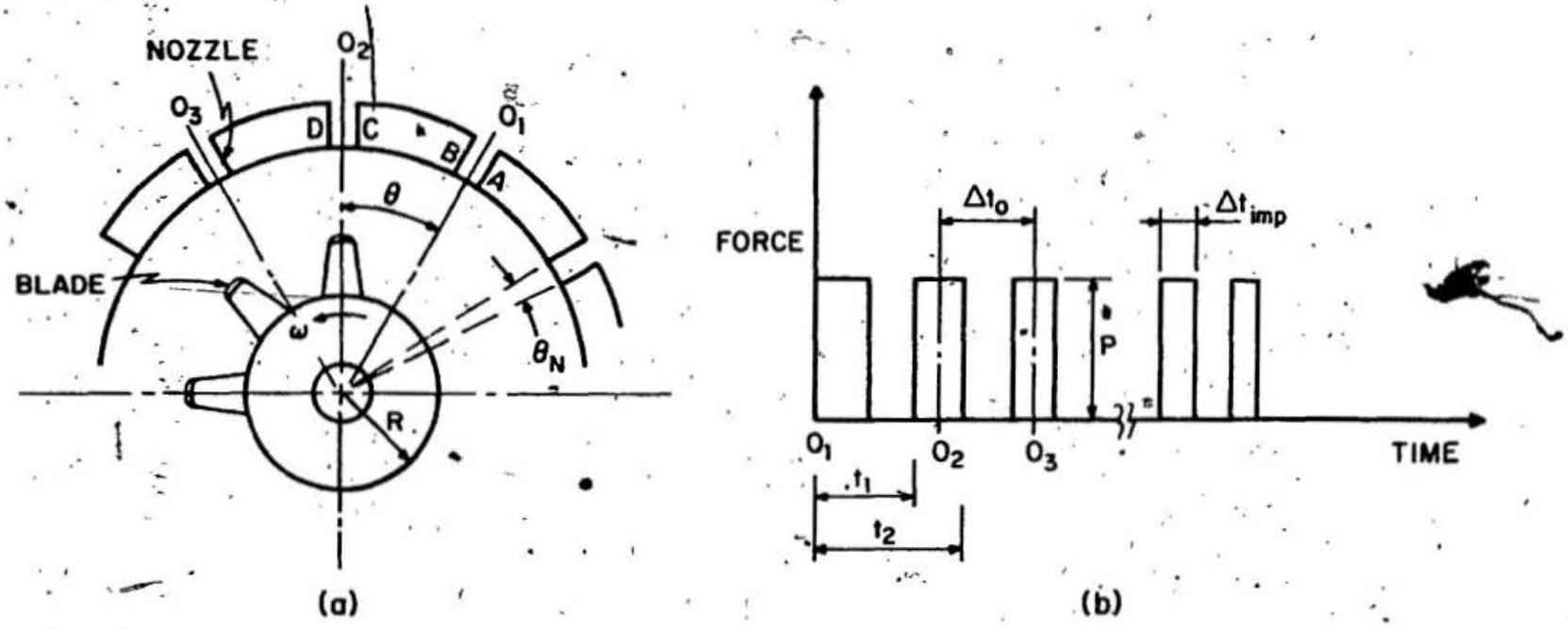

FIG.4.1 (a) Schematic of the blade, nozzle and rotor configuration; (b) The representation of the nozzle excitation forces as a series of impulses.

Fig. 4.1a shows the position of a rotor blade at O_2. It started from rest with an angular acceleration α from its position at O_1. The location of the position of the rotor blade at various instants of time can be known by solving kinematic equations. From this figure one can see that the time taken by the blade to move from O_1 to C will be

$$t_1 = \sqrt{\frac{2(\theta - \theta_N/2)}{\alpha}} \qquad (4.1)$$

Similarly, the blade will be at D at the instant

$$t_2 = \sqrt{\frac{2(\theta + \theta_N/2)}{\alpha}} \qquad (4.2)$$

Therefore the duration of the impulse, Δt_{imp}, will be equal to $(t_2 - t_1)$. It should be borne in mind that θ is the total angle measured counter-clockwise from O_1 to the centre-line of the nozzle.

The instantaneous speed of the rotor can be calculated as

$$\omega_i = \omega_{i-1} + \alpha(t_i - t_{i-1}) \qquad (4.3)$$

The ω_i is needed further on in the calculation of transient vibration response of the blade due to centrifugal forces in the Section 4.2.3. Also, the time gap between the occurence of any two impulses will be

$$\Delta t_0 = t_{1_i} + \frac{(\Delta t_{imp})_i}{2} - \left(t_{1_{i-1}} + \frac{(\Delta t_{imp})_{i-1}}{2}\right) \qquad (4.4)$$

where i in Eqns. (4.3) and (4.4) represents the sequential order of the impulses.

The forces due to gas pressure are distributed along the entire length of the blade. The actual magnitude of the pressure distribution would depend upon the type and operating conditions of the turbine. To demonstrate the applicability of the present work, the values for the magnitude of the height of the impulse were taken from [32]. The existence of the normal modes of the lightly damped system is assumed here.

4.2.2 The Transient Response Due to Nozzle Excitation Forces

One of the convenient ways of calculating the response due to the series of impulses occuring at various instants of time would be by using the following equation

$$q_k(t) = \frac{P\ \Delta t_{imp}}{m_k\ \omega_{nk}(1 - \xi_k^2)^{1/2}}\ e^{(-\xi_k \omega_{nk} t)} \sin(\omega_{dk} t) \qquad (4.5)$$

The Eqn. (4.5) can be used to calculate the response of each mode by decoupling the following equations of motion

$$\left[M^G\right]\left\{\ddot{U}\right\} + \left[C^G\right]\left\{\dot{U}\right\} + \left[KS^G\right]\left\{U\right\} = \left\{F(t)^G\right\} \qquad (4.6)$$

The procedure for decoupling the equations of motion is given in Appendix B. In Eqn. (4.5) the subscript k corresponds to the mode number. In Fig. 4.1b the displacement response at any instant of time between O_1 and O_2 can be calculated using Eqn. (4.5) and the velocity response by differentiating this equation. The displacement and the velocity response values between O_2 and O_3

can be calculated due to the occurence of the impulse at O_2, and the velocity and the displacement values at O_2 due to the previous impulse. In this way one can calculate the respone at any instant of time.

4.2.3 The Transient Response Due to Centrifugal Forces

The centrifugal forces in the rotor blade arise due to the radial location of the element with reference to the axis of rotation of the rotor shaft. If the mass of the element is m, then the centrifugal force acting on this mass will be

$$F_{cen} = m \omega^2_{rotor} (R + z) \qquad (4.7)$$

where R is the radius of the rotor disk and z is the distance from the root to the center of gravity of the element. This force which acts at the center of gravity can be replaced by eight equivalent forces each of which act at the corner nodes.

To calculate the dynamic response due to the centrifugal forces one has to first recognize that these are time variant because ω_{rotor} in Eqn. (4.7) is a variable and is calculated using Eqn. (4.3). To calculate the response one has to decouple the equations of motion using the matrix of eigenvectors and this procedure is given in Appendix B. Now the forcing function corresponding to the Eqn. (4.7) will be

$$F_{cen} = (R + z)(\alpha t)^2 m \qquad (4.8)$$

To calculate the modal response one has to use the convolution

$$q_k(t) = \frac{1}{\omega_{dk}} \int_0^t (R + z)(\alpha\tau)^2 \, m \, e^{(-\xi_k \omega_{nk}(t-\tau))} \sin(\omega_{dk}(t-\tau)) d\tau \quad (4.9)$$

The solution for this equation can be written as [37],

$$q_k(t) = \frac{(R + z)}{\omega_{dk}} \alpha^2 \sin(\omega_{dk} t) \, e^{(-\xi_k \omega_{nk} t)}$$

$$\left[e^{(\xi_k \omega_{nk} \tau)} \sum_{r=0}^{2} \frac{(-1)^r \, 2! \, (\tau)^{2-r}}{\left(\xi_k^2 \, \omega_{nk}^2 + \omega_{dk}^2\right)^{\frac{r+1}{2}} (2 - r)!} \right.$$

$$\left. \cos\left[\omega_{dk}\tau - (r + 1) \tan^{-1}\left(\frac{\omega_{dk}}{\xi_k \, \omega_{nk}}\right)\right] \right]_0^t$$

$$- \frac{(R + z)\alpha^2}{\omega_{dk}} \cos(\omega_{dk} t) \, e^{(-\xi_k \omega_{nk} t)} \left[e^{(\xi_k \omega_{nk} \tau)} \right.$$

$$\sum_{r=0}^{2} \frac{(-1)^r \, 2! \, (\tau)^{2-r}}{\left(\xi_k^2 \, \omega_{nk}^2 + \omega_{dk}^2\right)^{\frac{r+1}{2}} (2 - r)!} \sin\left[\omega_{dk}\tau \right.$$

$$\left. \left. - (r + 1) \tan^{-1}\left(\frac{\omega_{dk}}{\xi_k \, \omega_{nk}}\right)\right] \right]_0^t \quad (4.10)$$

4.2.4 The Calculation of Vibratory Stresses

Once the total response of the turbine blade due to various excitation forces is known, the strains in each element can be obtained from the isoparametric finite element formulation as

$$\underset{6\times1}{\{\gamma\}} = \underset{6\times60}{[B]} \; \underset{60\times1}{\{U\}} \quad (4.11)$$

and the dynamic stresses can then be evaluated as

$$\underset{6\times1}{\{\sigma\}} = \underset{6\times6}{[D]}\ \underset{6\times1}{\{\gamma\}} \tag{4.12}$$

This stress vector can then be used to obtain the principal stresses in each element of the blade by solving the following cubic equation [38]:

$$S^3 - (\sigma_x + \sigma_y + \sigma_z)\, S^2 + (\sigma_x\sigma_y + \sigma_y\sigma_z + \sigma_x\sigma_z - \tau_{yz}^2 - \tau_{xz}^2 - \tau_{xy}^2)\, S - (\sigma_x\sigma_y\sigma_z + 2\tau_{yz}\,\tau_{xz}\,\tau_{xy} - \sigma_x\tau_{yz}^2 - \sigma_y\tau_{xz}^2 - \sigma_x\tau_{xy}^2) = 0 \tag{4.13}$$

The roots of Eqn. (4.13) yield the three principal stresses as σ_1, σ_2 and σ_3. In order to calculate the design stress for the safe operation of the turbine blade, various failure theories can be used. One commonly used theory is the distortion energy theory. This theory can be used to calculate the design stress (σ_d) from the principal stresses as

$$\sigma_d = \frac{1}{\sqrt{2}}\,[(\sigma_1 - \sigma_2)^2 + (\sigma_2 - \sigma_3)^2 + (\sigma_3 - \sigma_1)^2]^{1/2} \tag{4.14}$$

Thus σ_d would be a reliable indicator of the state of stress in each element.

4.3 Numerical Example

The discretization of the turbine blade into solid isoparametric finite elements was the same as shown in Fig. 3.3. After

carrying out the thermal stress analysis in Chapter 2 it was stated that the T_{gas} versus time curve was an infeasible path because the thermal stresses in the blade for that particular heating rate exceed the yield stress. This phenomena of high thermal stresses is resolved in the case of an actual turbine by extracting work from it in two stages. Let us assume that for the final stage the gas temperature rises from 400°C to 870°C and is then maintained at 870°C. The transient temperatures and thermal stresses are then calculated for this T_{gas} versus time curve using the theory developed in Chapter 2.

The dynamic loading on the turbine blade is caused by assuming that there are 12 nozzles placed at equiangular intervals all along the periphery of the rotor. The various sections along the height of the turbine blade are shown in the Appendix C and the computer programmes used to calculate all types of stresses are given in the Appendix D.

4.4 A Study of the Coupled Effects of Thermal and Vibratory Loads on the Transient Stresses in the Blade

4.4.1 The Thermal Stress Analysis of the Turbine Blade

The thermal stresses can be calculated once the temperature distribution at any cross-section of the blade is known. For the cross-section shown in the Fig. 2.1, the temperature distribution was calculated using Eqn. (2.22) and once the temperature

distribution at various elements was known, the thermal stresses were calculated using Eqn. (2.26). The variations of temperatures and stresses with time are shown in the Fig. 4.2 at some of the important points of this cross-section. One can clearly see in this figure that the stresses build up to a maximum value and then decrease as the temperatures of various points on the blade approach the gas temperature. The maximum stresses occur at the element number 78, the location of which is shown in Fig. 2.1. The stress values in this figure have been normalized with respect to the yield stress of the element which itself varies as the element temperature changes. It should be added here that these stresses will become negligible when the blade temperature approaches the steady state temperature.

4.4.2 The Vibratory Stress Analysis of the Turbine Blade

To carry out the vibratory stress analysis, the rotor blade was divided into 35 twenty-noded elements which were arranged in five layers as shown in Fig. 3.3. The various other details of the turbine blade etc. are given in Table. 3.2. Since the total degrees of freedom for this system were 924, the Guyan's reduction technique was used to reduce the size of the system matrices. The reduced degrees of freedom were 200 and the criteria for this reduction was that the change in the first five natural frequencies was less than 1%.

The value of E used in this section only was 2.0×10^{11} Pa and the corresponding first natural frequency was 636.01 Hz (3180 RPM).

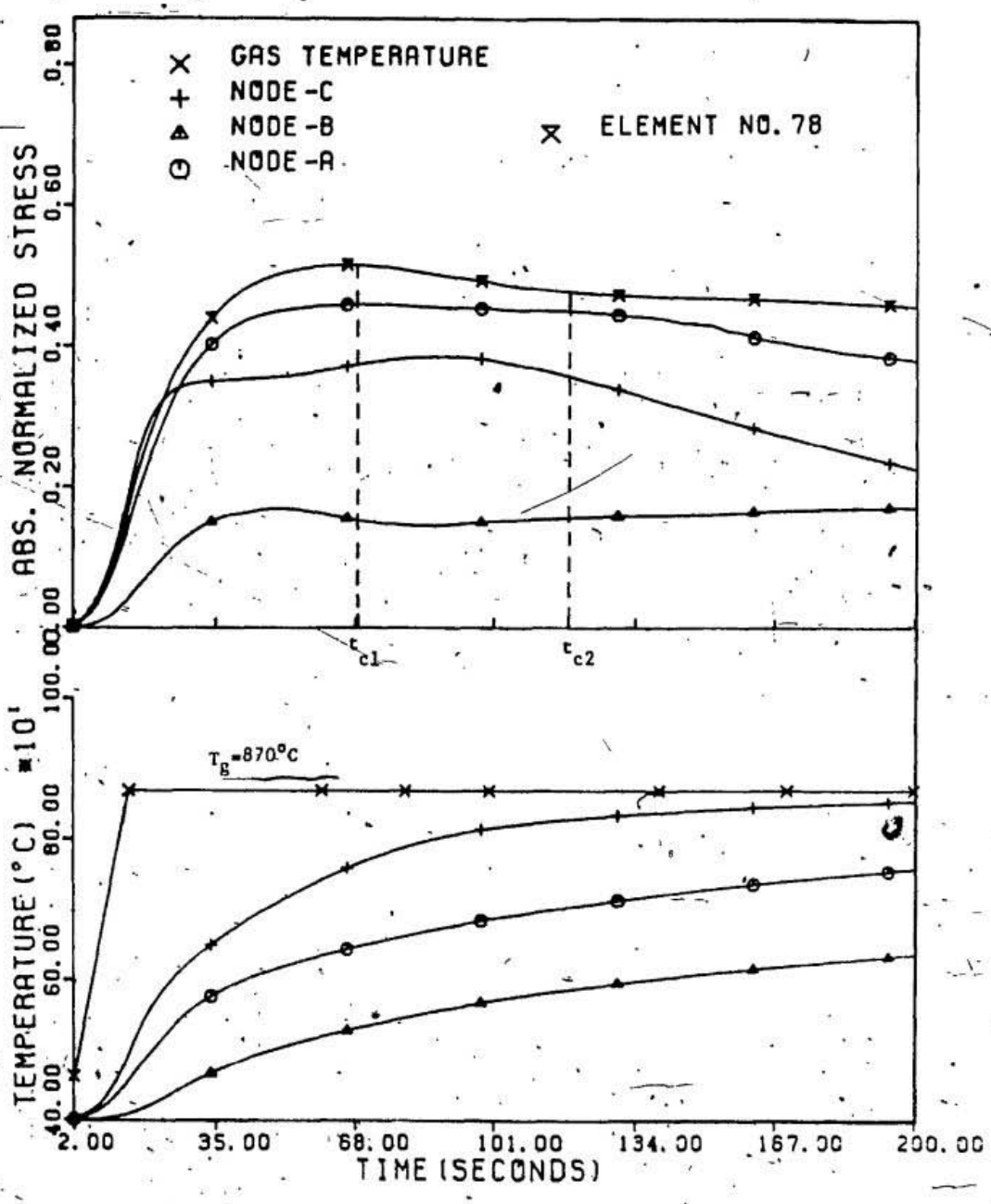

FIG.4.2 THE TRANSIENT TEMPERATURE AND THERMAL STRESS DISTRIBUTION IN THE BLADE FOR THE FEASIBLE HEATING RATE OF 31.33 C/SEC & FINAL T_g=870°C

The transient vibration response was calculated with this value in mind. Figs. 4.3 to 4.5 show the variations of the nozzle excitation stresses along the height of the blade at the leading edge, trailing edge and at the element number 78. In the Fig. 4.3 the maximum stresses occur close to the tip of the blade and among all the maxima, the global maxima takes place at 3180 RPM which corresponds to the first natural frequency. At half-order excitation i.e. at 1590 RPM the stresses are again quite significant. This figure also shows reasonably low value of stresses at 4000 RPM which is the maximum operating speed for the present analysis. Similar behaviour, as far as the speeds are concerned, can be seen in Figs. 4.4 and 4.5 also. The maximum stresses in these two figures are also nearer to the tip than the root. Among all the peaks in these three figures, the maximum peak value of the stress is in Fig. 4.4. The stress values in these three figures have been normalized with respect to the global maxima of the Fig. 4.4.

In all these three figures, the stress values have been connected by straight lines and each point corresponds to the element-joint along the height of the blade. If one desires to know the value of stress at any other point then one can calculate this value using polynomial interpolation used for this particular finite element. It should be noted in all these figures that the maximum stress does not occur at the root. This is because the cross-sectional area of the root is higher, which is generally the case, and the variation of the stress along the height is not very regular

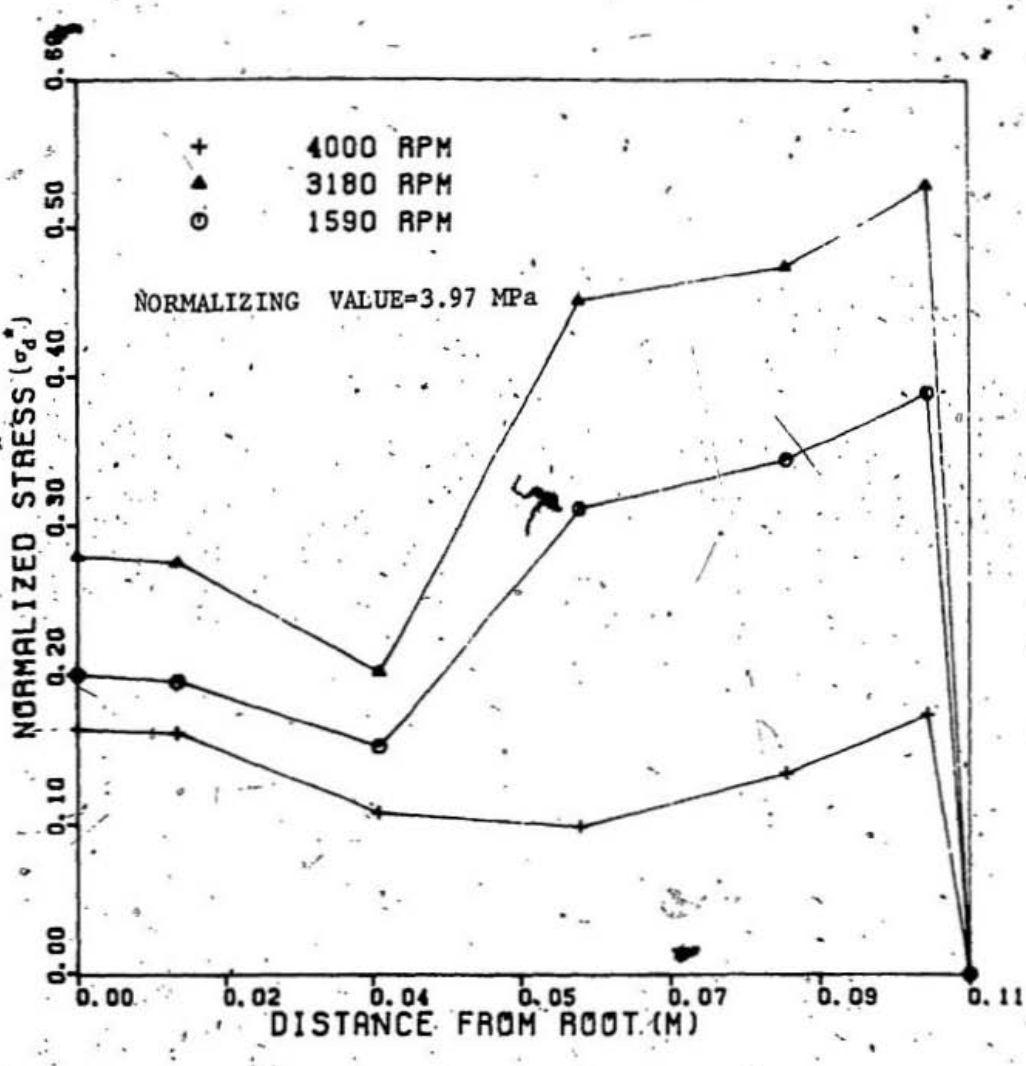

FIG.4.3 THE VARIATION OF NOZZLE EXCITATION STRESSES AT THE LEADING EDGE AT VARIOUS SPEEDS

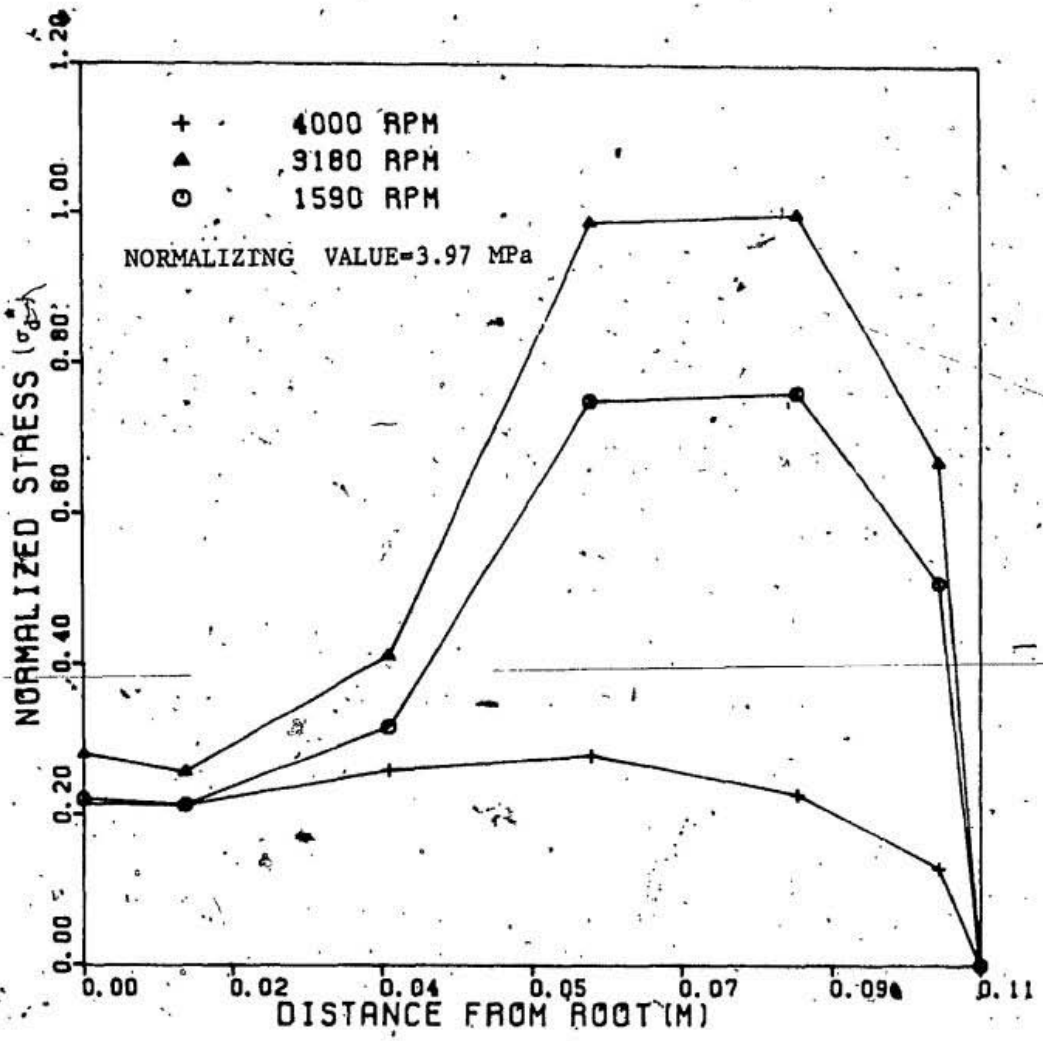

FIG.4.4 THE VARIATION OF NOZZLE EXCITATION STRESSES AT THE TRAILING EDGE AT VARIOUS SPEEDS

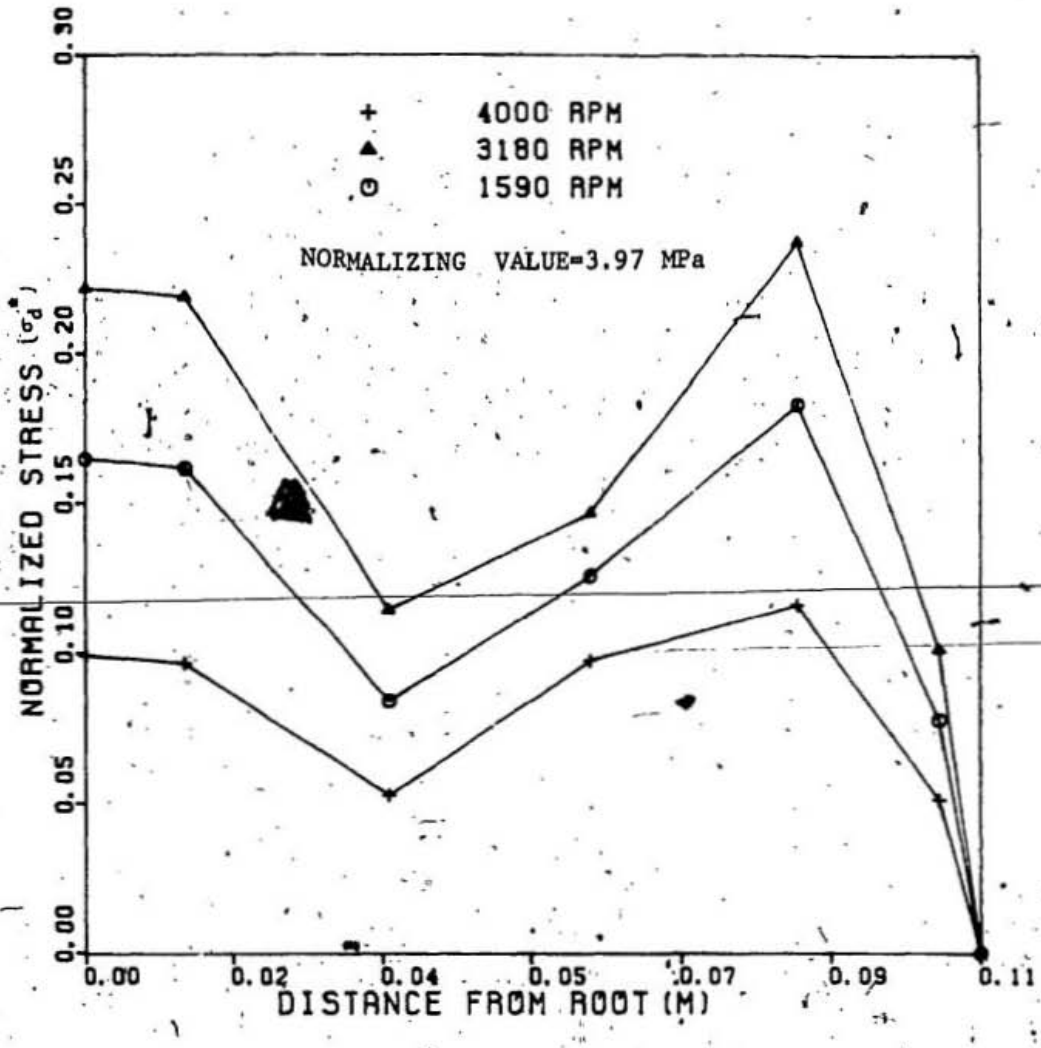

FIG.4.5 THE VARIATION OF NOZZLE EXCITATION STRESSES AT THE ELEMENT NO.78 AT VARIOUS SPEEDS

because of the complicated three-dimensional geometry of the blade.

Fig. 4.6 shows the centrifugal stress distribution when the rotor speed reaches 4000 RPM. At this speed the peak value of the stress was more than the peak value at other speeds. Among the leading edge, trailing edge and element number 78, the peak stress of each occur at different distances from the root. From the design point of view, even in this case the magnitude of the stresses are more near the tip than the root. This figure has also been normalized with the same value as that used in Figs. 4.3 to 4.5.

4.4.3 The Stress Analysis of the Turbine Blade Due to the Combined Effects

In the Section 4.4.1, the stresses due to the thermal effects were discussed and the maximum transient stresses were found to be quite significant. In the dynamic analysis, the value for the height of the impulse, P, was chosen to be a low value and it was used just to illustrate the calculation of the transient stresses. In the design of an actual turbine blade, the transient forces have to be exactly known, and for this type of a linear system the dynamic stresses would be in the same proportion as the actual force is to P. Therefore, the actual design would involve the summation of all the stresses first of all at any instant of time, and then finding the global maxima of these type of combined stresses as the time varies.

To understand the critical instants of time from the stress point of view one should look at the Figs. 4.2 - 4.6. The rotor

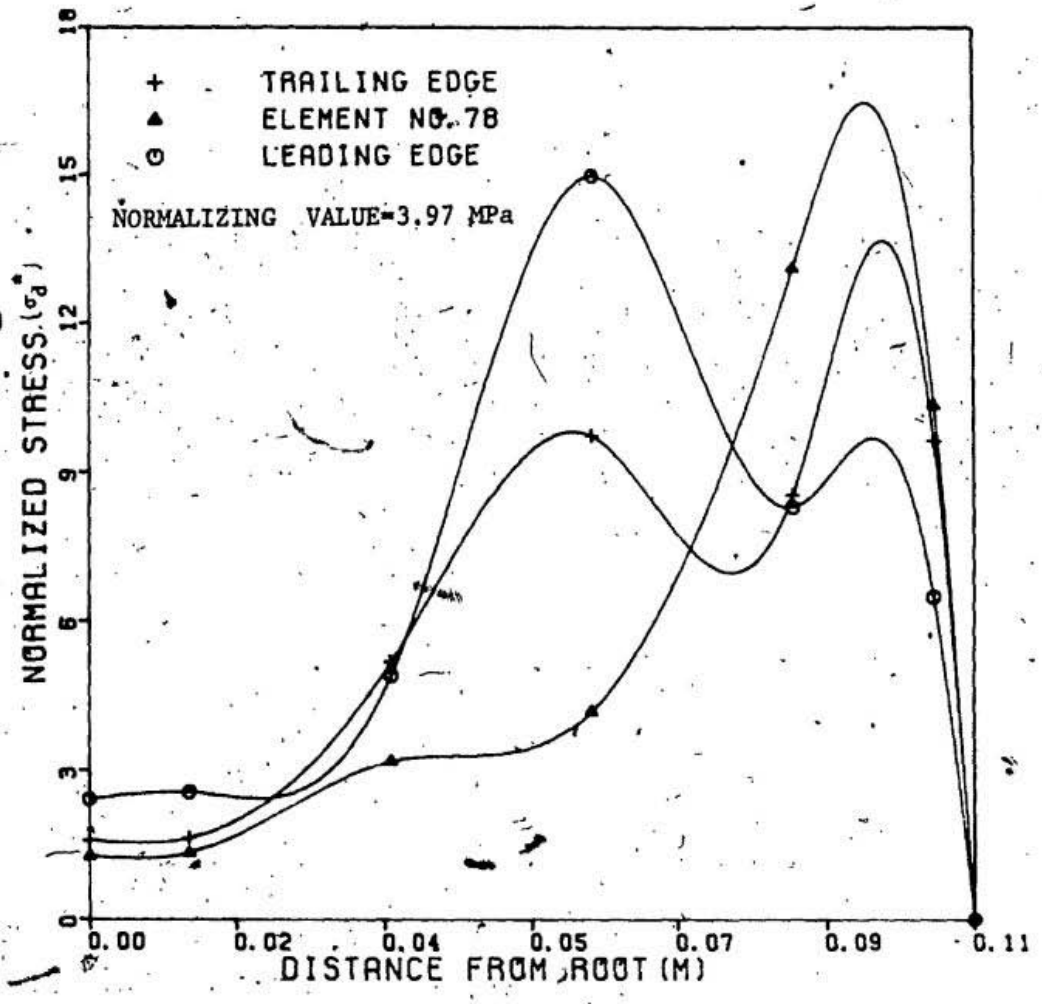

FIG.4.6 THE VARIATION OF CENTRIFUGAL STRESSES AT THE ROTOR SPEED OF 4000 RPM.

accelerates from rest and at t = 70 seconds the shaft speed is 933.33 RPM. At this instant, (t_{c1} in Fig. 4.2), the maximum thermal stresses occur at element number 78. These stresses decrease very slowly with time. The second critical event (t_{c2} in Fig. 4.2) occurs due to the half-order excitation at 1590 RPM (t = 119.25 seconds). Here the critical point is the trailing edge. This is due to the dynamic stresses as shown in the Fig. 4.4. The centrifugal stresses, not shown in any of the figures, are very low at this speed. The thermal stress at the trailing edge is also quite significant. The most critical stresses take place at 3180 RPM (t = 238.5 seconds) as the rotor goes through the first natural frequency. The maximum dynamic stresses shown in Fig. 4.4 are again at the trailing edge, In addition, the thermal stresses are also not very low. At 4000 RPM the dynamic stresses in Figs. 4.3 to 4.5 are much lower. The thermal stresses, however, are still quite high (not shown in the figures). However, the peaks of the centrifugal stresses are significant. If we compare the magnitudes of the peaks of the centrifugal stresses shown in the Fig. 4.6 and the thermal stresses, the centrifugal stresses are still much lower. Therefore, the blade is not under very high stress at 4000 RPM as compared to the first critical instant of time (t_{c1}). From all this discussion one can see that the thermal stresses are quite important in the design of the turbine blades. As a point of clarification it should be stated again that the dynamic stresses in Figs. 4.3 to 4.5 were low because the value of P in Fig. 4.1b was very small. In actual

operation of the turbomachinery P would be very large, whereas the stresses in Figs. 4.2 and 4.6 are not affected by the value of P.

4.5 Conclusion

In this chapter, the transient temperature variations were obtained using a finite element analysis in two-dimensions. The finite element equations also included the effect of non-linear variation of properties as well as the non-linear boundary conditions. From the temperature distribution the normal thermal stresses in the z-direction were calculated. To calculate the stresses due to the pressure and centrifugal forces the three-dimensional solid finite elements were used. The transient forces were modelled as a series of impulses occurring at instants of time which were known by solving kinematic equations. The response due to these forces were calculated using modal analysis. The response values were then used to calculate the dynamic stress vector. The principal stresses in three-dimensions were obtained by solving the cubic equation. The design criteria for the blade was based on the distortion energy theory.

Based on the study carried out in this chapter, the following conlusions can be drawn:

1. The maximum value of the thermal stresses occur at the element number 78 during the transient period.
2. The peak values of the distortion energy stress, σ_d, occur at the trailing edge along the blade and amongst these maxima, the global maxima takes place close to the tip.

3. The stresses, σ_d, due to centrifugal forces increase with the increase in speed.
4. The thermal stresses are quite significant during the acceleration period and must be included in the design of rotor blades.

CHAPTER 5

CONCLUSIONS AND RECOMMENDATIONS

5.1 A Brief Discussion About This Investigation and the Conclusions

The objective of this investigation was to analyse the state of stress in the turbine blade due to the coupled effects of dynamic and thermal loading. This was achieved by separately carrying out the heat transfer and vibration analyses of a gas turbine blade and then adding up the effects due to each. The transient temperatures in the blade were calculated using non-linear finite element analysis in two-dimensions. These temperatures were then used to calculate the thermal gradients and thermal stresses in the blade. For the thermal analysis, the material properties of the blade were a function of its temperature and the coefficient of convective heat transfer varied along the pressure and suction surfaces of the airfoil cross-section of the turbine blade.

The dynamic analysis was carried out using solid, quadratic, twenty-noded isoparametric finite elements. A dynamic coordinate reduction scheme was used to condense the system matrices. The effect of a thermal environment on the natural frequencies of the blade was studied. Also, the effect of pre-twist on the blade natural frequencies was determined. The vibratory stresses due to nozzle excitation forces and centrifugal forces were calculated.

Based on the studies carried out in this investigation, the following conclusions can be drawn:

1. The heat transfer process within the blade can be studied by deriving the equations using the non-linear finite element analysis.
2. The effect of radiative heat transfer is quite significant in the transient temperature analysis and so it should be considered for the thermal analysis of a gas turbine engine.
3. The maximum thermal stress occurs at element number 78 at all instants of time irrespective of the heating path followed by the incoming hot gases.
4. The study of the thermal gradients in the blade help us to better understand the complex dynamics of the heat transfer process.
5. The solid isoparametric finite elements can be successfully used to accurately predict the natural frequencies of the rotor blade.
6. The blade natural frequencies vary quite significantly during the transient heating period.
7. The dynamic coordinate reduction scheme can be very fruitfully utilized in the case of rotor blades.
8. The variation of the pre-twist angle has a significant influence on the blade natural frequencies. The bending natural frequencies decrease with the increase in the angle of pre-twist but the torsional natural frequencies increase with the increase in the angle of pre-twist.

9. The gas turbine engine has to be pre-heated to about 400°C in order to limit the thermal stresses to within 50 percent of the yield stress. Otherwise, if the gases heat up the blade from room temperature to 870°C, the thermal stresses would be more than the yield stress of the blade.
10. The kinematic equations can be successfully used to model the nozzle excitation forces as a series of impulses.
11. The nozzle excited stresses are the highest when the rotor passes through the first natural frequency.
12. The peak values of the nozzle excited stress, using distortion enegy criteria, occur at the trailing edge along the height of the blade.
13. Amongst the various maxima of the dynamic stresses, the global maxima takes place close to the tip.
14. The distortion energy stresses due to centifugal forces increase with the increase in speed.
15. Besides the dynamic stresses, the thermal stresses are very significant during the acceleration period and must be included in the design of rotor blades.

5.2 Limitations of the Present Investigation and Recommendations For Future Work

1. In the non-linear temperature distribution calculations, the surrounding gases were assumed to be at a uniform temperature. Since this is not the practical case, the present finite element

model can be revised to include the non-uniform gas temperature distribution around the blade.

2. The creep behaviour of the material of the blade was not taken into account in the present analysis. This phenomena can be an interesting area of study for the thermal stress calculation in future research work.

3. Even though the normal thermal stress along the z-direction in the blade is most significant, a more rigorous three-dimensional thermal stress analysis can be carried out in future work.

4. For the dynamic response calculation only viscous damping as a function of rotor speed was considered in this investigation. But the non-linearity in the damping due to dry-friction damping at the root of the blade, where it is attached to the rotor disk, should also be taken into account.

5. The nozzle excitation forces have been distributed along the height of the blade in the x and y directions and have been neglected in the z-direction. But in actual practice, much more experimental work is required to predict the magnitude, direction and location of these pressure forces.

6. An interesting problem to work on in future would be to determine the fatigue life of the turbine blade.

REFERENCES

1. Faires, V. M., "Thermodynamics", The Macmillan Company, London, 1970, pp. 356.

2. Csanady, G. T., "Theory of Turbomachines", McGraw-Hill Book Company, 1964, pp. 17.

3. Roeder, A., "The Influence of Material Properties on the Design of Large Steam Turbines", First Parsons Int. Turbine Conference, University of Dublin, June, 1984, pp. 153.

4. Daniels, L. D. and Browne, W. B., "Calculation of Heat Transfer Rates to Gas Turbine Blades", Int. Journal of Heat and Mass Transfer, Vol. 24, No. 5, 1981, pp. 871-879.

5. Mohanty, A. K., Raghavachar, T. S. and Nanda, R. S., "Heat Transfer from Rotating Short Radial Blades", Int. Journal of Heat and Mass Transfer, Vol. 20, 1977, pp. 1417-1425.

6. Maya, T., Katsumata, I., and Itoh, M., "A Study of Thermal Fatigue Life Prediction of Air-Cooled Turbine Blades", 1978, ASME Paper No. 78-GT-63.

7. Mukherjee, D. K., "Stresses in Turbine Blades Due to Temperature and Load Variation", 1978, ASME Paper No. 78-GT-158.

8. Allen, J. M., "Effect of Temperature Dependent Mechanical Properties on Thermal Stresses in Cooled Turbine Blades", Journal of Engineering for Power, Trans. ASME, Vol. 104, April 1982, pp. 349-353.

9. Bogov, I. A., "Influence of Turbine Blade Airfoil and Root Thickness Variation along the Blade on its Thermal Stress State:, Energomashinostroenie, No. 8, 1978, pp. 10-12.

10. Gryaznov, B. A., Zaslotskaya, L. A., Konoplyanikov, E. G., and Mitchenko, E. I., "Experimental Verification of Finite Element Calculation of the Thermal Stress State of Gas Turbine Blades", Probl. Procn., No. 9, Sept. 1979, pp. 34-37.

11. Rao, J. S. and Carnegie, W., "Solution of the Equation of Motion of Coupled Bending, Bending-Torsion Vibrations of Turbine Blades by the Method Ritz-Galerkin", Int. J. of Mech. Sci., Vol. 12, 1970, pp. 875.

12. Mabie, H. H. and Rogers, C. B., "Transverse Vibrations of a Doubly Tapered Cantilever Beam with an End Mass and End Support", J. of Acou. Soc. America, Vol. 55, 1974, pp. 986.

13. Sato, K., "Transverse Vibrations of Linearly Tapered Beam with Ends Restrained Elastically Against Rotation and Subjected to Axial Force", Int. J. of Mech. Sci., Vol. 22, 1980, pp. 109.

14. Banerji, J. R. and Wiliams, F. W., "Exact Bernoulli-Euler Dynamic Stiffness Matrix for a Range of Tapered Beams", Intl. J. of Numerical Methods in Engineering, Vol. 21, 1985, pp. 2289.

15. Hutchinson, J. R. and Zillmer, S. D., "On the Transverse Vibration of Beams of Rectangular Cross-section", J. of Applied Mechanics, ASME, Vol. 53, 1986, pp. 278.

16. Subrahmanuam, K. B. and Leissa, A. W., "An improved Finite Difference Analysis of Uncoupled Vibrations of Cantilever Beams", J. of Sound and Vibration, Vol. 98, 1985, pp. 1.

17. Gupta, A. K., "Vibration of Tapered Beams", J. of Structural Engineering, ASCE, Vol. 111, 1985, pp. 19.

18. Sisto, F. and Chang, A. T., "A Finite Element for Vibration Analysis of Twisted Blades Based on Beam Theory", AIAA Journal, Vol. 22, 1984, pp. 1646-1651.

19. Nagarajan, P. and Alwar, R. S., "A Three Dimensional Approach to Blade Packet Vibrations", J. of Sound and Vibration, Vol. 95(3), 1984, pp. 295-303.

20. Rao, J. S., "Single Blade Dynamics", Session Proc. Tech. Comm. on Rotordynamics, Sixth IFToMM Congress, 1983, New Delhi, pp. 41.

21. Rieger, N. F., "Blade Fatigue", Session Proc. Tech. Comm. on Rotordynamics, Sixth IFToMM Congress, 1983, New Delhi, pp. 66.

22. Srinivasan, A. V. "Vibration of Bladed Disc Assemblies - A Selected Review", Session Proc. Tech. Comm. on Rotordynamics, Sixth IFToMM Congress, 1983, New Delhi.

23. Ramamurthy, V. and Balasubramaniam, P., "Analysis of Turbomachine Blades - A Review", Sh.V.B., Aug. 1984, pp. 7.

24. Segerlind, L. J., "Applied Finite Element Analysis", John Wiley and Sons, Inc, 1976, pp. 71-77; 212-222.

25. Littler, D. J., "Thermal Stresses and Thermal Fatigue", Proceedings of the Int. Conference held at Berkeley Castle, Gloucestershire, England, Sept. 22-26, 1969, pp. 374-386.

26. Cubberly, W. H., "ASM Metals Reference Book, American Society for Metals", Metals Park, Ohio, Ed. 9, 1980, Vol. 3, pp. 248- 249.

27. Bahree, R. and Sharan, A. M., "The Heat Transfer and Thermal Stress Analysis in Turbine Blades Subjected to Radiative Boundary Conditions", SCS Summer Computer Simulation Conference, Montreal, Canada, July 1987, pp. 826-831.

28. Bahree, R. and Sharan, A. M., "The Computer-Aided Transient Heat Transfer Analysis in Turbine Blades Using the Non-Linear Finite Element Method", to be published in the Ninth National Heat and Mass Transfer Conference, Indian Institute of Science, Bangalore, India, December, 1987.

29. Zienkiewicz, O. C., "The Finite Element Method", McGraw-Hill Book Company (UK) Ltd., 1977, pp. 169-171.

30. Cook, R. D., "Concepts and Applications of Finite Element Analysis", John Wiley and Sons, Inc., 1981, pp. 113-121.

31. Huebner, K. H. and Thornton, E. A., "The Finite Element Method for Engineers", John Wiley and Sons, Inc., 1982, pp. 187.

32. Guyan, R. J., "Reduction of Stiffness and Mass Matrices", AIAAJ, Vol. 3, No. 2, 1965, pp. 380.

33. Thomson, W. T., "Theory of Vibration with Applications", Prentice-Hall, Inc., 1981, pp. 464-466; 92-94; 25-29.

34. Vyas, N. S., "Vibratory Stress Analysis and Fatigue Life Estimation of Turbine Blade", Ph.D. Thesis, I.I.T. Delhi, India, 1986, pp. 37-39.

35. Rao, J. S., and Vyas, N. S., "Response of Steam Turbine Blades Subjected to Distributed Harmonic Nozzle Excitation", 3rd Int. Modal Analysis Conference, Orlando, Florida, 1985, pp. 618-626.

36. Rao, S. S., "Mechanical Vibrations", Addison-Wesley Publishing Co., 1986, pp. 294-296.

37. Weast, R. C., "Handbook of Chemistry and Physics", CRC Press, Inc., 1975, pp. A155-A156.

38. Timoshenko, S. P. and Goodier, J. N., "Theory of Elasticity", McGraw-Hill Book Co., 1970, pp. 223-224.

39. Akin, J. E., "Application and Implementation of Finite Element Methods", Academic Press Inc. (London) Ltd., 1982, pp. 65-77.

APPENDIX A

THE EXPRESSIONS FOR THE ELEMENTAL MATRICES AND VECTORS FOR THE LINEAR TRIANGULAR ELEMENT

The shape functions for the linear triangular element are (refer to the Fig. A.1)

$$N_\beta = \frac{1}{2A^e}(a_\beta + b_\beta x + c_\beta y), \quad \beta = i,j,k \tag{A.1}$$

where
$$a_i = x_j y_k - x_k y_j$$
$$b_i = y_j - y_k$$
$$c_i = x_k - x_j$$
$$a_j = x_k y_i - y_k x_i$$
$$b_j = y_k - y_i \tag{A.2}$$
$$c_j = x_i - x_k$$
$$a_k = x_i y_j - x_j y_i$$
$$b_k = y_i - y_j$$
$$c_k = x_j - x_i$$

The elemental capacitance matrix can be expressed as

$$\left[CP^e\right] = \int_{V^e} \rho c^e \left[N^e\right]^T \left[N^e\right] dV \tag{A.3}$$

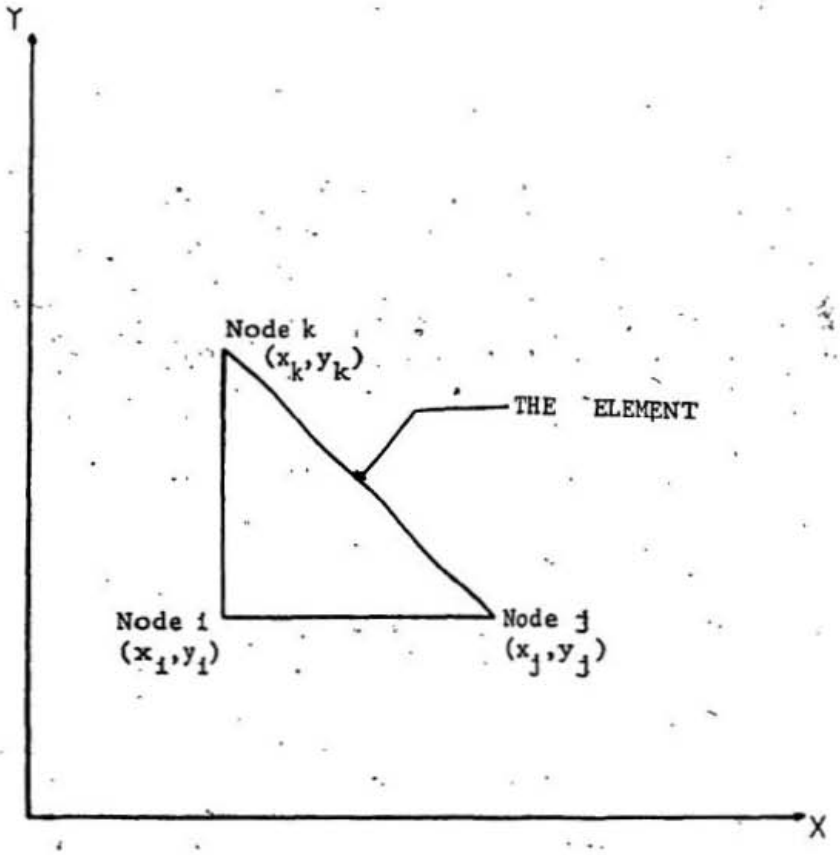

FIG.A.1 THE DETAILS OF THE TRIANGULAR ELEMENT

This can be written in matrix form by evaluating the volume integral for unit thickness as

$$\left[CP^e\right] = \frac{\rho c^e A^e}{12}\begin{bmatrix} 2 & 1 & 1 \\ 1 & 2 & 1 \\ 1 & 1 & 2 \end{bmatrix} \tag{A.4}$$

The conduction matrix can be expressed as

$$\left[K^e\right] = \int_{V^e} \left[B^e\right]^T \left[D^e\right] \left[B^e\right] dV + \int_{S_2^e} h^e \left[N^e\right]^T \left[N^e\right] dS . \tag{A.5}$$

In Eqn. (A.5) the surface integral becomes zero if none of the sides of the triangular element exchange heat by convection. Evaluating the two integrals of Eqn. (A.5) using the volume and area coordinates, the expression for the $\left[K^e\right]$ matrix can be written as

$$\left[K^e\right] = \frac{K_x^e}{4A^e}\begin{bmatrix} b_ib_i & b_ib_j & b_ib_k \\ b_jb_i & b_jb_i & b_jb_k \\ b_kb_i & b_kb_j & b_kb_k \end{bmatrix}$$

$$+ \frac{K_y^e}{4A^e}\begin{bmatrix} c_ic_i & c_ic_j & c_ic_k \\ c_jc_i & c_jc_i & c_jc_k \\ c_kc_i & c_kc_j & c_kc_k \end{bmatrix}$$

$$+ \frac{h^e L_{ij}}{6}\begin{bmatrix} 2 & 1 & 0 \\ 1 & 2 & 0 \\ 0 & 0 & 0 \end{bmatrix} \tag{A.6}$$

Here L_{ij} represents the length of the side i-j of the triangle experiencing heat transfer by convection.

The force vector due to the convective heat transfer can be written as

$$\left\{F_c^e\right\} = \int_{S_2^e} h^e \, T_\infty \left[N^e\right]^T dS \qquad (A.7)$$

This vector for the side i-j of the triangular element can be written as

$$\left\{F_c^e\right\} = \frac{h^e \, T_\infty \, L_{ij}}{2} \begin{Bmatrix} 1 \\ 1 \\ 0 \end{Bmatrix} \qquad (A.8)$$

The force vector due to radiative heat transfer can be expressed as

$$\left\{F_r^e\right\} = \int_{S_2^e} \sigma \in T_\infty^4 \left[N^e\right]^T dS - \int_{S_2^e} \sigma \in \left[N^e\right]^T \left(\left[N^e\right]\left\{T^e\right\}\right)^4 dS \qquad (A.9)$$

The vector can now be written for the side i-j of the element experiencing heat transfer by radiation as

$$\left\{F_c^e\right\} = \frac{\sigma \in L_{ij} \, T_\infty^4}{2} \begin{Bmatrix} 1 \\ 1 \\ 0 \end{Bmatrix} - \frac{\sigma \in L_{ij}}{30} \begin{Bmatrix} 5T_i^4 + 4T_i^3T_j + 3T_i^2T_j^2 + 2T_iT_j^3 + T_j^4 \\ 5T_j^4 + 4T_j^3T_i + 3T_j^2T_i^2 + 2T_jT_i^3 + T_i^4 \\ 0 \end{Bmatrix} \qquad (A.10)$$

APPENDIX B

DECOUPLING OF THE EQUATIONS OF MOTION FOR MODAL ANALYSIS

The equations of motion for a damped system can be expressed as

$$\left[M^G\right]\left\{\ddot{U}\right\} + \left[C^G\right]\left\{\dot{U}\right\} + \left[K^G\right]\left\{U\right\} = \left\{F^G\right\} \qquad (B.1)$$

Now, the displacement vector in the cartesian coordinate system can be expressed as a linear combination of the natural modes of the undamped system. Hence,

$$\{U(t)\} = [\phi]\{q(t)\} \qquad (B.2)$$

Substituting Eqn. (B.2) into Eqn. (B.1) we obtain

$$\left[M^G\right][\phi]\left\{\ddot{q}\right\} + \left[C^G\right][\phi]\left\{\dot{q}\right\} + \left[K^G\right][\phi]\{q\} = \left\{F^G\right\} \qquad (B.3)$$

Premultiplication of Eqn. (B.3) by $[\phi]^T$ leads to

$$[\phi]^T\left[M^G\right][\phi]\left\{\ddot{q}\right\} + [\phi]^T\left[C^G\right][\phi]\left\{\dot{q}\right\} + [\phi]^T\left[K^G\right][\phi]\{q\} = [\phi]^T\left\{F^G\right\} \qquad (B.4)$$

This leads to the diagonalization of the global mass, damping and stiffness matrices respectively. Thus we obtain

$$\left[M\right]\left\{\ddot{q}\right\} + \left[C\right]\left\{\dot{q}\right\} + \left[K\right]\{q\} = \{Q\} \qquad (B.5)$$

In this way we decouple the equations of motion and express the

entire system by individual single degree of freedom systems.

Now, if the matrix of eigenvectors is mass-orthonormalized, then instead of Eqn. (B.5), we obtain

$$\{\ddot{q}\} + 2\xi\omega_n \{\dot{q}\} + \omega_n^2 \{q\} = \{QF\} \tag{B.6}$$

This equation can be expressed for the individual modes as

$$\ddot{q}_i(t) + 2\xi_i\omega_{n_i} \dot{q}_i(t) + \omega_{n_i}^2 q_i(t) = QF_i(t) \tag{B.7}$$

where i represents the mode number.

APPENDIX C

THE TURBINE BLADE AIRFOIL CROSS-SECTIONS

The turbine blade has a complicated geometry. It is twisted, tapered, asymmetric and has an airfoil cross-section. In this Appendix, the blade profiles at various cross-sections from the root to the tip are shown. One can get a good idea of the blade geometry by looking at these cross-sections.

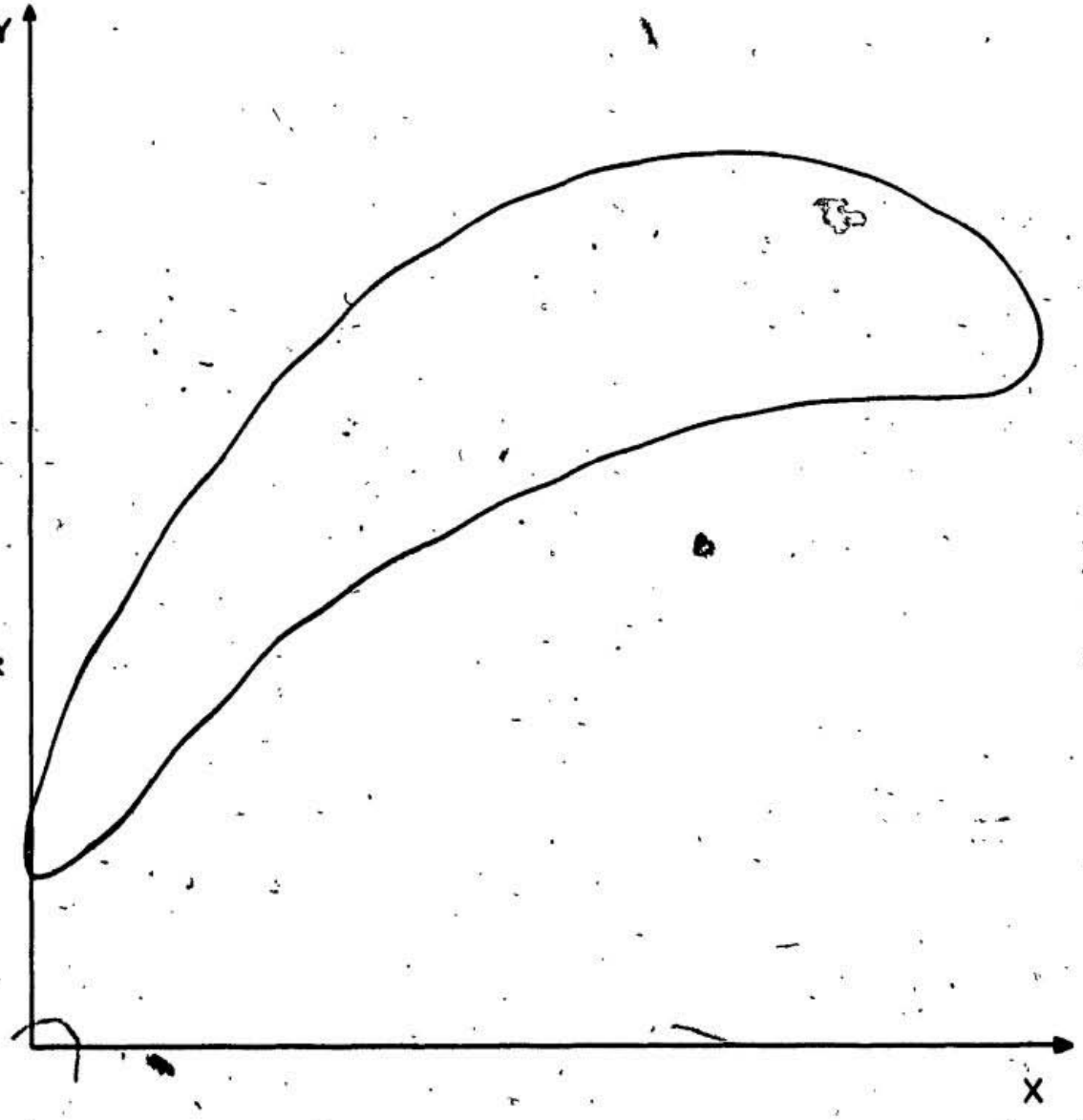

Fig. C.1 The Turbine Blade Airfoil Cross-section at the Root (Z = 0.0 m)

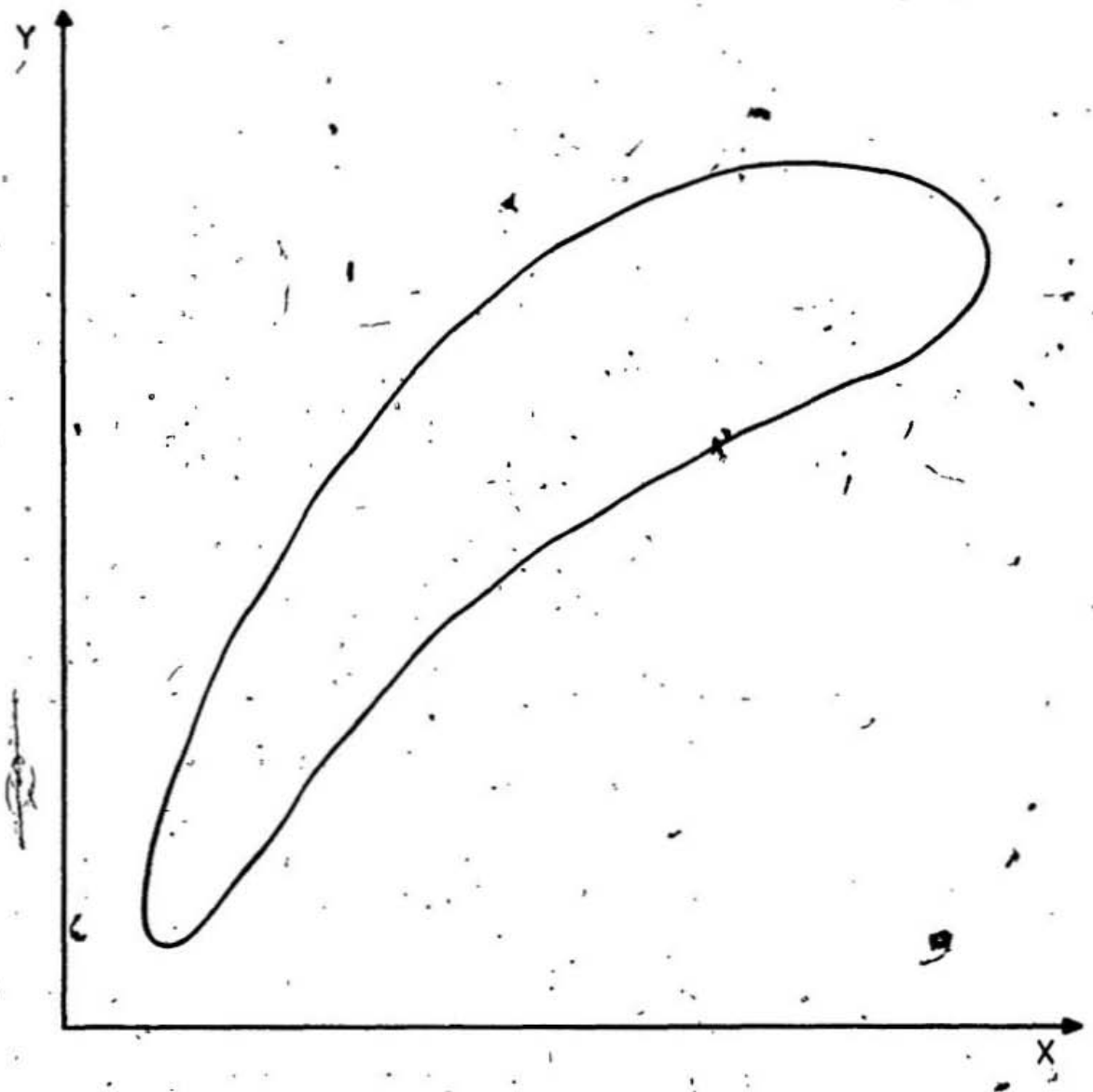

Fig. C.2 The Turbine Blade Airfoil Cross-section at Z=0.025m

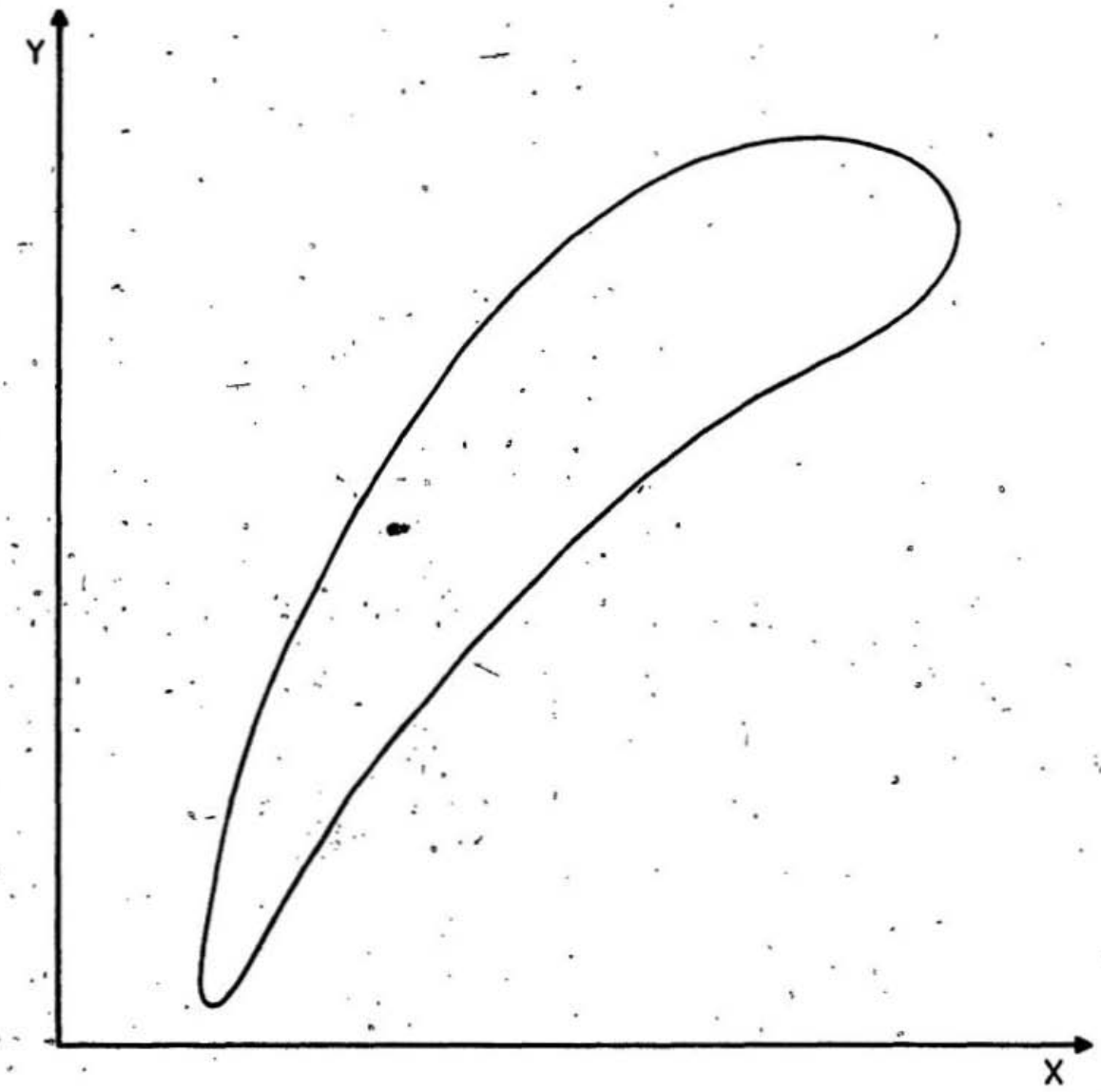

Fig. C.3 The Turbine Blade Airfoil Cross-section at Z=0.05 m.

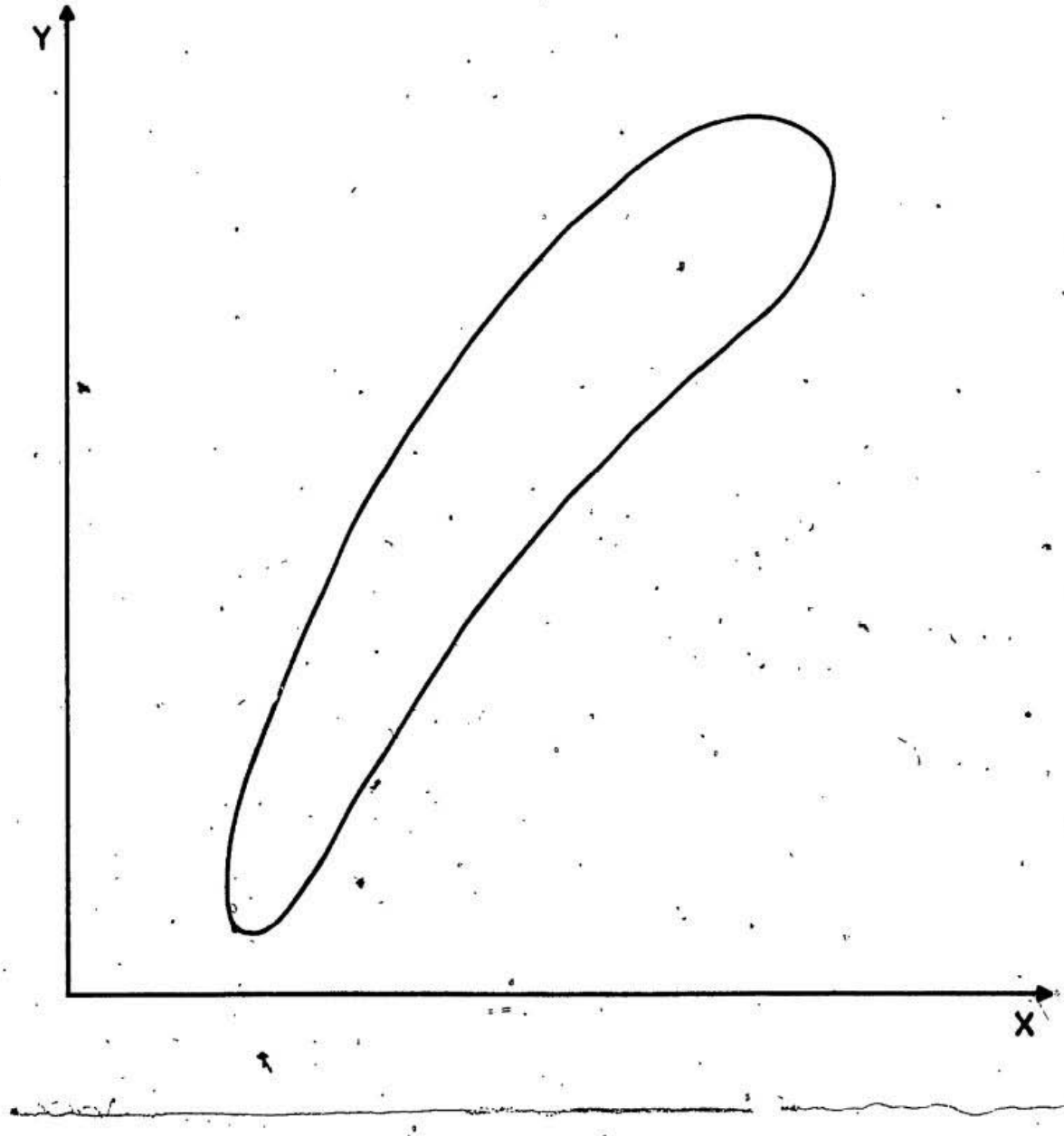

Fig. C.4 The Turbine Blade Airfoil Cross-section at Z=0.075m

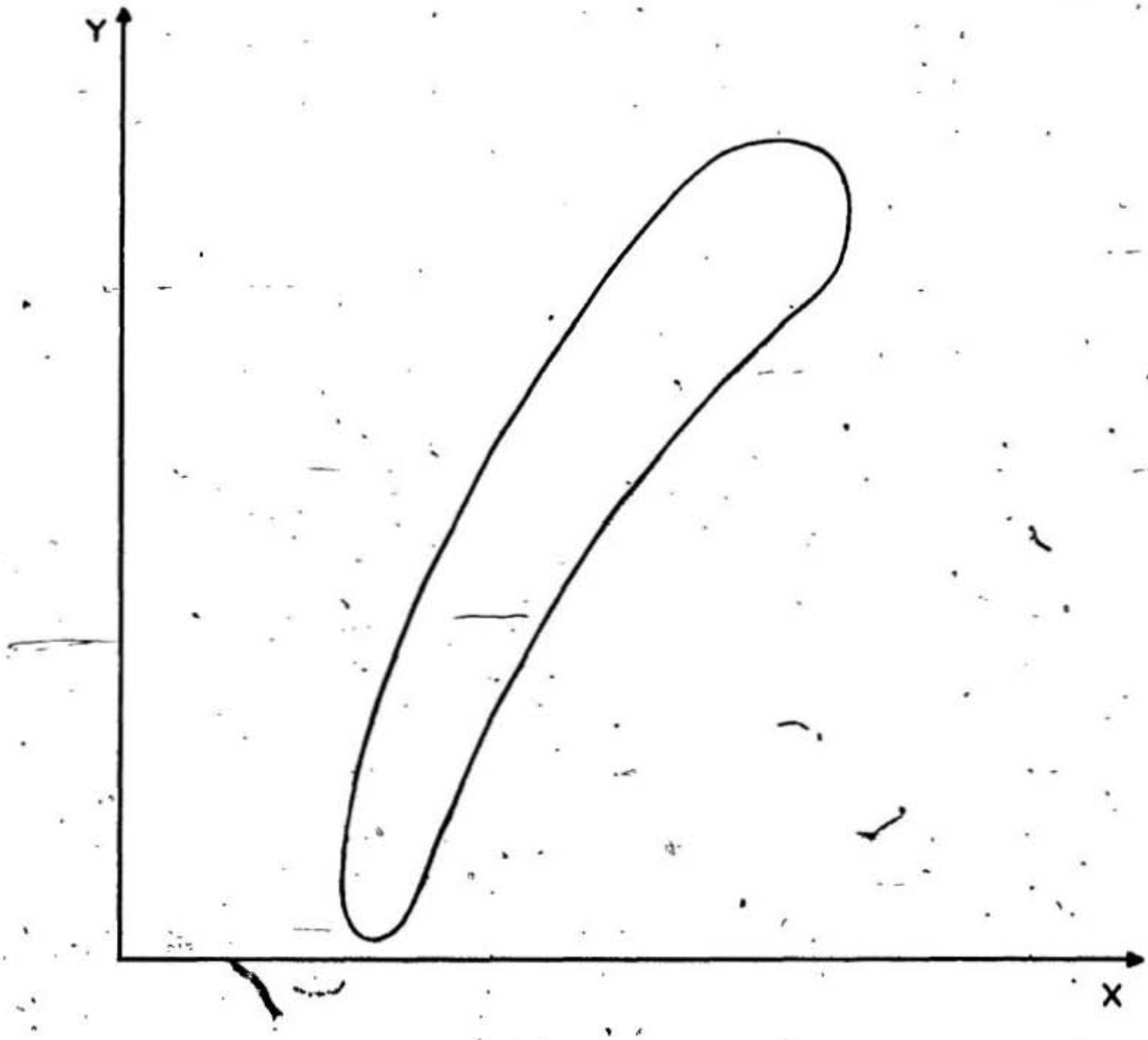

Fig. C.5 The Turbine Blade Airfoil Cross-section at Z = 0.1 m

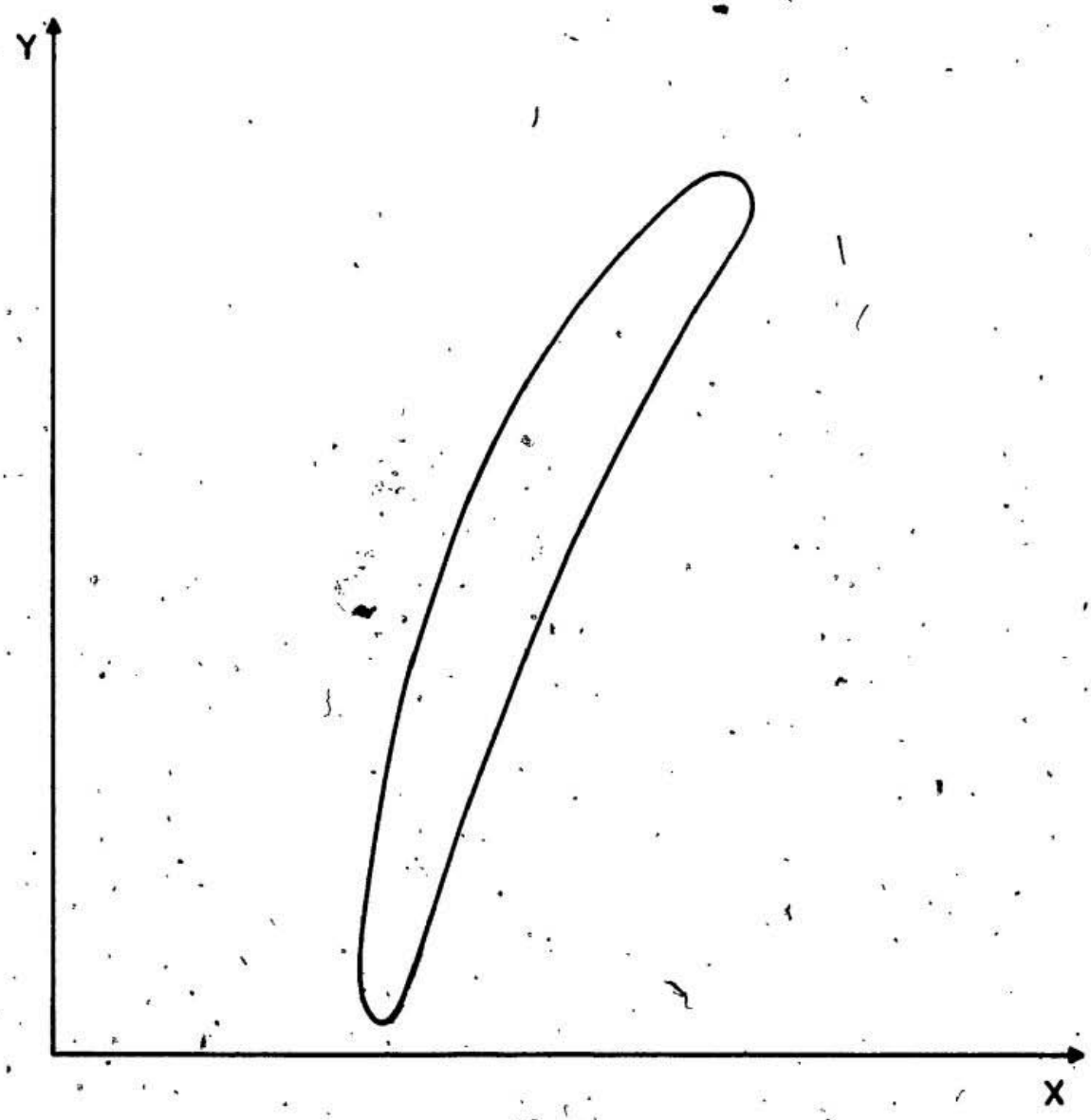

Fig. C.6 The Turbine Blade Airfoil Cross-section at the Tip (Z = 0.11 m)

APPENDIX D

DESCRIPTION AND LISTING OF THE COMPUTER PROGRAMS

The computer software for this thesis was developed in the FORTRAN language and the computations were carried out on the VAX 8800 digital computer. A listing of all of the computer programs is given in this Appendix. These programs can be executed by using suitable input and output data files. A number of IMSL subroutines are used in these programs for matrix multiplication, transposition and inversion. IMSL subroutines are also used in the free vibration analysis to determine the eigenvalues and eigenvectors. A brief description about each program is given below.

The program MESH generates the triangular mesh within an airfoil cross-section of the blade. The coordinates of the airfoil cross-section are input as data for both the pressure and suction surfaces respectively. The value of the y-intercept for any value of x was achieved by using cubic interpolation routine SPLFIT.

The program TEMPGRAD calculates the transient temperatures and temperature gradient distribution within the turbine blade cross-section. The temperature dependent material properties of the blade were input as data and the properties at any value of temperature were interpolated by using the cubic interpolation routine SPLFIT. The heat transfer coefficient distribution was also input for both

pressure and suction surfaces respectively. The value of 'h' was also dependent on the temperature of the blade and this too was fed as input. A flow chart depicting the various steps to be followed in the program is shown in Fig. D.1.

The program TSTRESS calculates the thermal stress within each element after the nodal temperatures are known. Once again the input data consists of the temperature dependent material properties of the blade and the use of SPLFIT to interpolate the material properties at any temperature. The stresses are summed up according to their nature after every time increment.

The program ISO calculates the natural frequencies of the uncondensed system matrices using the twenty-noded isoparametric finite element formulation. The shape function for each node and its derivatives are calculated in the subroutine SHAPE20. These are then used in the integration of the stiffness and mass matrices for each Gauss point within the 20-noded element in the subroutine STIFFMASS20. In the subroutine SHAPE20, each of the 20 nodes of the 20-noded element is defined by its local coordinates ξ, η and ζ which are input as data. The shape functions and their derivatives are calculated using these values of ξ, η and ζ. In the subroutine STIFFMASS20, the elemental stiffness and mass matrices for each Gauss point are of the order 60×60. The total element stiffness and mass matrices are obtained by adding up the stiffness and mass matrices evaluated at each Gauss point. A general guidance

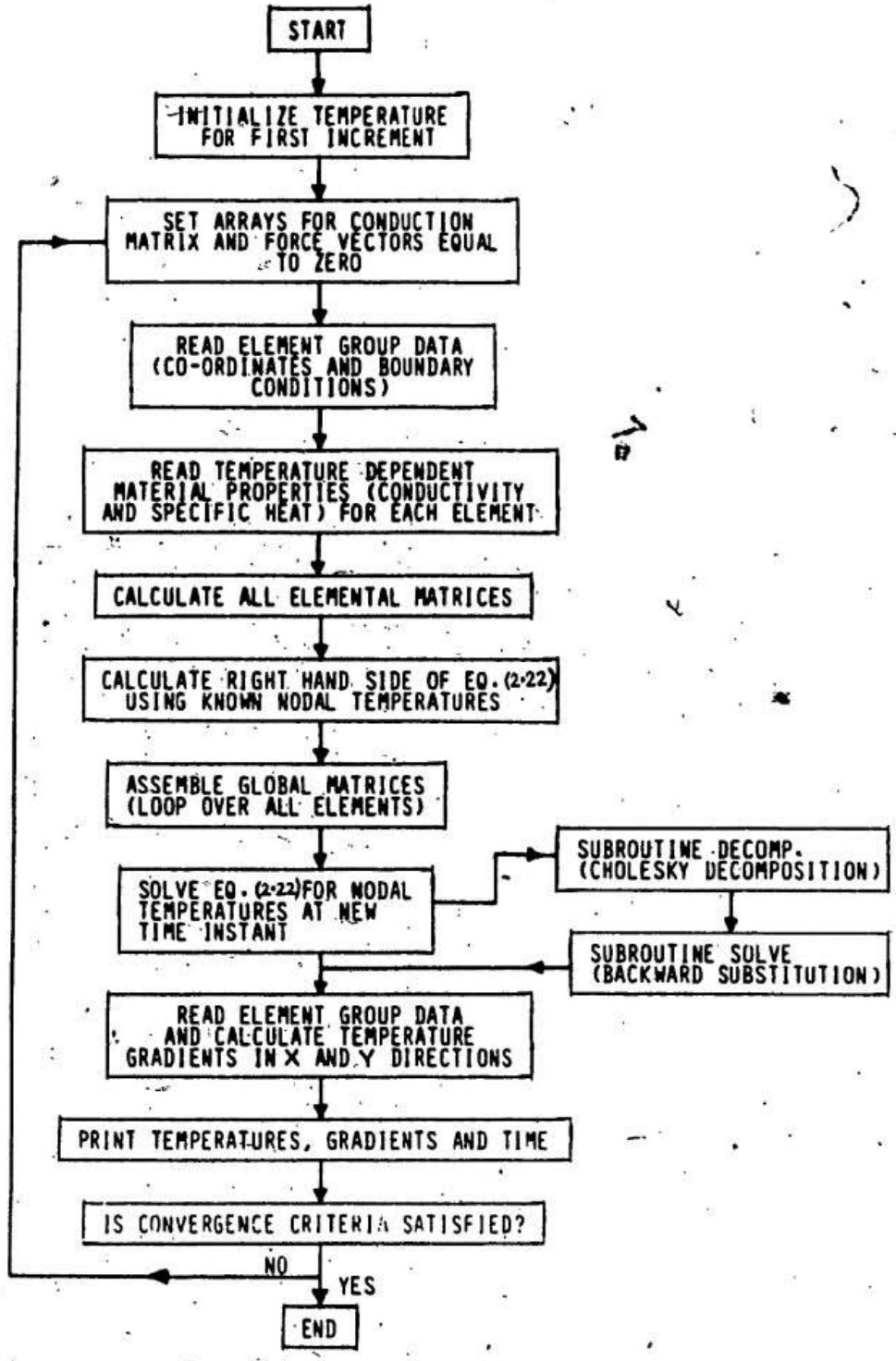

FIG.D.1 THE FLOW CHART FOR THE TRANSIENT STATE THERMAL ANALYSIS

in the programming of isoparametric finite elements was obtained from [39]. The effect of temperature on the natural frequencies was studied by making use of the temperatures achieved at every time instant from the program TEMPGRAD. The modulus of elasticity was evaluated at these temperatures. This caused the stiffness matrix to become temperature dependent.

The program FREQ calculates the undamped natural frequencies of the turbine blade by condensing the global stiffness and mass matrices by using the Guyan's dynamic matrix reduction scheme. This program also calculates the matrix of eigenvectors for the condensed system. The dynamic equations of motion are decoupled using the modal matrix. The modal matrix is then mass-orthonormalized. The frequencies, the transformation matrix and the mass-orthonormalized modal matrix are then stored for further use in the calculation of the dynamic response and stresses.

The program TRANSVIB calculates the transient dynamic response and the dynamic stresses due to nozzle excitation and centrifugal forces respectively. The program is so structured that the dynamic response and stresses due to either nozzle excitation or centrifugal forces can be determined by making use of appropriate comment statements. The nozzle excitation forces are distributed along the height of the blade in the x and y directions respectively. The equations of kinematics are used to calculate every impulse impinging on the blade in the time domain as the rotor

accelerates with an angular acceleration of 800 RPM/min.

The vibratory stress vector is calculated by feeding in the values of the nodal displacements at every time instant. This stress vector is calculated by the subroutine STRESS20 by making use of the isoparametric finite element formulation. The principal stresses are calculated from this stress vector and then the distortion energy stress is calculated.

```
C*********************************************************************
C*
C* LISTING OF THE PROGRAM **MESH**
C* PROGRAM TO GENERATE TRIANGULAR FINITE ELEMENT
C* MESH IN BLADE AIRFOIL CROSS-SECTION
C*
C*********************************************************************

      DIMENSION XT(28),YT(28),YB(31),XB(31)
      DIMENSION X(1000),Y(1000)
      DIMENSION P(100),Q(100),R(100),S(100),T(100)

      DATA XT/0.0,0.01,0.17,0.51,1.07,1.9,3.05,4.57,6.47,8.73,
     + 11.26,13.9,16.46,18.83,20.96,22.83,24.46,25.87,27.08,
     + 28.11,28.99,29.73,30.33,30.83,31.22,31.51,31.72,31.88/

      DATA YT/12.1,12.81,13.71,14.76,15.94,17.21,18.51,19.76,
     + 20.85,21.66,22.05,21.96,21.41,20.48,19.27,17.88,16.39,
     + 14.85,13.31,11.82,10.4,9.08,7.89,6.85,5.98,5.27,4.77,
     + 4.36/

      DATA XB/0.0,0.11,0.32,0.17,1.19,1.87,2.69,3.64,4.68,5.8,
     + 6.96,8.14,9.32,10.48,11.68,12.92,14.26,15.69,17.16,18.71
     + ,20.25,21.75,23.2,24.57,25.85,27.02,28.07,28.97,29.63,
     + 30.33,31.11/

      DATA YB/12.1,11.78,11.27,11.11,11.07,11.13,11.29,11.54,
     + 11.85,12.2,12.57,12.89,13.16,13.35,13.44,13.4,13.2,12.84,
     + 12.32,11.68,10.89,10.06,9.2,8.33,7.49,6.7,5.97,5.33,4.79,
     + 4.35,3.78/

      COMMON U,X1(28),Y1(28),A1(28),B1(28),C1(28)
      COMMON W,X2(31),Y2(31),A2(31),B2(31),C2(31)

C*********************************************************************
C DATA XT,YT REPRESENT COORDINATES OF THE SUCTION
C SURFACE OF THE BLADE AIRFOIL CROSS-SECTION
C
C DATA XB,YB REPRESENT COORDINATES OF THE PRESSURE
C SURFACE OF THE BLADE AIRFOIL CROSS-SECTION
C*********************************************************************

      DO 1 I=1,28
      X1(I)=XT(I)
```

```
 1   Y1(I)=YT(I)

DO 2 I=1,31
X2(I)=XB(I)
 2   Y2(I)=YB(I)

OPEN(UNIT=2,FILE='NODE.DAT',TYPE='NEW')
OPEN(UNIT=3,FILE='NMESH.DAT',TYPE='NEW')

U=28
W=31

X(1)=0.0
Y(1)=12.10
X(106)=31.88
Y(106)=4.36
X(100)=31.11
Y(100)=3.78

X(2)=31.88/15.0
DX=31.88/15.0

II=2
III=7
ICOUNT=1

 15 DO 5 I=II,III+1
 5 X(I)=X(II)

DO 10 I=II,III
XD=X(I)
CALL SPLFIT(U,X1,Y1,A1,B1,C1)
Y(III+1)=SUCTION(XD)
CALL SPLFIT(W,X2,Y2,A2,B2,C2)
Y(II)=PRESSURE(XD)
DY=(Y(III+1)-Y(II))/7.0
INC=I+1

IF(I.EQ.(II))DY=DY/2.0
IF(I.EQ.(II+1))DY=DY
IF(I.EQ.(II+2))DY=2*DY
IF(I.EQ.(II+3))DY=2*DY
IF(I.EQ.(II+4))DY=DY
IF(I.EQ.(II+5))DY=DY/2.0
```

```
Y(INC)=Y(I)+DY
 10 CONTINUE

IP=II
ICOUNT=ICOUNT+1
II=II+7
III=III+7
X(II)=X(IP)+DX
IF(ICOUNT.LE.14)GO TO 15
DXX=(X(106)-X(100))/6.0
SL=(Y(106)-Y(100))/(X(106)-X(100))
DO 100 I=101,105
I1=I-1
  X(I)=X(I1)+DXX
 100  Y(I)=SL*DXX+Y(I1)

IC=1
NF1=8
II=1
III=6
ID=2
L=1
NEL=7

DO 103 IM=2,99
 103 WRITE(2,93)X(IM),Y(IM),IM

 93 FORMAT(10X,2F10.4,I5)
 94 FORMAT(I3,2X,I3,2X,I3,2X,I3,2X,F7.4,2X,F7.4,2X,
    + F7.4,2X,F7.4,2X,F7.4,2X,F7.4)
 95 FORMAT(17X,F7.4,2X,F7.4,2X,F7.4,2X,F7.4,2X,F7.4
    + ,2X,F7.4)

IN=1
WRITE(3,95)X(1),Y(1),X(8),Y(8),X(7),Y(7)
WRITE(3,95)X(1),Y(1),X(7),Y(7),X(6),Y(6)
WRITE(3,95)X(1),Y(1),X(6),Y(6),X(5),Y(5)
WRITE(3,95)X(1),Y(1),X(5),Y(5),X(4),Y(4)
WRITE(3,95)X(1),Y(1),X(4),Y(4),X(3),Y(3)
WRITE(3,95)X(1),Y(1),X(3),Y(3),X(2),Y(2)

 305 CONTINUE
```

```
      DO 105 I=II,III
      IT1=ID
      IT2=ID+1
      IT3=NF1+1
      IT4=NF1+2
      WRITE(3,94)NEL,IT1,IT4,IT3,X(IT1),Y(IT1),X(IT4),
     1 Y(IT4),X(IT3),Y(IT3)
      NEL=NEL+1
      WRITE(3,94)NEL,IT2,IT4,IT1,X(IT2),Y(IT2),X(IT4),
     1 Y(IT4),X(IT1),Y(IT1)
      NEL=NEL+1

      ICOUNT=IN*7
      ID=ID+1
      NF1=NF1+1
      IC=IC+1
      IN=IN+1
  105 CONTINUE

      ID=ID+1
      NF1=NF1+1
      L=L+1
      IF(L.LE.14)GO TO 305

      STOP
      END


      FUNCTION SUCTION(XF)
      COMMON U,X1(28),Y1(28),A1(28),B1(28),C1(28)
      COMMON W,X2(31),Y2(31),A2(31),B2(31),C2(31)
      DO 10 I=1,U
      IF(X1(I).GT.XF) GO TO 20
   10 CONTINUE
   20 I=I-1
      DX=XF-X1(I)
      SUCTION=Y1(I)+DX*(A1(I)+DX*(B1(I)+DX*C1(I)))
C     WRITE(5,*)YT,A1,B1,C1
      RETURN
      END


      FUNCTION PRESSURE(ST)
      COMMON U,X1(28),Y1(28),A1(28),B1(28),C1(28)
```

```
COMMON W,X2(31),Y2(31),A2(31),B2(31),C2(31)
DO 100 I=1,W
IF(X2(I).GT.ST)GO TO 200
 100 CONTINUE
 200 I=I-1
DXX=ST-X2(I)
PRESSURE=Y2(I)+DXX*(A2(I)+DXX*(B2(I)+DXX*C2(I)))
RETURN
END

SUBROUTINE SPLFIT(V,X,Y,B,C,D)
  DIMENSION X(V),Y(V),B(V),C(V),D(V)
VM1=V-1
IF(V.LT.2) RETURN
IF(V.LT.3) GO TO 50
D(1)=X(2)-X(1)
C(2)=(Y(2)-Y(1))/D(1)
DO 10 I=2,VM1
D(I)=X(I+1)-X(I)
B(I)=2.*(D(I-1)+D(I))
C(I+1)=(Y(I+1)-Y(I))/D(I)
C(I)=C(I+1)-C(I)
 10 CONTINUE
B(1)=-D(1)
B(V)=-D(V-1)
C(1)=0.
C(V)=0.
IF(V.EQ.3) GO TO 15
C(1)=C(3)/(X(4)-X(2))-C(2)/(X(3)-X(1))
C(V)=C(V-1)/(X(V)-X(V-2))-C(V-2)/(X(V-1)-X(V-3))
C(1)=C(1)*D(1)**2/(X(4)-X(1))
C(V)=-C(V)*D(V-1)**2/(X(V)-X(V-3))
 15 DO 20 I=2,V
T=D(I-1)/B(I-1)
B(I)=B(I)-T*D(I-1)
C(I)=C(I)-T*C(I-1)
 20 CONTINUE
C(V)=C(V)/B(V)
DO 30 IB=1,VM1
I=V-IB
C(I)=(C(I)-D(I)*C(I+1))/B(I)
 30 CONTINUE
B(V)=(Y(V)-Y(VM1))/D(VM1)+D(VM1)*(C(VM1)+2.*C(V))
```

```
      DO 40 I=1,VM1
      B(I)=(Y(I+1)-Y(I))/D(I)-D(I)*(C(I+1)+2.*C(I))
      D(I)=(C(I+1)-C(I))/D(I)
      C(I)=3.*C(I)
   40 CONTINUE
      C(V)=3.*C(V)
      D(V)=D(V-1)
      RETURN
   50 B(1)=(Y(2)-Y(1))/(X(2)-X(1))
      C(1)=0.
      D(1)=0.
      B(2)=B(1)
      C(2)=0.
      D(2)=0.
      RETURN
      END
```

```
C*****************************************************************
C*
C* LISTING OF THE PROGRAM **TEMPGRAD**
C* PROGRAM TO CALCULATE TRANSIENT TEMPERATURES AND
C* TEMPERATURE GRADIENTS IN A TURBINE BLADE USING F.E.M.
C*
C*****************************************************************

    REAL LENG,LAMBDA,ITEMP,COUNT
DIMENSION XX(11),YY(11),XXX(11),YYY(11),XS(11),HS(11)
DIMENSION NS(3),ESM1(3,3),EF(3),X(3),Y(3),B(3),C(3)
DIMENSION D(10000),T(60000),A(60000),G(60000),DXTG(11)
DIMENSION EF1(3),EF2(3),EF3(3),EF4(3),ISIDE(2),XT(8)
DIMENSION CAP(3,3),ESM2(3,3),PM(3),AK(3),ESM(3,3)
DIMENSION XP(11),HP(11),DYTG(11),YT(8)

DATA NCL/1/
DATA XX/21.0,93.0,205.0,315.0,425.0,540.0,650.0,760.0,
     1 870.0,980.0,1090.0/
DATA YY/12.7,13.0,13.5,13.8,15.1,15.2,17.3,14.0,21.6,24.9
     1 ,29.7/
DATA XXX/21.0,93.0,205.0,315.0,425.0,540.0,650.0,760.0,
     1 870.0,980.0,1090.0/
DATA YYY/400.0,400.0,395.0,420.0,440.0,420.0,460.0,480.0,
     1 500.0,525.0,565.0/
DATA XS/0.0,0.109,0.1359,0.2709,0.4059,0.5409,0.6219,0.6759,
     1 0.8109,0.9459,1.0/
DATA HS/2470.6,1117.65,1176.47,2000.0,2588.23,2941.0,3000.0,
     1 ,2941.0,2823.5,2588.2,2529.0/
DATA XP/0.0,0.0549,0.1359,0.2709,0.3249,0.4059,0.5409,0.6759,
     1 0.8109,0.9459,1.0/
DATA HP/2470.6,1294.1,1764.7,1470.6,1411.78,1410.0,1529.4,
     1 1647.0,1764.7,1823.5,1825.0/
DATA DXTG/0.0,5.0,10.0,15.0,20.0,25.0,30.0,35.0,40.0,45.0,
     1 100.0/
DATA DYTG/303.0,573.0,863.0,1143.0,1143.0,1143.0,1143.0,
     1 1143.0,1143.0,1143.0,1143.0/
DATA XT/0.0,6.0,12.0,18.0,24.0,30.0,36.0,100.0/
DATA YT/0.1,0.14,0.17,0.2,0.26,0.34,0.37,0.4/

COMMON Z,X4(11),Y4(11),A4(11),B4(11),C4(11)
COMMON Q,X5(11),Y5(11),A5(11),B5(11),C5(11)
COMMON V,X2(11),Y2(11),A2(11),B2(11),C2(11)
COMMON U,X1(11),Y1(11),A1(11),B1(11),C1(11)
```

```
      COMMON W,X6(11),Y6(11),A6(11),B6(11),C6(11)
      COMMON S,X7(8),Y7(8),A7(8),B7(8),C7(8)

C*****************************************************************
C
C AKTEH    THERMALCOND. OF MAT.
C H     CONVECTION HEAT TRANSFER COEFF.
C DELTA  TIME STEP IN SECS.
C TO     FLUID TEMP. AT PREVIOUS TIME INSTANCE
C TN     FLUID TEMP. AT CURRENT TIME INSTANCE
C SIGMA  STEFAN BOLTZMANN CONSTANT
C NCL    NO. OF LOADING CASES
C ISIDE  SIDE WITH CONVECTION AND RADIATION BOUNDARY
C LENG   LENGTH OF THE SIDE
C DATA XX,XXX   TEMPERATURES
C DATA YY   SPECIFIC HEAT
C DATA YYY  CONDUCTIVITY
C DATA HS   CONVECTIVE  HEAT TRANSFER COEFF.(SUCTION SURFACE)
C DATA HP   CONVECTIVE  HEAT TRANSFER COEFF.(PRESSURE SURFACE)
C DATA XS   CHORD LENGTH RATIO (SUCTION SURFACE)
C DATA XP   CHORD LENGTH RATIO (PRESSURE SURFACE)
C DATA XT,DXTG   TIME
C DATA YT   H/HO RATIO
C DATA DYTG   GAS, TEMPERATURE  VARIATION
C
C*****************************************************************

      RHO=8526.0
      TEMP1=0.0
      TOTAL=0.0
      CHORD=0.3188
      DELTA=0.5
      EPSI=0.7
      SIGMA=5.669E-8
      PRO=EPSI*SIGMA
      COUNT=2.0

      OPEN(UNIT=2,FILE='NMESH.DAT',TYPE='OLD')
      OPEN(UNIT=3,FILE='T.DAT',TYPE='NEW')

      U=11
      V=11
      Q=11
      Z=11
```

```
W=11
S=8

IS=0
IK=0

NP=106
NE=174
NBW=16

C*****************************************************************
C INITIALIZING DATA
C*****************************************************************

DO 5 I=1,11
X2(I)=XXX(I)
 5 Y2(I)=YYY(I)

DO 6 I=1,11
X1(I)=XX(I)
 6 Y1(I)=YY(I)

DO 7 I=1,11
X5(I)=XS(I)
 7 Y5(I)=HS(I)

DO 8 I=1,11
X4(I)=XP(I)
 8 Y4(I)=HP(I)

DO 9 I=1,11
X6(I)=DXTG(I)
 9 Y6(I)=DYTG(I)

DO 4 I=1,8
X7(I)=XT(I)
 4 Y7(I)=YT(I)

JGF=NP
JGSM=JGF*2
JEND=JGSM+NP+NBW

DO 100 I=1,JEND
 100 A(I)=0.0
```

```
      DO 110 I=1,JGF
      A(I)=303.0
       110 CONTINUE
       10 CONTINUE

      DO 120 I=JGF+1,JEND
      A(I)=0.0
       120 CONTINUE

      C*********************************************************************
      C READ   ELEMENT   GROUP   DATA
      C*********************************************************************

       DO  130 KK=1,NE
      READ(2,*) NEL,NS,X(1),Y(1),X(2),Y(2),X(3),Y(3),ISIDE(1)
          1 ,ISIDE(2)

      DO 302 I=1,3
      X(I)=X(I)/100.0
      302 Y(I)=Y(I)/100.0

      B(1)=Y(2)-Y(3)
      B(2)=Y(3)-Y(1)
      B(3)=Y(1)-Y(2)
      C(1)=X(3)-X(2)
      C(2)=X(1)-X(3)
      C(3)=X(2)-X(1)
      AR4=ABS((X(2)*Y(3)+X(3)*Y(1)+X(1)*Y(2)-X(2)*Y(1)
          +   -X(3)*Y(2)-X(1)*Y(3)))*2.0
      ITEMP=(((A(NS(1))+A(NS(2))+A(NS(3)))/3.0)-273.0)

      IF(ITEMP.LE.21.0)THEN
      AKTEH=12.7
      SPEHT=400.0
      ELSE
      CALL SPLFIT(U,X1,Y1,A1,B1,C1)
      AKTEH=BKTH(ITEMP)
      CALL SPLFIT(V,X2,Y2,A2,B2,C2)
      SPEHT=SPHEAT(ITEMP)
      END IF

       1 LAMBDA=RHO*SPEHT
      PTIME=TIME-DELTA
```

```
IF(TIME.EQ.0.0)THEN
FACT=0.1
ELSE
CALL SPLFIT(S,X7,Y7,A7,B7,C7)
FACT=RATIO(TIME)
END IF

IF(TIME.GT.36.0)FACT=(0.03*TIME/64.0)+0.37
IF(TIME.GT.100.0)FACT=0.4

IF(TIME.LE.15.0)THEN
TN=(TIME*31.533)+303.0
TO=((TIME-DELTA)*31.533)+303.0
ELSE
TN=1143.0
TO=1143.0
END IF

IF(TIME.EQ.0.0)TN=303.0
IF(TIME.EQ.0.0)TO=303.0

DO 140 I=1,3
AK(I)=A(NS(I))
 140 CONTINUE

C*********************************************************************
C CALCULATE ELEMENT CONDUCTION AND CAPACITANCE
C MATRICES AND THE FORCE VECTORS DUE TO
C CONVECTION AND RADIATION
C*********************************************************************

DO 150 I=1,3
EF(I)=0.0
PM(I)=0.0
DO 150 J=1,3
ESM(I,J)=(AKTEH*B(I)*B(J)+AKTEH*C(I)*C(J))/AR4
 150 CONTINUE

DO 160 I=1,2
IF (ISIDE(I).LE.0)GO TO 160

J=ISIDE(I)
K=J+1
IF(J.EQ.3)K=1
```

```
LENG=SQRT((X(K)-X(J))**2.+(Y(K)-Y(J))**2.)
XBAR=(X(K)+X(J))/2.0
CRATIO=XBAR/CHORD
IF(ISIDE(I).EQ.1)GO TO 151
IF(ISIDE(I).EQ.3)GO TO 152
 151 CALL SPLFIT(Q,X5,Y5,A5,B5,C5)
H=HTCS(CRATIO)
H=H*FACT

GO TO 153

 152 CALL SPLFIT(Z,X4,Y4,A4,B4,C4)
H=HTCP(CRATIO)
H=H*FACT
 153 HL=H*LENG
EF(J)=HL*TO/2.0
EF(K)=HL*TO/2.0
M=NS(J)
N=NS(K)


EF1(J)=PRO*LENG*(TO**4)/2.0
EF2(K)=PRO*LENG*(TO**4)/2.0
EF31=((5*A(M)**4)+(4*A(N)*A(M)**3)+(3*A(M)*A(M)
     +    *A(N)*A(N))+(2*A(M)*A(N)**3)+(A(N)**4))
EF3(J)=(PRO*LENG/30.0)*(EF31)
EF41=((5*A(N)**4)+(4*A(M)*A(N)**3)+(3*A(M)*A(M)
     +  *A(N)*A(N))+(2*A(N)*A(M)**3)+(A(M)**4))
EF4(K)=(PRO*LENG/30.0)*(EF41)

EF(J)=EF(J)-EF3(J)+EF1(J)
EF(K)=EF(K)-EF4(K)+EF2(K)

ESM(J,J)=ESM(J,J)+(HL*2)/6.0
ESM(J,K)=ESM(J,K)+HL/6.0
ESM(K,J)=ESM(J,K)
ESM(K,K)=ESM(K,K)+(HL*2)/6.0

 160 CONTINUE

DP=LAMBDA*AR4/48.0
CAP(1,1)=DP*2
CAP(1,2)=DP*1
CAP(1,3)=DP*1
```

```
CAP(2,1)=DP*1
CAP(2,2)=DP*2
CAP(2,3)=DP*1
CAP(3,1)=DP*1
CAP(3,2)=DP*1
CAP(3,3)=DP*2

C*****************************************************************
C CALCULATE  R.H.S.  OF EQN.(2.22) USING  CRANK-NICOLSON
C FINITE DIFFERENCE SCHEME FOR PREVIOUS  INSTANT OF TIME
C*****************************************************************

DO 170 I=1,3
DO 170 J=1,3
ESM1(I,J)=(2.*CAP(I,J)/DELTA)-ESM(I,J)
 170 CONTINUE

DO 180 I=1,3
DO 180 J=1,3
PM(I)=PM(I)+(ESM1(I,J)*AK(J))
 180 CONTINUE

DO 210 I=1,3
EF(I)=PM(I)+EF(I)
 210 CONTINUE

DO 130 I=1,3
II=NS(I)
J5=NP+II
A(J5)=A(J5)+EF(I)
IK=IK+1
 130 CONTINUE

REWIND 2

DO 300 I=1,JGSM
 300 D(I)=A(I)

 270 DO 301 I=1,JGF
A(I)=0.5*(A(I)+D(I))
 301 D(I)=A(I)
TEMP2=0.0

C*****************************************************************
```

```
C READ  ELEMENT  GROUP  DATA & CALCULATE  R.H.S. OF
C EQN.(2.22) FOR THE NEXT INSTANT INSTANT  OF TIME
C*****************************************************************

DO 436 KK=1,NE
READ(2,*) NEL,NS,X(1),Y(1),X(2),Y(2),X(3),Y(3),ISIDE(1)
     1 ,ISIDE(2)

DO 303 I=1,3
X(I)=X(I)/100.0
 303 Y(I)=Y(I)/100.0

B(1)=Y(2)-Y(3)
B(2)=Y(3)-Y(1)
B(3)=Y(1)-Y(2)
C(1)=X(3)-X(2)
C(2)=X(1)-X(3)
C(3)=X(2)-X(1)
AR4=ABS((X(2)*Y(3)+X(3)*Y(1)+X(1)*Y(2)-X(2)*Y(1)
     +  -X(3)*Y(2)-X(1)*Y(3)))*2.0

ITEMP=(((A(NS(1))+A(NS(2))+A(NS(3)))/3.0)-273.0)

IF(ITEMP.LE.21.0)THEN
AKTEH=12.7
SPEHT=400.0
ELSE
CALL SPLFIT(U,X1,Y1,A1,B1,C1)
AKTEH=BKTH(ITEMP)

CALL SPLFIT(V,X2,Y2,A2,B2,C2)
SPEHT=SPHEAT(ITEMP)
END IF

 2 LAMBDA=RHO*SPEHT

PTIME=TIME-DELTA

IF(TIME.EQ.0.0)THEN
FACT=0.1
ELSE
CALL SPLFIT(S,X7,Y7,A7,B7,C7)
FACT=RATIO(TIME)
END IF
```

```
IF(TIME.GT.36.0)FACT=(0.03*TIME/64.0)+0.37
IF(TIME.GT.100.0)FACT=0.4

IF(TIME.LE.15.0)THEN
TN=(TIME*31.533)+303.0
TO=((TIME-DELTA)*31.533)+303.0
ELSE
TN=1143.0
TO=1143.0
END IF

IF(TIME.EQ.0.0)TN=303.0
IF(TIME.EQ.0.0)TO=303.0

DO 450 I=1,3
EF(I)=0.0
DO 450 J=1,3
ESM(I,J)=(AKTEH*B(I)*B(J)+AKTEH*C(I)*C(J))/AR4
 450 CONTINUE

DO 460 I=1,2
IF(ISIDE(I).LE.0) GO TO 460
J=ISIDE(I)
K=J+1
IF(J.EQ.3)K=1
LENG=SQRT((X(K)-X(J))**2.+(Y(K)-Y(J))**2.)
XBAR=(X(K)+X(J))/2.0
CRATIO=XBAR/CHORD

IF(ISIDE(I).EQ.1)GO TO 451
IF(ISIDE(I).EQ.3)GO TO 452

 451 CALL SPLFIT(Q,X5,Y5,A5,B5,C5)
H=HTCS(CRATIO)
H=H*FACT

GO TO 453

 452 CALL SPLFIT(Z,X4,Y4,A4,B4,C4)
H=HTCP(CRATIO)
H=H*FACT

 453 HL=H*LENG
```

```
      EF(J)=HL*TH/2.0
      EF(K)=HL*TH/2.0
      M=NS(J)
      N=NS(K)

      EF1(J)=PRO*LENG*(TH**4)/2.0
      EF2(K)=PRO*LENG*(TH**4)/2.0
      EF31=((5*A(M)**4)+(4*A(N)*A(M)**3)+(3*A(M)*A(M)
     +  *A(N)*A(N))+(2*A(M)*A(N)**3)+(A(N)**4))
      EF3(J)=(PRO*LENG/30.0)*(EF31)
      EF41=((5*A(N)**4)+(4*A(M)*A(N)**3)+(3*A(M)*A(M)
     +   *A(N)*A(N))+(2*A(N)*A(M)**3)+(A(M)**4))
      EF4(K)=(PRO*LENG/30.0)*(EF41)

      EF(J)=EF(J)-EF3(J)+EF1(J)
      EF(K)=EF(K)-EF4(K)+EF2(K)

      ESM(J,J)=ESM(J,J)+(HL*2.)/6.0
      ESM(J,K)=ESM(J,K)+HL/6.0
      ESM(K,J)=ESM(J,K)
      ESM(K,K)=ESM(K,K)+(HL*2.)/6.0

  460 CONTINUE

      DP=LAMBDA*AR4/48.0
      CAP(1,1)=DP*2
      CAP(1,2)=DP*1
      CAP(1,3)=DP*1
      CAP(2,1)=DP*1
      CAP(2,2)=DP*2
      CAP(2,3)=DP*1
      CAP(3,1)=DP*1
      CAP(3,2)=DP*1
      CAP(3,3)=DP*2

      DO 470 I=1,3
      DO 470 J=1,3
      ESM2(I,J)=(2.*CAP(I,J)/DELTA)+ESM(I,J)
  470 CONTINUE

C*****************************************************************
C ASSEMBLE GLOBAL MATRICES
C*****************************************************************
```

```
      DO 430 I=1,3
      II=NS(I)
      J5=NP+II
      A(J5)=A(J5)+EF(I)
      DO 190 J=1,3
      JJ=NS(J)
      JJ=JJ-II+1
      IF(JJ)190,190,200
  200 J5=JGSM+(JJ-1)*NP+II
      A(J5)=A(J5)+ESM2(I,J)
  190 CONTINUE
  430 CONTINUE

      REWIND 2

C*****************************************************************
C SOLUTION  OF EQN.(2.24) FOR  UNKNOWN  NODAL TEMPERATURES
C BY CHOLESKY  DECOMPOSITION  &  BACKWARD  SUBSTITUTION
C*****************************************************************

      CALL DECOMP(A(JGSM+1),NP,NBW)
      CALL SOLVE(A(JGSM+1),A(JGF+1),A(1),NP,NBW,NCL)

C*****************************************************************
C TEST  FOR  CONVERGENCE  IN  NODAL  TEMPERATURES
C*****************************************************************

      DO 240 I=1,JGF
      IF(ABS(D(I)-A(I)).GE.0.01)GO TO 250
  240 CONTINUE

      GO TO 290

  250 CONTINUE

      DO 260 I=JGF+1,JEND
  260 A(I)=0.0

      DO 280 I=JGF+1,JGSM
      A(I)=D(I)
  280 CONTINUE

      GO TO 270
```

```
 290 CONTINUE

TIME=TIME+DELTA
IF(TIME.EQ.COUNT)GO TO 1000

GO TO 1001

 1000 DO 291 I=1,106
G(I)=A(I)-273.0
 291 CONTINUE

 1001 REWIND 2

IF(TIME.EQ.COUNT)GO TO 1002
GO TO 1003

C*************************************************************************
C READ  ELEMENT  GROUP  DATA  &  CALCULATE  TEMPERATURE
C GRADIENTS  IN  X & Y DIRECTIONS
C*************************************************************************

 1002 DO 292 I=1,NE
READ(2,*)NEL,NS,X(1),Y(1),X(2),Y(2),X(3),Y(3),ISIDE(1),ISIDE(2)

T(I)=(A(NS(1))+A(NS(2))+A(NS(3)))/3.0-273.0

B(1)=(Y(2)-Y(3))/100.0
B(2)=(Y(3)-Y(1))/100.0
B(3)=(Y(1)-Y(2))/100.0
C(1)=(X(3)-X(2))/100.0
C(2)=(X(1)-X(3))/100.0
C(3)=(X(2)-X(1))/100.0
XC=((X(1)+X(2)+X(3))/(3.0*CHORD))

AR2=ABS((X(2)*Y(3)+X(3)*Y(1)+X(1)*Y(2)-X(2)*Y(1)-X(3)*Y(2)
     + -X(1)*Y(3)))/10000.0
GRADX=0.0
GRADY=0.0

DO 299 J=1,3
GRADX=GRADX+(B(J)*A(NS(J)))/AR2
GRADY=GRADY+(C(J)*A(NS(J)))/AR2
 299 CONTINUE
```

```
      WRITE(3,2233)NEL,T(I),TIME,XC,GRADX,GRADY
 2233 FORMAT(I3,2X,F10.4,2X,F10.4,2X,F10.4,2X,F15.4,2X,F15.4)

  292 CONTINUE

      COUNT=COUNT+2

      REWIND 2

 1003 IF(TIME.LT.200.0)GO TO 10

      STOP
      END


C SUBROUTINE  *** DECOMP ***


      SUBROUTINE DECOMP(GSM,NP,NBW)
      DIMENSION GSM(NP,NBW)
      IO=61
      NP1=NP-1
      DO 226 I=1,NP1
      MJ=I+NBW-1
      IF(MJ.GT.NP)MJ=NP
      NJ=I+1
      MK=NBW
      IF((NP-I+1).LT.NBW) MK=NP-I+1
      ND=0
      DO 225 J=NJ,MJ
      MK=MK-1
      ND=ND+1
      NL=ND+1
      DO 225 K=1,MK
      NK=ND+K
  225 GSM(J,K)=GSM(J,K)-GSM(I,NL)*GSM(I,NK)/GSM(I,1)
  226 CONTINUE
      RETURN
      END


C SUBROUTINE  *** SOLVE ***
```

```
      SUBROUTINE SOLVE(GSM,GF,X,NP,NBW,NCL)
      DIMENSION GSM(NP,NBW),GF(NP,NCL),X(NP,NCL)
      IO=61
      NP1=NP-1
      DO 265 KK=1,NCL
      JM=KK
      DO 250 I=1,NP1
      MJ=I+NBW-1
      IF(MJ.GT.NP) MJ=NP
      NJ=I+1
      L=1
      DO 250 J=NJ,MJ
      L=L+1
  250 GF(J,KK)=GF(J,KK)-GSM(I,L)*GF(I,KK)/GSM(I,1)
      X(NP,KK)=GF(NP,KK)/GSM(NP,1)
      DO 252 K=1,NP1
      I=NP-K
      MJ=NBW
      IF((I+NBW-1).GT.NP) MJ=NP-I+1
      SUM=0.0
      DO 251 J=2,MJ
      N=I+J-1
  251 SUM=SUM+GSM(I,J)*X(N,KK)
  252 X(I,KK)=(GF(I,KK)-SUM)/GSM(I,1)
  265 CONTINUE
      RETURN
      END


      FUNCTION RATIO(TIM)
      COMMON Z,X4(11),Y4(11),A4(11),B4(11),C4(11)
      COMMON Q,X5(11),Y5(11),A5(11),B5(11),C5(11)
      COMMON V,X2(11),Y2(11),A2(11),B2(11),C2(11)
      COMMON U,X1(11),Y1(11),A1(11),B1(11),C1(11)
      COMMON W,X6(11),Y6(11),A6(11),B6(11),C6(11)
      COMMON S,X7(8),Y7(8),A7(8),B7(8),C7(8)
      DO 1 I=1,S
      IF(X7(I).GT.TIM)GO TO 2
    1 CONTINUE
    2 I=I-1
      DX=TIM-X7(I)
      RATIO=Y7(I)+DX*(A7(I)+DX*(B7(I)+DX*C7(I)))
```

```
      RETURN
      END

      FUNCTION SPHEAT(XF)
      COMMON Z,X4(11),Y4(11),A4(11),B4(11),C4(11)
      COMMON Q,X5(11),Y5(11),A5(11),B5(11),C5(11)
      COMMON V,X2(11),Y2(11),A2(11),B2(11),C2(11)
      COMMON U,X1(11),Y1(11),A1(11),B1(11),C1(11)
      COMMON W,X6(11),Y6(11),A6(11),B6(11),C6(11)
      COMMON S,X7(8),Y7(8),A7(8),B7(8),C7(8)
      DO 10 I=1,V
      IF(X2(I).GT.XF) GO TO 20
       10 CONTINUE
       20 I=I-1
      DX=XF-X2(I)
      SPHEAT=Y2(I)+DX*(A2(I)+DX*(B2(I)+DX*C2(I)))
      RETURN
      END

      FUNCTION BKTH(XSS)
      COMMON Z,X4(11),Y4(11),A4(11),B4(11),C4(11)
      COMMON Q,X5(11),Y5(11),A5(11),B5(11),C5(11)
      COMMON V,X2(11),Y2(11),A2(11),B2(11),C2(11)
      COMMON U,X1(11),Y1(11),A1(11),B1(11),C1(11)
      COMMON W,X6(11),Y6(11),A6(11),B6(11),C6(11)
      COMMON S,X7(8),Y7(8),A7(8),B7(8),C7(8)
      DO 100 I=1,U
      IF(X1(I).GT.XSS) GO TO 200
       100 CONTINUE
       200 I=I-1
      DXX=XSS-X1(I)
      BKTH=Y1(I)+DXX*(A1(I)+DXX*(B1(I)+DXX*C1(I)))
      RETURN
      END

      FUNCTION HTCS(SU)
      COMMON Z,X4(11),Y4(11),A4(11),B4(11),C4(11)
      COMMON Q,X5(11),Y5(11),A5(11),B5(11),C5(11)
      COMMON V,X2(11),Y2(11),A2(11),B2(11),C2(11)
      COMMON U,X1(11),Y1(11),A1(11),B1(11),C1(11)
      COMMON W,X6(11),Y6(11),A6(11),B6(11),C6(11)
```

```
      COMMON S,X7(8),Y7(8),A7(8),B7(8),C7(8)
      DO 10 I=1,Q
      IF(X5(I).GT.SU)GO TO 20
       10 CONTINUE
       20 I=I-1
      DXX=SU-X5(I)
      HTCS=Y5(I)+DXX*(A5(I)+DXX*(B5(I)+DXX*C5(I)))
      RETURN
      END


      FUNCTION HTCP(PR)
      COMMON Z,X4(11),Y4(11),A4(11),B4(11),C4(11)
      COMMON Q,X5(11),Y5(11),A5(11),B5(11),C5(11)
      COMMON V,X2(11),Y2(11),A2(11),B2(11),C2(11)
      COMMON U,X1(11),Y1(11),A1(11),B1(11),C1(11)
      COMMON W,X6(11),Y6(11),A6(11),B6(11),C6(11)
      COMMON S,X7(8),Y7(8),A7(8),B7(8),C7(8)
      DO 100 I=1,Z
      IF(X4(I).GT.PR)GO TO 200
       100 CONTINUE
       200 I=I-1
      DZ=PR-X4(I)
      HTCP=Y4(I)+DZ*(A4(I)+DZ*(B4(I)+DZ*C4(I)))
      RETURN
      END


      FUNCTION TTM(T)
      COMMON Z,X4(11),Y4(11),A4(11),B4(11),C4(11)
      COMMON Q,X5(11),Y5(11),A5(11),B5(11),C5(11)
      COMMON V,X2(11),Y2(11),A2(11),B2(11),C2(11)
      COMMON U,X1(11),Y1(11),A1(11),B1(11),C1(11)
      COMMON W,X6(11),Y6(11),A6(11),B6(11),C6(11)
      COMMON S,X7(8),Y7(8),A7(8),B7(8),C7(8)
      DO 100 I=1,W
      IF(X6(I).GT.T)GO TO 200
       100 CONTINUE
       200 I=I-1
      DW=T-X6(I)
      TTM=Y6(I)+DW*(A6(I)+DW*(B6(I)+DW*C6(I)))
      RETURN
      END
```

```
SUBROUTINE SPLFIT(V,X,Y,B,C,D)
  DIMENSION X(V),Y(V),B(V),C(V),D(V)
VM1=V-1
IF(V.LT.2) RETURN
IF(V.LT.3) GO TO 50
D(1)=X(2)-X(1)
C(2)=(Y(2)-Y(1))/D(1)
DO 10 I=2,VM1
D(I)=X(I+1)-X(I)
B(I)=2.*(D(I-1)+D(I))
C(I+1)=(Y(I+1)-Y(I))/D(I)
C(I)=C(I+1)-C(I)
 10 CONTINUE
B(1)=-D(1)
B(V)=-D(V-1)
C(1)=0.
C(V)=0.
IF(V.EQ.3) GO TO 15
C(1)=C(3)/(X(4)-X(2))-C(2)/(X(3)-X(1))
C(V)=C(V-1)/(X(V)-X(V-2))-C(V-2)/(X(V-1)-X(V-3))
C(1)=C(1)*D(1)**2/(X(4)-X(1))
C(V)=-C(V)*D(V-1)**2/(X(V)-X(V-3))
 15 DO 20 I=2,V
T=D(I-1)/B(I-1)
B(I)=B(I)-T*D(I-1)
C(I)=C(I)-T*C(I-1)
 20 CONTINUE
C(V)=C(V)/B(V)
DO 30 IB=1,VM1
I=V-IB
C(I)=(C(I)-D(I)*C(I+1))/B(I)
 30 CONTINUE
B(V)=(Y(V)-Y(VM1))/D(VM1)+D(VM1)*(C(VM1)+2.*C(V))
DO 40 I=1,VM1
B(I)=(Y(I+1)-Y(I))/D(I)-D(I)*(C(I+1)+2.*C(I))
D(I)=(C(I+1)-C(I))/D(I)
C(I)=3.*C(I)
 40 CONTINUE
C(V)=3.*C(V)
D(V)=D(V-1)
RETURN
 50 B(1)=(Y(2)-Y(1))/(X(2)-X(1))
```

```
C(1)=0.
D(1)=0.
B(2)=B(1)
C(2)=0.
D(2)=0.
RETURN
END
```

```
C*****************************************************************
C*
C* LISTING  OF  THE  PROGRAM **TSTRESS**
C* PROGRAM  TO  CALCULATE  THE  THERMAL  STRESSES  IN
C* THE  BLADE  FROM  THE  TRANSIENT  TEMPERATURE
C* DISTRIBUTION
C*
C*****************************************************************

C*****************************************************************
C NP       NO. OF GLOBAL DISPLACEMENTS OR D.O.F.
C NE       NO. OF ELEMENTS
C NBW      BANDWIDTH
C ITEMP    ELEMENT TEMP. (INPUT)
C ELASTIC  ELASTIC MODULUS
C PR       POISSON'S RATIO
C ALPHA    COEFF. OF THERMAL EXPN
C TEMP     INITIAL TEMP.
C T        ELEMENT THICKNESS
C DT       RISE  IN  TEMPERATURE  OF  THE  ELEMENT
C*****************************************************************

REAL ITEMP
DIMENSION NS(6),ND(3),ESM(6,6),EF(6),B(3,6),C(6,3),D(3,3)
DIMENSION STRA(3),STRE(3),ET(3),U(6),A(50000),SIGMA(20000)
DIMENSION AX(10),AY(10),EX(10),EY(10),ISIDE(2),DEL(174)
DIMENSION XYS(6),YYS(6),TEMP(174),DT(174),DDT(174),DELTA(174)

DATA AX/0.0,205.0,315.0,425.0,540.0,650.0,760.0,870.0,980.0,
     1 1090.0/
DATA AY/0.0000110,0.0000119,0.0000124,0.0000128,0.0000131,
     1 0.0000135,0.000014,0.0000148,0.0000158,0.000017/
DATA EX/0.0,93.0,205.0,315.0,425.0,540.0,650.0,760.0,870.0,
     1 980.0/
DATA EY/220.0E9,215.0E9,215.0E9,195.0E9,190.0E9,185.0E9,
     1 175.0E9,170.0E9,160.0E9,145.0E9/
DATA XYS/21.0,540.0,650.0,760.0,870.0,980.0/
DATA YYS/840.0E+6,850.0E+6,855.0E+6,840.0E+6,760.0E+6,
     1 470.0E+6/
DATA NCL/1/,ID1/0/,IELR/0/

C*****************************************************************
C DATA  AX,AY  REPRESENT  ALFA v/s TEMPERATURE
C DATA  EX,EY  REPRESENT  ELASTIC v/s TEMPERATURE
```

```
C DATA  XYS,YYS  REPRESENT  YIELD STRESS v/s TEMPERATURE
C*********************************************************************
COMMON P,PX(10),PY(10),AP(10),BP(10),CP(10)
COMMON Q,QX(10),QY(10),AQ(10),BQ(10),CQ(10)
COMMON V,RX(6),RY(6),AR(6),BR(6),CR(6)

OPEN(UNIT=60,FILE='NMESH.DAT',TYPE='OLD')
OPEN(UNIT=70,FILE='STRESS.DAT',TYPE='NEW')
OPEN(UNIT=63,FILE='T.DAT',TYPE='OLD')

T=1.0
P=10
Q=10
V=6

C*********************************************************************
C INITIALIZING  DATA
C*********************************************************************

DO 1 I=1,10
PX(I)=AX(I)
 1 PY(I)=AY(I)

DO 2 I=1,10
QX(I)=EX(I)
 2 QY(I)=EY(I)

DO 3 I=1,6
RX(I)=XYS(I)
 3 RY(I)=YYS(I)

NP=212
NE=174
NBW=16
PR=0.25

  DO 13 I=1,174
 13 TEMP(I)=303.0

C*********************************************************************
C READ  ELEMENTAL  TRANSIENT  TEMPERATURES  AND CARRY
C OUT  THE  SUMMATION  FOR  EACH  ELEMENT  AS  IN
C EQN.(2.26)
```

```
C**********************************************************************

  DO 300 KM=1,100
 115  READ(63,63)(I,A(I),TIME,I=1,174)
 63 FORMAT(I3,2X,F10.4,2X,F10.4)

    SUM1=0.0
SUM2=0.0
SUM3=0.0
SUM4=0.0
SUM5=0.0
SUM6=0.0

DO 7 KK=1,NE
 114 READ(60,*)NEL,ND,X1,Y1,X2,Y2,X3,Y3,ISIDE
ITEMP=A(NEL)
DT(I)=ITEMP-TEMP(NEL)

X1=(X1-15.33)/100.0
X2=(X2-15.33)/100.0
X3=(X3-15.33)/100.0
Y1=(Y1-15.0)/100.0
Y2=(Y2-15.0)/100.0
Y3=(Y3-15.0)/100.0

IF(ITEMP.LE.0.0) THEN
ELASTIC=220.0E+09
ALPHA=0.0000106
ELSE
CALL SPLFIT(Q,QX,QY,AQ,BQ,CQ)
ELASTIC=ELAST(ITEMP)
CALL SPLFIT(P,PX,PY,AP,BP,CP)
ALPHA=ALFA(ITEMP)
END IF

XC=(X1+X2+X3)/3.0
YC=(Y1+Y2+Y3)/3.0

ARR=ABS(X2*Y3+X3*Y1+X1*Y2-X2*Y1-X3*Y2-X1*Y3)/2.0

SUM1=SUM1+(ALPHA*ELASTIC*ARR*DT(I))
SUM2=SUM2+(ARR*ELASTIC)
SUM3=SUM3+(ARR*ELASTIC*ALPHA*DT(I)*XC)
SUM4=SUM4+(ARR*ELASTIC*XC**2)
```

```
      SUM5=SUM5+(ARR*ELASTIC*ALPHA*DT(I)*YC)
      SUM6=SUM6+(ARR*ELASTIC*YC**2)
       7 CONTINUE

      REWIND 60

C*****************************************************************
C CALCULATE THE THERMAL STRESS IN EACH ELEMENT
C*****************************************************************

      DO 45 I=1,NE
      READ(60,*)NEL,ND,X1,Y1,X2,Y2,X3,Y3,ISIDE

      X1=(X1-15.33)/100.0
      X2=(X2-15.33)/100.0
      X3=(X3-15.33)/100.0
      Y1=(Y1-15.0)/100.0
      Y2=(Y2-15.0)/100.0
      Y3=(Y3-15.0)/100.0

      XC=(X1+X2+X3)/3.0
      YC=(Y1+Y2+Y3)/3.0
      ITEMP=A(NEL)
      DT(I)=ITEMP-TEMP(NEL)

      IF(ITEMP.LE.30.0) THEN
      ELASTIC=220.0E+09
      ALPHA=0.0000116
      YIELD=840.0E+6
      ELSE
      CALL SPLFIT(Q,QX,QY,AQ,BQ,CQ)
      ELASTIC=ELAST(ITEMP)
      CALL SPLFIT(V,RX,RY,AR,BR,CR)
      YIELD=FUN(ITEMP)
      CALL SPLFIT(P,PX,PY,AP,BP,CP)
      ALPHA=ALFA(ITEMP)
      END IF

      IF(DT(I).LT.0.0)THEN
      SIGMA(I)=SIGMA(I)-(ELASTIC*((SUM1/SUM2)+(XC*SUM3/SUM4)
           1 +(YC*SUM5/SUM6)-(ALPHA*DT(I))))/YIELD
      ELSE
      SIGMA(I)=SIGMA(I)+(ELASTIC*((SUM1/SUM2)+(XC*SUM3/SUM4)
           1 +(YC*SUM5/SUM6)-(ALPHA*DT(I))))/YIELD
```

```
END IF

 71 FORMAT(I4,2X,E15.8,2X,E15.8,2X,E15.8)
 45 CONTINUE

C*****************************************************************
C LOCATE  THE  MAX. & MIN. VALUES  OF  THERMAL,STRESS
C*****************************************************************
SIGMAX=0.0
SIGMIN=0.0
DO 1111 I=1,NE
IF(SIGMA(I).GT.SIGMAX)SIGMAX=SIGMA(I)
IF(SIGMA(I).LT.SIGMIN)SIGMIN=SIGMA(I)
 1111 CONTINUE
WRITE(70,1112)SIGMA(1),SIGMA(78),SIGMA(163),SIGMIN,
     1 SIGMAX,TIME
1112 FORMAT(2X,E10.4,2X,E10.4,2X,E10.4,2X,E10.4,2X,E10.4,
     1 2X,E10.4)

REWIND 60

DO 2233 I=1,174
 2233 TEMP(I)=A(I)

 300 CONTINUE

 200 STOP
END
```

```
C*****************************************************************
C*
C* LISTING  OF  THE  PROGRAM **ISO**
C* PROGRAM  TO  CALCULATE  NATURAL  FREQUENCIES  OF
C* A  TURBINE  BLADE  USING  20-NODED  ISOPARAMETRIC
C*  FINITE  ELEMENTS
C*
C*****************************************************************

C IMPLICIT REAL*8 (A-H,O-Z)

DIMENSION COORD(20,3),STIFF(60,60),DERIV(8,3,20)
DIMENSION SHAPE(8,20),ST(60,60),EMASS(60,60)
DIMENSION ND(20),X(20),Y(20),Z(20),NS(60)
DIMENSION GSTIFF(924,924),D(38),GMASS(924,924)
DIMENSION WK(1850),AWK(2),G(2,2),GSINV(924,924)
COMPLEX EV(924),DYN(924,924),ZV(1,1)

EQUIVALENCE (GMASS(1),DYN(1))

OPEN(UNIT=2,FILE='FREQ.DAT',TYPE='NEW')
OPEN(UNIT=3,FILE='MESH.DAT',TYPE='OLD')
OPEN(UNIT=7,FILE='DISP.DAT',TYPE='OLD')

TVOL=0.0
GSUM=0.0

DO 30 I=1,924
DO 30 J=1,924
GMASS(I,J)=0.0
 30 GSTIFF(I,J)=0.0

C*************************************************************
C READ  ELEMENT  COORDINATES
C*************************************************************

DO 20 NELM=1,35
READ(3,*)NEL
DO 10 I=1,20
READ(3,*)ND(I),X(I),Y(I),Z(I)
 10 CONTINUE

DO 1 J=1,3
DO 1 I=1,20
```

```
      IF(J.EQ.1)COORD(I,J)=(X(I))/1000.0
      IF(J.EQ.2)COORD(I,J)=(Y(I))/1000.0
      IF(J.EQ.3)COORD(I,J)=(Z(I))/100.0
       1 CONTINUE

      C*****************************************************************
      C EVALUATE  ELEMENT  SHAPE  FUNCTIONS & THEIR  DERIVATIVES
      C*****************************************************************

      CALL SHAPE20(SHAPE,DERIV)

      C*****************************************************************
      C CALCULATE  ELEMENT  STIFFNESS & MASS  MATRICES
      C*****************************************************************

      CALL STIFFMASS20(NEL,COORD,SHAPE,DERIV,STIFF,EMASS,VOL)

      C*****************************************************************
      C ASSEMBLE  ELEMENTAL  MATRICES  INTO  THEIR
      C GLOBAL  LOCATIONS & FORM  THE SYSTEM MATRICES
      C*****************************************************************

      DO 7 I=1,20
      DO 7 IDOFN=1,3
      IF(IDOFN.EQ.1)NROWS=ND(I)*3-2
      IF(IDOFN.EQ.1)NROWE=I*3-2
      IF(IDOFN.EQ.2)NROWS=ND(I)*3-1
      IF(IDOFN.EQ.2)NROWE=I*3-1
      IF(IDOFN.EQ.3)NROWS=ND(I)*3
      IF(IDOFN.EQ.3)NROWE=I*3
      DO 7 J=1,20
      DO 7 JDOFN=1,3
      IF(JDOFN.EQ.1)NCOLS=ND(J)*3-2
      IF(JDOFN.EQ.1)NCOLE=J*3-2
      IF(JDOFN.EQ.2)NCOLS=ND(J)*3-1
      IF(JDOFN.EQ.2)NCOLE=J*3-1
      IF(JDOFN.EQ.3)NCOLS=ND(J)*3
      IF(JDOFN.EQ.3)NCOLE=J*3
      GSTIFF(NROWS,NCOLS)=GSTIFF(NROWS,NCOLS)+STIFF(NROWE,NCOLE)
      GMASS(NROWS,NCOLS)=GMASS(NROWS,NCOLS)
           1 +EMASS(NROWE,NCOLE)
       7 CONTINUE
      TVOL=TVOL+VOL
       20 CONTINUE
```

```
C*****************************************************************
C APPLY  BOUNDARY  CONDITIONS AT ROOT OF THE BLADE AT  THE
C PROPER  ROWS & COLUMNS  OF  GLOBAL [K] & [M] MATRICES
C*****************************************************************

DO 200 I=1,38
READ(7,*)D(I)
NROW1=D(I)*3-2
NROW2=D(I)*3-1
NROW3=D(I)*3
NCOL1=NROW1
NCOL2=NROW2
NCOL3=NROW3
DO 100 K=1,924
GSTIFF(NROW1,K)=0.0
GSTIFF(NROW2,K)=0.0
GSTIFF(NROW3,K)=0.0
GSTIFF(K,NCOL1)=0.0
GSTIFF(K,NCOL2)=0.0
GSTIFF(K,NCOL3)=0.0
GMASS(NROW1,K)=0.0
  GMASS(NROW2,K)=0.0
GMASS(NROW3,K)=0.0
GMASS(K,NCOL1)=0.0
GMASS(K,NCOL2)=0.0
GMASS(K,NCOL3)=0.0
 100 CONTINUE

 200 CONTINUE

DO 300 I=1,924
DO 300 J=1,924
IF(I.EQ.J.AND.GSTIFF(I,J).EQ.0.0)THEN
GSTIFF(I,J)=1.0E+15
GMASS(I,J)=1.0E-6
ELSE
GO TO 300
END IF
 300 CONTINUE

C*****************************************************************
C INVERT [K] MATRIX & FORM  DYNAMIC  MATRIX
C*****************************************************************
```

```
      CALL LINV1F(GSTIFF,924,924,GSINV,0,WK,IER)
      CALL VMULFF(GSINV,GMASS,924,924,924,924,924,GSTIFF,924,IER)

      DO 400 I=1,924
      DO 400 J=1,924
      DYN(I,J)=CMPLX(GSTIFF(I,J))
  400 CONTINUE

C*****************************************************************
C CALCULATE  EIGENVALUES  USING  DYNAMIC  MATRIX
C*****************************************************************

      CALL EIGCC(DYN,924,924,0,EV,ZV,1,WK,IER)

      DO 500 I=1,924
  500 EV(I)=1./(SQRT(EV(I))*2*3.14159)

      WRITE(2,*)(EV(I),I=1,924)
      STOP
      END


      SUBROUTINE SHAPE20(SHAPE,DERIV)
C     IMPLICIT REAL*8 (A-H,O-Z)
      DIMENSION SHAPE(8,20),DERIV(8,3,20),F(2),ZTA(20)
      DIMENSION SI(20),F1(24),NTA(20)

      DATA F/-0.577350269189626,+0.577350269189626/
      DATA ZTA/-1.,+1.,+1.,-1.,-1.,1.,1.,-1.,-1.,1.,1.,-1.,0.0,
     1 1.,0.0,-1.,0.0,1.,0.0,-1./
      DATA NTA/-1.,-1.,1.,1.,-1.,-1.,1.,1.,-1.,-1.,1.,1.,-1.,
     1 0.0,1.,0.0,-1.,0.0,1.,0.0/
      DATA SI/-1.,-1.,-1.,1.,1.,1.,1.,1.,0.0,0.0,0.0,0.0,-1.,
     1 -1.,-1.,-1.,1.,1.,1.,1./

C*****************************************************************
C DATA  ZTA(1),NTA(1),SI(1) REPRESENT THE  LOCAL COORDINATES
C OF  THE  FIRST  NODE  OF  THE  20-NODED  ELEMENT & SO ON
C*****************************************************************

      KK=0
      DO 101 K=1,2
      DO 101 J=1,2
```

```
      DO 101 I=1,2
      KK=KK+1
      F1(KK)=F(I)
      KK=KK+1
      F1(KK)=F(J)
      KK=KK+1
      F1(KK)=F(K)
       101 CONTINUE

      DO 10 NN=1,8
      NN1=(NN-1)*3+1

      GZ=F1(NN1)
      GN=F1(NN1+1)
      GR=F1(NN1+2)

      DO 20 I=1,8
      SHAPE(NN,I)=(1.0/8.0)*(1.0+GZ*ZTA(I))*(1.0+GN*NTA(I))*(1.0+GR*
     1 SI(I))*(GZ*ZTA(I)+GN*NTA(I)+GR*SI(I)-2.0)
      DERIV(NN,1,I)=(1./8.0)*ZTA(I)*(1.0+GN*NTA(I))*(1.0+GR*SI(I))*
     1 (2.0*ZTA(I)*GZ+GN*NTA(I)+GR*SI(I)-1.0)
      DERIV(NN,2,I)=(1.0/8.0)*NTA(I)*(1+GZ*ZTA(I))*(1+GR*SI(I))*
     1 (GN*NTA(I)*2.0+GZ*ZTA(I)+GR*SI(I)-1.0)
      DERIV(NN,3,I)=(1.0/8.0)*SI(I)*(1.+GZ*ZTA(I))*(1.+GN*NTA(I))*
     1 (GZ*ZTA(I)+GN*NTA(I)+2.0*GR*SI(I)-1.0)
       20 CONTINUE

      DO 30 J=9,12
      SHAPE(NN,J)=(1./4.)*(1.0-GR**2)*(1.+GZ*ZTA(J))*(1.+GN*NTA(J))
      DERIV(NN,1,J)=(1./4.)*ZTA(J)*(1.0-GR**2)*(1.+GN*NTA(J))
      DERIV(NN,2,J)=(1./4.)*NTA(J)*(1.-GR**2)*(1.+ZTA(J)*GZ)
      DERIV(NN,3,J)=(-1./2.)*GR*(1.+GZ*ZTA(J))*(1.+GN*NTA(J))
       30 CONTINUE

      DO 40 L=13,16
      IF(L.EQ.16)K=19
      IF(L.EQ.15)K=17
      IF(L.EQ.14)K=15
      IF(L.EQ.13)K=13
      SHAPE(NN,K)=(1./4.)*(1.-GZ**2)*(1.+GN*NTA(K))*(1.+GR*SI(K))
      DERIV(NN,1,K)=(-1./2.)*GZ*(1.+NTA(K)*GN)*(1.+SI(K)*GR)
      DERIV(NN,2,K)=(1./4.)*NTA(K)*(1.-GZ**2)*(1.+SI(K)*GR)
      DERIV(NN,3,K)=(1./4.)*SI(K)*(1.-GZ**2)*(1.+NTA(K)*GN)
       40 CONTINUE
```

```
      DO 50 K=17,20
      IF(K.EQ.17)L=14
      IF(K.EQ.18)L=16
      IF(K.EQ.19)L=18
      IF(K.EQ.20)L=20
      SHAPE(NN,L)=(1./4.)*(1.-GN**2)*(1.+GZ*ZTA(L))*(1.+SI(L)*GR)
      DERIV(NN,1,L)=(1./4.)*ZTA(L)*(1.0-GN**2)*(1.+SI(L)*GR)
      DERIV(NN,2,L)=(-1./2.)*GN*(1.+ZTA(L)*GZ)*(1.+SI(L)*GR)
      DERIV(NN,3,L)=(1./4.)*SI(L)*(1.-GN**2)*(1.+ZTA(L)*GZ)
       50 CONTINUE

       10 CONTINUE

      RETURN
      END


      SUBROUTINE STIFFMASS20(NEL,COORD,SHAPE,DERIV,STIFF,
     1 EMASS,VOL)

      C IMPLICIT REAL*8 (A-H,O-Z)

      DIMENSION STIFF(60,60),ESM(60,60),B(6,60),AJACOB(3,3)
      DIMENSION AJINV(3,3),DERIV(8,3,20),COORD(20,3),P(6,9)
      DIMENSION R(9,60),PQ(6,9),D(6,6),BTD(60,6),W(3),FWT(8)
      DIMENSION TSM(60,3),SM(3,60),EMM(60,60),EMASS(60,60)
      DIMENSION SHAPE(8,20),BT(60,6),Q(9,9)

      DATA W/1.0,1.0,1.0/
      INTEGER IER
      RHO=8526.0

      C*****************************************************************************
      C INITIALIZE ALL MATRICES TO BE ZERO
      C*****************************************************************************

      DO 1 I=1,60
      DO 1 J=1,60
      EMM(I,J)=0.0
      EMASS(I,J)=0.0
      ESM(I,J)=0.0
       1 STIFF(I,J)=0.0
```

```
      VOL=0.0
      NN=0

C*****************************************************************************
C INTIGRATE  AT  EACH  GAUSS  POINT (2 IN EACH DIRECTION)
C*****************************************************************************

      DO 105 KK=1,2
      DO 105 JJ=1,2
      DO 105 II=1,2
      NN=NN+1

C*****************************************************************************
C SET [B] & [J] MATRICES EQUAL TO ZERO FOR EACH GAUSS POINT
C*****************************************************************************

      DO 50 L=1,6
      DO 50 K=1,60
   50 B(L,K)=0.0

      DO 51 I=1,3
      DO 51 J=1,3
   51 AJACOB(I,J)=0.0

C*****************************************************************************
C FORM  THE  JACOBIAN  MATRIX [J]
C*****************************************************************************

      DO 52 I=1,3
      DO 52 J=1,3
      SUM=0.0
      DO 53 K=1,20
      SUM=SUM+DERIV(NN,I,K)*COORD(K,J)
   53 CONTINUE
      AJACOB(I,J)=SUM
   52 CONTINUE

C*****************************************************************************
C CALCULATE  THE  INVERSE & THE  DETERMINANT  OF [J]
C*****************************************************************************

      CALL INVERSE(AJACOB,AJINV,DET)
```

```
FWT(NN)=DET*W(KK)*W(JJ)*W(II)

C*****************************************************************
C EVALUATE  [P],[Q] & [R] AT EACH G.P. TO FORM [B] MATRIX
C*****************************************************************

DO 54 I=1,6
DO 54 J=1,9
 54 P(I,J)=0.0
P(1,1)=1.0
P(2,5)=1.0
P(3,9)=1.0
P(4,2)=1.0
P(4,4)=1.0
P(5,3)=1.0
P(5,7)=1.0
P(6,6)=1.0
P(6,8)=1.0


DO 55 I=1,9
DO 55 J=1,9
 55 Q(I,J)=0.0
DO 56 I=1,3
DO 56 J=1,3
 56 Q(I,J)=AJINV(I,J)
DO 58 L=4,6
DO 58 M=4,6
I=L-3
J=M-3
 58 Q(L,M)=AJINV(I,J)
DO 59 L=7,9
DO 59 M=7,9
I=L-6
J=M-6
 59 Q(L,M)=AJINV(I,J)


DO 60 I=1,9
DO 60 J=1,60
 60 R(I,J)=0.0
DO 61 I=1,3
K=1
DO 61 J=1,20
```

```
      R(I,K)=DERIV(NN,I,J)
      K=K+3
       61 CONTINUE
      DO 62 I=4,6
      K=2
      DO 62 J=1,20
      L=I-3
      R(I,K)=DERIV(NN,L,J)
      K=K+3
       62 CONTINUE
      DO 63 I=7,9
      K=3
      DO 63 J=1,20
      L=I-6
      R(I,K)=DERIV(NN,L,J)
      K=K+3
       63 CONTINUE

      CALL VMULFF(P,Q,6,9,9,6,9,PQ,6,IER)
      CALL VMULFF(PQ,R,6,9,60,6,9,B,6,IER)

      C*****************************************************************
      C FORM  THE  MATERIAL  PROPERTY  MATRIX [D]
      C*****************************************************************

      E=2.0E+11
      PR=0.25
      DO 64 I=1,6
      DO 64 J=1,6
       64 D(I,J)=0.0
      EPR=E*(1.-PR)/((1.+PR)*(1.-2*PR))
      D(1,1)=1.*EPR
      D(1,2)=(PR/(1.-PR))*EPR
      D(1,3)=D(1,2)
      D(2,2)=D(1,1)
      D(2,3)=D(1,2)
      D(3,3)=D(1,1)
      D(4,4)=EPR*(1.-2*PR)/(2.*(1.-PR))
      D(5,5)=D(4,4)
      D(6,6)=D(4,4)
      D(2,1)=D(1,2)
      D(3,1)=D(1,3)
      D(3,2)=D(2,3)
```

```
C*********************************************************************
C FORM  TRANSPOSE  OF  THE  [B] MATRIX
C*********************************************************************

DO 65 I=1,6
DO 65 J=1,60
BT(J,I)=B(I,J)
 65 CONTINUE

C*********************************************************************
C FORM  SHAPE FUNCTION MATRIX TO BE USED IN THE
C CALULATION  OF THE  ELEMENT  MASS  MATRIX
C*********************************************************************

DO 70 I=1,3
K=I
DO 70 J=1,20
SN(I,K)=SHAPE(NN,J)
K=K+3
 70 CONTINUE

DO 71 I=1,3
DO 71 J=1,60
TSN(J,I)=SN(I,J)
 71 CONTINUE

C*********************************************************************
C FORM  ELEMENT [K] & [M] MATRICES
C*********************************************************************

CALL VMULFF(BT,D,60,6,6,60,6,BTD,60,IER)
CALL VMULFF(BTD,B,60,6,60,60,6,ESM,60,IER)
CALL VMULFF(TSN,SN,60,3,60,60,3,EMM,60,IER)

C*********************************************************************
C SUM. UP  THE  ELEMENTAL  [K] & [M]  MATRICES  AT
C EACH  G.P. TO FORM THE TOTAL  ELEMENTAL [K] & [M]
C MATRICES
C*********************************************************************

DO 66 I=1,60
DO 66 J=1,60
```

```
      STIFF(I,J)=FWT(NN)*ESM(I,J)+STIFF(I,J)
      EMASS(I,J)=RHO*FWT(NN)*EMM(I,J)+EMASS(I,J)
   66 CONTINUE

      VOL=VOL+DET*RHO

  105 CONTINUE
      RETURN
      END


      SUBROUTINE INVERSE(A,AJINV,DET)
C     IMPLICIT REAL*8 (A-H,O-Z)
      DIMENSION A(3,3),AJINV(3,3)
      INTEGER IER
      AJINV(1,1)=A(2,2)*A(3,3)-A(3,2)*A(2,3)
      AJINV(2,1)=-A(2,1)*A(3,3)+A(3,1)*A(2,3)
      AJINV(3,1)=A(2,1)*A(3,2)-A(3,1)*A(2,2)
      AJINV(1,2)=-A(1,2)*A(3,3)+A(3,2)*A(1,3)
      AJINV(2,2)=A(1,1)*A(3,3)-A(3,1)*A(1,3)
      AJINV(3,2)=-A(1,1)*A(3,2)+A(3,1)*A(1,2)
      AJINV(1,3)=A(1,2)*A(2,3)-A(2,2)*A(1,3)
      AJINV(2,3)=-A(1,1)*A(2,3)+A(2,1)*A(1,3)
      AJINV(3,3)=A(1,1)*A(2,2)-A(2,1)*A(1,2)

      DET=A(1,1)*AJINV(1,1)+A(1,2)*AJINV(2,1)+A(1,3)*AJINV(3,1)
      DO 20 J=1,3
      DO 10 I=1,3
   10 AJINV(I,J)=AJINV(I,J)/DET
   20 CONTINUE
      DO 30 I=1,3
      DO 30 J=1,3
   30 CONTINUE
      RETURN
      END
```

```
C*****************************************************************
C*
C* LISTING  OF  THE  PROGRAM  **FREQ**
C* PROGRAM  TO  CALCULATE  THE  NATURAL  FREQUENCIES  OF
C* THE  BLADE  USING  GUYAN'S  REDUCTION  TECHNIQUE AND
C* THEN  DECOUPLING  THE  EQUATIONS  OF  MOTION
C*
C*****************************************************************

C IMPLICIT REAL*8 (A-H,O-Z)

REAL MAX
DIMENSION COORD(20,3),STIFF(60,60),DERIV(8,3,20)
DIMENSION SHAPE(8,20),ST(60,60),EMASS(60,60)
DIMENSION ND(20),X(20),Y(20),Z(20),NS(60)
DIMENSION D(38),WKAREA(2000)
DIMENSION GKK(924,924),GMM(924,924)
REAL GKKINV(200,200),LAMDA(200,200),
     1 F(924),KSS(724,724),TEMP8(724,200),KSSINV(724,724)
REAL R(924),TEMP1(924),TEMP2(924),KMS(200,724),T(924,200),
     1 TEMP4(200,924),GKR(200,200),GMR(200,200),TEMP7(924),
     1 TEMP3(200,924),EVR(200,200)
REAL TEMP6(200,200),GMMM(200,200),EV(200,200),TT(724,200)
REAL TEMP10(200,200),EME(200,200),EVV(200,200)

COMPLEX ILAMDA(200,200),EIGVAL(200),EIGVEC(200,200)

OPEN(UNIT=2,FILE='IDMASS.DAT',TYPE='NEW')
OPEN(UNIT=3,FILE='MESH.DAT',TYPE='OLD')
OPEN(UNIT=7,FILE='DISP.DAT',TYPE='OLD')
OPEN(UNIT=11,FILE='PHI.DAT',TYPE='NEW')
OPEN(UNIT=12,FILE='TRANS.DAT',TYPE='NEW')
OPEN(UNIT=8,FILE='EIGEN.DAT',TYPE='NEW')

TVOL=0.0
GSUM=0.0

DO 30 I=1,924
DO 30 J=1,924
GMM(I,J)=0.0
 30 GKK(I,J)=0.0

DO 20 NELM=1,35
READ(3,*)NEL
```

```
      DO 10 I=1,20
      READ(3,*)ND(I),X(I),Y(I),Z(I)
       10 CONTINUE

      DO 1 J=1,3
      DO 1 I=1,20
      IF(J.EQ.1)COORD(I,J)=(X(I))/1000.0
      IF(J.EQ.2)COORD(I,J)=(Y(I))/1000.0
      IF(J.EQ.3)COORD(I,J)=(Z(I))/100.0
       1 CONTINUE

      CALL SHAPE20(SHAPE,DERIV)

      CALL STIFFMASS20(NEL,COORD,SHAPE,DERIV,STIFF,EMASS,VOL)

      C*****************************************************************
      C DIRECT  ASSEMBLY  OF  SYSTEM  [K] & [M] MATRICES
      C*****************************************************************

      DO 7 I=1,20
      DO 7 IDOFN=1,3
      IF(IDOFN.EQ.1)NROWS=ND(I)*3-2
      IF(IDOFN.EQ.1)NROWE=I*3-2
      IF(IDOFN.EQ.2)NROWS=ND(I)*3-1
      IF(IDOFN.EQ.2)NROWE=I*3-1
      IF(IDOFN.EQ.3)NROWS=ND(I)*3
      IF(IDOFN.EQ.3)NROWE=I*3
      DO 7 J=1,20
      DO 7 JDOFN=1,3
      IF(JDOFN.EQ.1)NCOLS=ND(J)*3-2
      IF(JDOFN.EQ.1)NCOLE=J*3-2
      IF(JDOFN.EQ.2)NCOLS=ND(J)*3-1
      IF(JDOFN.EQ.2)NCOLE=J*3-1
      IF(JDOFN.EQ.3)NCOLS=ND(J)*3
      IF(JDOFN.EQ.3)NCOLE=J*3
      GKK(NROWS,NCOLS)=GKK(NROWS,NCOLS)+STIFF(NROWE,NCOLE)
      GMM(NROWS,NCOLS)=GMM(NROWS,NCOLS)+EMASS(NROWE,NCOLE)
       7 CONTINUE

       20 CONTINUE

      C*****************************************************************
      C APPLY  BOUNDARY  CONDITIONS
      C*****************************************************************
```

```
      DO 200 I=1,38
      READ(7,*)D(I)
      NROW1=D(I)*3-2
      NROW2=D(I)*3-1
      NROW3=D(I)*3
      NCOL1=NROW1
      NCOL2=NROW2
      NCOL3=NROW3
      DO 100 K=1,924
      IF(NROW1.EQ.K)GKK(NROW1,K)=0.0
      IF(NROW2.EQ.K)GKK(NROW2,K)=0.0
      IF(NROW3.EQ.K)GKK(NROW3,K)=0.0
       100 CONTINUE
       200 CONTINUE

      DO 300 I=1,924
      DO 300 J=1,924
      IF((I.EQ.J).AND.(GKK(I,J).EQ.0.0))THEN
      GKK(I,J)=1.0E+16
      GMM(I,J)=1.0E-5
      ELSE
      GO TO 300
      END IF.
       300 CONTINUE

      C*************************************************************************
      C  DYNAMIC CONDENSATION
      C       CONDENASTION IS CARRIED OUT FOR NSD=724
      C*************************************************************************
      C N = TOTAL NO. OF D.O.F.
      C NSD=NO. OF SLAVE D.O.F
      C NR =NO. OF RETAINED MASTER D.O.F.
      C*************************************************************************

      N=924
      NN=N
      NSD=724
      NR=N-NSD
      C*************************************************************************
      C THE CONDENSATION STARTS HERE
      C*************************************************************************

      DO 2000 II=1,NSD
```

```
      MAX=0.
      DO 60 I=1,N
      60 R(I)=GKK(I,I)/GMM(I,I)
      DO 70 I=1,N
      IF(R(I).GT.MAX) THEN
      MAX=R(I)
      IMAX=I
      ELSE
      GO TO 70
      ENDIF
      70 CONTINUE

      DO 80 J=1,NN
      TEMP1(J)=GMM(IMAX,J)
      TEMP2(J)=GKK(IMAX,J)
      80 TEMP7(J)=F(IMAX)
      DO 90 I=IMAX,N-1
      DO 90 J=1,NN
      GMM(I,J)=GMM(I+1,J)
      GKK(I,J)=GKK(I+1,J)
      90 F(I)=F(I+1)
      DO 1000 J=1,NN
      GMM(N,J)=TEMP1(J)
      GKK(N,J)=TEMP2(J)
      1000 F(N)=TEMP7(J)
      DO 110 I=1,NN
      TEMP1(I)=GMM(I,IMAX)
      TEMP2(I)=GKK(I,IMAX)
       110 CONTINUE
      DO 120 J=IMAX,N-1
      DO 120 I=1,NN
      GMM(I,J)=GMM(I,J+1)
      GKK(I,J)=GKK(I,J+1)
       120 CONTINUE
      DO 130 I=1,NN
      GMM(I,N)=TEMP1(I)
      GKK(I,N)=TEMP2(I)
       130 CONTINUE
      N=N-1
      2000 CONTINUE

      N=NN

      DO 140 I=1,NSD
```

```
      DO 140 J=1,NSD
  140 KSS(I,J)=-1.*GKK(I+NR,J+NR)

      DO 1100 I=1,NR
      DO 1100 J=1,NSD
 1100 KMS(I,J)=GKK(I,J+NR)

      IDGT=0
      CALL LINV1F(KSS,NSD,724,KSSINV,IDGT,WKAREA,IER)
      CALL VMULFP(KSSINV,KMS,NSD,NSD,NR,724,200,TEMP8,724,IER)

C*********************************************************************
C FORM  THE  TRANSFORMATION  MATRIX [T]
C*********************************************************************

      DO 160 I=1,NR
  160 T(I,I)=1.

      DO 170 I=1,NSD
      DO 170 J=1,NR
  170 T(I+NR,J)=TEMP8(I,J)

      DO 171 I=1,NSD
      DO 171 J=1,NR
  171 TT(I,J)=T(I+NR,J)

      WRITE(12,998)TT

C*********************************************************************
C FORM  THE  REDUCED  SYSTEM  [K] & [M] MATRICES
C*********************************************************************

      CALL VMULFM(T,GKK,924,NR,924,924,924,TEMP3,200,IER)
      CALL VMULFF(TEMP3,T,NR,924,NR,200,924,GKR,200,IER)
      CALL VMULFM(T,GMM,924,NR,924,924,924,TEMP4,200,IER)
      CALL VMULFF(TEMP4,T,NR,924,NR,200,924,GMR,200,IER)

      N=NR

C*********************************************************************
C INVERSION OF REDUCED [K]  MATRIX
C*********************************************************************

      IDGT =0
```

```
      CALL LINV1F (GKR,N,200,GKKINV,IDGT,WKAREA,IER)

C*****************************************************************
C MULTIPLICATION OF GKKINV AND GMM
C*****************************************************************

      CALL VMULFF (GKKINV,GMR,N,N,N,200,200,LAMDA,200,IER)
      DO 220 I=1,N
      DO 220 J=1,N
  220 ILAMDA(I,J)=CMPLX(LAMDA(I,J))

C*****************************************************************
C DETERMINATION OF EIGEN VALUES AND EIGENVECTORS
C*****************************************************************

      IJOB =1
      CALL EIGCC(ILAMDA,N,200,IJOB,EIGVAL,EIGVEC,200,WKAREA,IER)

      WRITE(8,*)EIGVAL
      DO 310 I=1,200
      DO 310 J=1,200
  310 EVR(I,J)=REAL(EIGVEC(I,J))

C*****************************************************************
C NORMALIZING  THE  EIGENVECTORS
C*****************************************************************
      DO 320 J=1,200
      ZN=EVR(1,J)
      DO 320 I=1,200
      EV(I,J)=EVR(I,J)/ZN
  320 CONTINUE

C*****************************************************************
C HERE  THE  REDUCED  MASS  MATRIX  IS  DIAGONALIZED
C*****************************************************************

      CALL VMULFM(EV,GMR,200,200,200,200,200,TEMP6,200,IER)
      CALL VMULFF(TEMP6,EV,200,200,200,200,200,GMMM,200,IER)
      WRITE(2,*)(GMMM(I,I),I=1,200)

C*****************************************************************
C HERE THE EIGENVECTORS ARE MASS-ORTHONORMALIZED
C*****************************************************************
```

```
      DO 400 J=1,200
      SUMM=1.0
      DO 430 I=1,200
  430 EVV(I,J)=(SUMM/SQRT(GMMM(J,J)))*EV(I,J)
  400 CONTINUE

      WRITE(11,998)EVV
  998 FORMAT(2X,E12.6,2X,E12.6,2X,E12.6,2X,E12.6,2X,E12.6,2X)

   11 CONTINUE

      STOP
      END
```

```
C*****************************************************************
C*
C* LISTING OF THE PROGRAM **TRANSVIB**
C* PROGRAM TO CALCULATE THE TRANSIENT RESPONSE
C* AND VIBRATORY STRESSES DUE TO NOZZLE EXCITATION
C* AND CENTRIFUGAL FORCES & THEN DIST. ENERGY STRESS
C*
C*****************************************************************

      REAL EV(200,200),T(924,200),TT(724,200),QV(200)
      REAL EIGEN(200),Q(200),TEMP1(200),U(924),SI(200)
      REAL GM(200,200),F(924),FC(200),FG(200),QC(200)
      REAL QI(200),QVI(200),QF(200),QVF(200),RPM(12)
      REAL EVINV(200,200),WK(500000),EVV(200,200)
      REAL TEMP2(200),QCF(200),UCF(924)
      REAL DDR1(12),DDR2(12),DDR3(12),DDR4(12)

      COMMON RPM1(12),DR1(12),A1(12),B1(12),C1(12)
      COMMON RPM2(12),DR2(12),A2(12),B2(12),C2(12)
      COMMON RPM3(12),DR3(12),A3(12),B3(12),C3(12)
      COMMON RPM4(12),DR4(12),A4(12),B4(12),C4(12)

      INTEGER IER

      DATA RPM/0.0,100.0,200.0,400.0,700.0,1000.0,1500.0,
     1 2000.0,2500.0,3000.0,3500.0,4000.0/
      DATA DDR1/0.034,0.0336,0.0284,0.0264,0.01525,0.00946,
     1 0.00802,0.007,0.00634,0.0058,0.00538,0.0050/
      DATA DDR2/0.04,0.03872,0.0336,0.03,0.016875,0.01,
     1 0.00904,0.0082,0.00766,0.00736,0.007,0.00676/
      DATA DDR3/0.045,0.04,0.037,0.0314,0.01875,0.0109,
     1 0.00946,0.0088,0.00832,0.00796,0.00772,0.0076/
      DATA DDR4/0.057,0.05,0.042,0.03727,0.02,0.0121,
     1 0.00985,0.00916,0.0088,0.00862,0.00844,0.00832/

C*****************************************************************
C DATA RPM,DDR1 REPRESENTS DAMPING RATIO OF 1ST MODE
C AS A FUNCTION OF ROTOR SPEED & SO ON FOR 1ST 4 MODES
C*****************************************************************

      OPEN(UNIT=2,FILE='PHI.DAT',TYPE='OLD')
      OPEN(UNIT=3,FILE='TRANS.DAT',TYPE='OLD')
      OPEN(UNIT=7,FILE='EIGEN.DAT',TYPE='OLD')
      OPEN(UNIT=8,FILE='MODE.DAT',TYPE='OLD')
```

```
OPEN(UNIT=9,FILE='IDMASS.DAT',TYPE='OLD')

C*****************************************************************
C INITIALIZING  DATA
C*****************************************************************
DO 7 I=1,12
RPM1(I)=RPM(I)
RPM2(I)=RPM1(I)
RPM3(I)=RPM2(I)
RPM4(I)=RPM3(I)
DR1(I)=DDR1(I)
DR2(I)=DDR2(I)
DR3(I)=DDR3(I)
DR4(I)=DDR4(I)
7 CONTINUE

DO 10 I=1,924
DO 10 J=1,200
10 T(I,J)=0.0

DO 20 I=1,200
20 T(I,I)=1.0

C*****************************************************************
C READING  IN  THE  TRANSFORMATION  MATRIX, NATURAL  FREQ.,
C DIAGONALIZED  MASSES  AND  MATRIX  OF  MODAL VECTORS
C*****************************************************************

READ(3,998)TT
998 FORMAT(2X,E12.6,2X,E12.6,2X,E12.6,2X,E12.6,2X,E12.6,2X)

DO 30 I=1,724
DO 30 J=1,200
30 T(I+200,J)=TT(I,J)

READ(2,998)EV
READ(7,*)EIGEN
READ(9,*)(GM(I,I),I=1,200)

DO 1 J=1,200
DO 1 I=1,200
1 EV(I,J)=EV(I,J)*(SQRT(ABS(GM(J,J))))

DO 2 I=1,200
```

```
      DO 2 J=1,200
    2 EVV(I,J)=EV(I,J)
C*****************************************************************
C INVERTING THE MATRIX OF MODAL VECTORS
C*****************************************************************
      IDGT=0
      CALL LINV2F(EVV,200,200,EVINV,IDGT,WK,IER)

      TIME=0.0

      DO 42 I=5,200
   42 SI(I)=0.01

C*****************************************************************
C INPUT KINEMATIC DATA & HEIGHT OF THE IMPULSE
C*****************************************************************

      THETAS=26.25*3.1415927/180.
      ALFA=(4000.0*0.10472)/300.0
      PX=0.0822*48.0
      PY=-0.0064*48.0
      OM=0.0

C*****************************************************************
C DISTRIBUTE AMPLITUDES OF FORCE VECTOR DUE TO IMPULSE
C ALONG THE HEIGHT OF THE BLADE
C*****************************************************************

      DO 50 J=1,5
      READ(8,*)NS1,NS2,NS3,ELEN
      NDX1=NS1*3-2
      NDX2=NS2*3-2
      NDX3=NS3*3-2
      NDY1=NS1*3-1
      NDY2=NS2*3-1
      NDY3=NS3*3-1
      F(NDX1)=PX*ELEN/3.0+F(NDX1)
      F(NDX2)=PX*ELEN/3.0+F(NDX2)
      F(NDX3)=PX*ELEN/3.0+F(NDX3)
      F(NDY1)=PY*ELEN/3.0+F(NDY1)
      F(NDY2)=PY*ELEN/3.0+F(NDY2)
      F(NDY3)=PY*ELEN/3.0+F(NDY3)
   50 CONTINUE
```

```
C*********************************************************************
C CONDENSE  THIS  FORCE VECTOR  &  CONVERT  IT  INTO
C MODAL  COORDINATES
C*********************************************************************
CALL VMULFM(T,F,924,200,1,924,924,FC,200,IER)
CALL VMULFF(EVINV,FC,200,200,1,200,200,FG,200,IER)

C*********************************************************************
C CALCULATE TRANSIENT VIBRATION RESPONSE
C*********************************************************************

TIN=0.0
KP=1
ICOUNT=1

101 CONTINUE

T1=SQRT(2*THETAS/ALFA)
T2=SQRT(2*(THETAS+(7.5*3.1415927/180.))/ALFA)
DT=T2-T1
DTIMP=T1+(DT/2.)
DDT=DTIMP-TIN
TIN=DTIMP
OM=OM+(ALFA*DDT)
THETAS=THETAS+(30.0*3.1415927/180.)

IF(OM.GE.332.0277)GO TO 102
GO TO 101

102 SPEED=OM/0.10472

CALL SPLFIT(RPM1,DR1,A1,B1,C1)
SI(1)=FW(SPEED)
CALL SPLFIT(RPM2,DR2,A2,B2,C2)
SI(2)=FX(SPEED)
CALL SPLFIT(RPM3,DR3,A3,B3,C3)
SI(3)=FY(SPEED)
CALL SPLFIT(RPM4,DR4,A4,B4,C4)
SI(4)=FZ(SPEED)

C*********************************************************************
C CALCULATE  RESPONSE  DUE TO  NOZZLE  EXCITATION
```

```
C*****************************************************************

IF(ICOUNT.EQ.1)THEN
CALL RESIMP(FG,DT,EIGEN,GM,SI,DDT,QI,QVI)
ELSE
CALL RESFREE(QI,QVI,DDT,SI,EIGEN,QF,QVF)
CALL RESIMP(FG,DT,EIGEN,GM,SI,DDT,QI,QVI)
END IF


DO 60 I=1,200
QI(I)=QI(I)+QF(I)
60 QVI(I)=QVI(I)+QVF(I)

TIME=DTIMP

C*****************************************************************
C CONVERT NOZZLE EXCITATION RESPONSE INTO CARTESIAN
C COORDINATES
C*****************************************************************

CALL VMULFF(EV,QI,200,200,1,200,200,TEMP1,200,IER)
80 CALL VMULFF(T,TEMP1,924,200,1,924,200,U,924,IER)

C*****************************************************************
C EVALUATE THE NOZZLE EXCITATION STRESSES
C*****************************************************************

CALL STRESS(1,U,OM,TIME)

C*****************************************************************
C CALCULATE THE RESPONSE DUE TO CENTRIFUGAL FORCES
C*****************************************************************

C CALL CENTRIFUGAL(EIGEN,SI,GM,ALFA,DTIMP,QCF)

C*****************************************************************
C CONVERT C.F. RESPONSE INTO CARTESIAN COORDINATES
C*****************************************************************

C CALL VMULFF(EV,QCF,200,200,1,200,200,TEMP2,200,IER)
C CALL VMULFF(T,TEMP2,924,200,1,924,200,UCF,924,IER)

C*****************************************************************
```

```
C CALCULATE  STRESSES  DUE  TO  C.F.
C*****************************************************************

C CALL STRESS(2,UCF,OM,TIME)

100 ICOUNT=ICOUNT+1
IF(OM.LE.333.09)GO TO 101

STOP
END

C ******* IMPULSE  RESPONSE  CALCULATION *************

SUBROUTINE RESIMP(FG,DT,EIGEN,GM,SI,DTIMP,QI,QVI)
REAL FG(200),SI(200),QI(200),QVI(200),EIGEN(200)
REAL GM(200,200)

DO 10 I=1,200
A=SQRT(1.-(SI(I)**2))
B=EXP(-SI(I)*EIGEN(I)*DTIMP)
C=SIN(A*EIGEN(I)*DTIMP)
D=COS(A*EIGEN(I)*DTIMP)
QI(I)=FG(I)*DT*B*C/(EIGEN(I)*A*GM(I,I))
QVI(I)=(FG(I)*DT)/(EIGEN(I)*A*GM(I,I))
QVI(I)=QVI(I)*((-SI(I)*EIGEN(I)*B*C)+(B*A*EIGEN(I)*D))
10 CONTINUE

RETURN
END

C ******FREE  VIBRATION  RESPONSE  CALCULATION **********

SUBROUTINE RESFREE(QI,QVI,DTIMP,SI,EIGEN,QF,QVF)
REAL QI(200),QVI(200),SI(200),EIGEN(200),QF(200)
REAL QVF(200)

DO 10 I=1,200
A=SQRT(1.-(SI(I)**2))
B=EXP(-SI(I)*EIGEN(I)*DTIMP)
C=SIN(A*EIGEN(I)*DTIMP)
D=COS(A*EIGEN(I)*DTIMP)
X=(QVI(I)+(SI(I)*EIGEN(I)*QI(I)))/(EIGEN(I)*A)
QF(I)=(B*X*C)+(B*QI(I)*D)
```

```
      QVF(I)=-SI(I)*EIGEN(I)*B*(I*C+QI(I)*D)
      QVF(I)=QVF(I)+B*(I*A*EIGEN(I)*D-(QI(I)*A*EIGEN(I)*C))
   10 CONTINUE

      RETURN
      END

C *******CENTRIFUGAL  FORCE  RESPONSE  CALCULATION ***********

      SUBROUTINE CENTRIFUGAL(EIGEN,SI,GM,ACC,TIME,QCF)
      DIMENSION EIGEN(200),SI(200),QCF(200),ED(200),GM(200,200)
      REAL INTA(2),INTB(2),I1(3),I2(3)
      REAL INT1,INT2,INT
      INTEGER R,R1

      ACCL=ACC
      T=TIME

      DO 30 I=1,200
      ED(I)=EIGEN(I)*SQRT(1.-SI(I)**2)
      A=SI(I)*EIGEN(I)
      B=ED(I)
      C=SQRT(A**2+B**2)
      ALFA=(ATAN(B/A))*180./3.14159

      IC=0.
      TU=0
   50 DO 10 K=1,3
      R=K-1
      R1=R
      TU1=TU
      IF(TU.EQ.0)TU1=1.0
      IF(R.EQ.0)R1=1

      ID=(-1)**R1
      IF(R.EQ.0)ID=1

      I1(K)=(ID)*2*((TU1)**(2-R))*SIN((B*TU-(R+1)*ALFA)
     1 *3.14159/180.)
      IF(K.EQ.1)I1(K)=I1(K)/((C**(R+1))*2)
      IF(K.NE.1)I1(K)=I1(K)/(C**(R+1))
      I2(K)=(ID)*2*((TU1)**(2-R))*COS((B*TU-(R+1)*ALFA)
     1 *3.14159/180.)
      IF(K.EQ.1)I2(K)=I2(K)/((C**(R+1))*2)
```

```
      IF(K.NE.1)I2(K)=I2(K)/(C**(R+1))
   10 CONTINUE

      IF(TU.EQ.0)INTA(1)=-EXP(A*(TU-T))*COS(ED(I)*T*3.14159
     1 /180.)*(I1(1)+I1(2)+I1(3))
      IF(TU.EQ.0)INTB(1)=EXP(A*(TU-T))*SIN(ED(I)*T*3.14159
     1 /180.)*(I2(1)+I2(2)+I2(3))
      IF(TU.EQ.T)INTA(2)=-EXP(A*(TU-T))*COS(ED(I)*T*3.14159
     1 /180.)*(I1(1)+I1(2)+I1(3))
      IF(TU.EQ.T)INTB(2)=EXP(A*(TU-T))*SIN(ED(I)*T*3.14159/
     1 /180.)*(I2(1)+I2(2)+I2(3))

      IC=IC+1
      TU=T
      IF(IC.EQ.1)GO TO 50

      INT1=INTA(2)-INTA(1)
      INT2=INTB(2)-INTB(1)
      INT=INT1+INT2
      QCF(I)=((ACCL)**2)*INT/(ED(I)*GM(I,I))
   30 CONTINUE

      RETURN
      END


      SUBROUTINE STRESS(INDEX,U,QM,TIME)
      C IMPLICIT REAL*8 (A-H,O-Z)
      DIMENSION COORD(20,3),DERIV(8,3,20)
      DIMENSION SHAPE(8,20),ST(60,60),UN(60)
      DIMENSION ND(20),X(20),Y(20),Z(20),NS(60),U(924)
      DIMENSION ESTRESS(6),IELM(15)

      OPEN(UNIT=3,FILE='MESH.DAT',TYPE='OLD')
      OPEN(UNIT=7,FILE='DISP.DAT',TYPE='OLD')
      OPEN(UNIT=12,FILE='VSTRESS.DAT',TYPE='NEW')
      OPEN(UNIT=14,FILE='CSTRESS.DAT',TYPE='NEW')

      RAD=0.5

      DO 20 NELM=1,35
      READ(3,*)NEL
      DO 10 I=1,20
      READ(3,*)ND(I),X(I),Y(I),Z(I)
```

```
 10 CONTINUE

C*****************************************************************
C EXTRACTING THE NODAL DISPLACEMENT VECTOR FOR
C EACH ELEMENT FROM THE GLOBAL DISPLACEMENT VECTOR
C*****************************************************************

K=1
DO 21 I=1,20
NS(K)=ND(I)*3-2
NS(K+1)=ND(I)*3-1
NS(K+2)=ND(I)*3
K=K+3
21 CONTINUE

DO 22 I=1,60
22 UN(I)=U(NS(I))

C*****************************************************************
C MULTIPLY C.F. RESPONSE WITH (R+Z) FOR EACH ELEMENT
C*****************************************************************

IF(INDEX.EQ.2)THEN
DO 30 I=1,60
30 UN(I)=UN(I)*(RAD+(Z(9))/100.)
ELSE
GO TO 35
END IF

35 DO 1 J=1,3
DO 1 I=1,20
IF(J.EQ.1)COORD(I,J)=(X(I))/1000.0
IF(J.EQ.2)COORD(I,J)=(Y(I))/1000.0
IF(J.EQ.3)COORD(I,J)=(Z(I))/100.0
 1 CONTINUE

IF(ON.GE.333.079)THEN

70 CALL SHAPE20(SHAPE,DERIV)

CALL STRESS20(INDEX,NEL,UN,COORD,SHAPE,DERIV,ESTRESS)

CALL PRINCIPAL(ESTRESS,DSTRESS)
```

```
IF(INDEX.EQ.1)WRITE(12,*)NEL,OM,TIME,DSTRESS
IF(INDEX.EQ.2)WRITE(14,*)NEL,OM,TIME,DSTRESS

ELSE
GO TO 60
END IF

60 CONTINUE

20 CONTINUE
REWIND 3
REWIND 7
RETURN
END

SUBROUTINE SHAPE20(SHAPE,DERIV)
C IMPLICIT REAL*8 (A-H,O-Z)
DIMENSION SHAPE(8,20),DERIV(8,3,20),F(2),ZTA(20)
DIMENSION SI(20),F1(24),NTA(20)

DATA F/-0.577350269189626,+0.577350269189626/
DATA ZTA/-1.,+1.,+1.,-1.,-1.,1.,1.,-1.,-1.,1.,1.,-1.,0.0,
    1 1.,0.0,-1.,0.0,1.,0.0,-1./
DATA NTA/-1.,-1.,1.,1.,-1.,-1.,1.,1.,-1.,-1.,1.,1.,-1.,
     1 0.0,1.,0.0,-1.,0.0,1.,0.0/
DATA SI/-1.,-1.,-1.,-1.,1.,1.,1.,1.,0.0,0.0,0.0,0.0,-1.,
     1 -1.,-1.,-1.,1.,1.,1.,1./

KK=0
DO 101 K=1,2
DO 101 J=1,2
DO 101 I=1,2
KK=KK+1
F1(KK)=F(I)
KK=KK+1
F1(KK)=F(J)
KK=KK+1
F1(KK)=F(K)
 101 CONTINUE

DO 10 NN=1,8
NN1=(NN-1)*3+1
```

```
      GZ=F1(NN1)
      GN=F1(NN1+1)
      GR=F1(NN1+2)

      DO 20 I=1,8
      SHAPE(NN,I)=(1.0/8.0)*(1.0+GZ*ZTA(I))*(1.0+GN*NTA(I))*(1.0+GR*
           1 SI(I))*(GZ*ZTA(I)+GN*NTA(I)+GR*SI(I)-2.0)
      DERIV(NN,1,I)=(1./8.0)*ZTA(I)*(1.0+GN*NTA(I))*(1+GR*SI(I))*
           1 (2.0*ZTA(I)*GZ+GN*NTA(I)+GR*SI(I)-1.0)
      DERIV(NN,2,I)=(1.0/8.0)*NTA(I)*(1+GZ*ZTA(I))*(1+GR*SI(I))*
           1 (GN*NTA(I)*2.0+GZ*ZTA(I)+GR*SI(I)-1.0)
      DERIV(NN,3,I)=(1.0/8.0)*SI(I)*(1.+GZ*ZTA(I))*(1.+GN*NTA(I))*
           1 (GZ*ZTA(I)+GN*NTA(I)+2.0*GR*SI(I)-1.0)
       20 CONTINUE

      DO 30 J=9,12
      SHAPE(NN,J)=(1./4.)*(1.0-GR**2)*(1.+GZ*ZTA(J))*(1.+GN*NTA(J))
      DERIV(NN,1,J)=(1./4.)*ZTA(J)*(1.0-GR**2)*(1.+GN*NTA(J))
      DERIV(NN,2,J)=(1./4.)*NTA(J)*(1.-GR**2)*(1.+ZTA(J)*GZ)
      DERIV(NN,3,J)=(-1./2.)*GR*(1.+GZ*ZTA(J))*(1.+GN*NTA(J))
       30 CONTINUE

      DO 40 L=13,16
      IF(L.EQ.16)K=19
      IF(L.EQ.15)K=17
      IF(L.EQ.14)K=15
      IF(L.EQ.13)K=13
      SHAPE(NN,K)=(1./4.)*(1.-GZ**2)*(1.+GN*NTA(K))*(1.+GR*SI(K))
      DERIV(NN,1,K)=(-1./2.)*GZ*(1.+NTA(K)*GN)*(1.+SI(K)*GR)
      DERIV(NN,2,K)=(1./4.)*NTA(K)*(1.-GZ**2)*(1.+SI(K)*GR)
      DERIV(NN,3,K)=(1./4.)*SI(K)*(1.-GZ**2)*(1.+NTA(K)*GN)
       40 CONTINUE

      DO 50 K=17,20
      IF(K.EQ.17)L=14
      IF(K.EQ.18)L=16
      IF(K.EQ.19)L=18
      IF(K.EQ.20)L=20
      SHAPE(NN,L)=(1./4.)*(1.-GN**2)*(1.+GZ*ZTA(L))*(1.+SI(L)*GR)
      DERIV(NN,1,L)=(1./4.)*ZTA(L)*(1.0-GN**2)*(1.+SI(L)*GR)
      DERIV(NN,2,L)=(-1./2.)*GN*(1.+ZTA(L)*GZ)*(1.+SI(L)*GR)
      DERIV(NN,3,L)=(1./4.)*SI(L)*(1.-GN**2)*(1.+ZTA(L)*GZ)
       50 CONTINUE
       10 CONTINUE
```

```
      RETURN
      END


      SUBROUTINE STRESS20(INDEX,NEL,UN,COORD,SHAPE,DERIV,SMAX)
C     IMPLICIT REAL*8 (A-H,O-Z)
      DIMENSION B(6,60),AJACOB(3,3),SHAPE(8,20),UN(60)
      DIMENSION AJINV(3,3),DERIV(8,3,20),COORD(20,3),P(6,9)
      DIMENSION R(9,60),PQ(6,9),D(6,6),BTD(60,6),AWK(100)
      DIMENSION STRAIN(6),STRESS(6),EPSILON(6),STRE(6,8)
      DIMENSION Q(9,9),VOL(8),SMAX(6)

      INTEGER IER
      RHO=8526.0

      DO 2 I=1,6
      STRAIN(I)=0.0
      EPSILON(I)=0.0
    2 STRESS(I)=0.0

      NN=0
      DO 105 KK=1,2
      DO 105 JJ=1,2
      DO 105 II=1,2
      NN=NN+1

      DO 50 L=1,6
      DO 50 K=1,60
   50 B(L,K)=0.0

      DO 51 I=1,3
      DO 51 J=1,3
   51 AJACOB(I,J)=0.0

      DO 52 I=1,3
      DO 52 J=1,3
      SUM=0.0
      DO 53 K=1,20
      SUM=SUM+DERIV(NN,I,K)*COORD(K,J)
   53 CONTINUE
      AJACOB(I,J)=SUM
   52 CONTINUE

      CALL INVERSE(AJACOB,AJINV,DET)
```